Influence of hypoxia on the proliferation and vincristine drug resistance in neuroblastoma cancer cell lines SHEP-2 and SH-SY5Y

December 2023 – September 2024

Master Thesis Project Biomedical Engineering

Meggie A. B. Stempher

Master thesis committee

Committee chair:	Prof. Dr. Armagan Kocer
Daily supervisor:	Hugo Markus MSc.
External UT supervisor:	Asst. Dr. Sandra Michel-Souzy
External supervisor:	Dr. Lieve Tytgat

BioElectric signaling and Engineering

UNIVERSITY OF TWENTE.

Acknowledgements

For the past 10 months, I have worked with great pleasure on my project in the Bio-Electrical Signaling and Engineering (Bio-EE) group. The feeling of being able to contribute and be a small part of the extensive and meaningful research within the group, gave me a profound sense of purpose. It provided an incredible boost of motivation to give the project my all and bring it to a purposeful conclusion.

I would like to express my deepest gratitude to Prof. Dr. Armagan Kocer for the opportunity to pursue this project in the Bio-EE group and for fostering a nurturing environment for learning and development. With the door always open, also for non-research-related talks, I have hardly ever felt more welcome and appreciated. Working with her has enhanced my feeling of being a competent researcher and believing in my abilities.

I want to extend my heartfelt appreciation to my daily supervisor Hugo Markus, who was always there for me, showing me the ropes and supporting me, and sharing his knowledge and experience with me. I have learned so much under his guidance, both theoretical and practical. I would also like to express my sincere appreciation to Dr. Sandra Michel-Souzy and Dr. Lieve Tytgat for being willing to be part of my master thesis committee and as such part of my academic journey. For evaluating this research and their valuable feedback and suggestions, especially during the midterm meeting and in the final stages of my assignment.

In addition, a warm thank you goes to the entire Bio-EE group for the great and warm working environment throughout all these months. Special thanks to all students for their enthusiasm, inspiration, incitement, and joy. Having a relaxing chat in between the arduous work, having our inside jokes, laughing with each other, supporting each other, cheering each other on and lifting each other up in case of a set-back. I have not just gained colleagues; I have gained friends. Also, special recognition goes to Edwin, Christian, Narges, Ingrid, and Connie, for helping with all kinds of arrangements of materials, for new perspectives and refreshing insights, for tips and advice, for a friendly chat in the hallways, labs or at lunch, and for making me feel welcome.

Finally, I would like to thank all of my family and friends for their unconditional support throughout my graduation journey and all those years working towards this moment.

I would like to thank everyone who was engaged in, contributed to, or was in any other way affiliated with the project or supported me throughout the process from the bottom of my heart.

Abstract

Neuroblastoma is currently one of the most common and deadly solid extracranial tumors in pediatric oncology. The primary site of metastasis of neuroblastoma is the bone marrow. A great obstacle in clinical oncology is chemotherapy resistance and relapse in pediatric patients, resulting in a poor prognosis. It is suggested the bone marrow microenvironment plays a crucial role in this process. This microenvironment in which metastatic neuroblastoma cells reside, is hypoxic. Hypoxia is known to affect the malignant behavior and phenotype of tumor cells. Moreover, hypoxia has been reported to activate bone marrow cells to mediate neuroblastoma drug resistance. However, the significance of hypoxia in pediatric cancer and the exact role of chronic hypoxia on the neuroblastoma cell characteristics has yet to be elucidated. Therefore, we aimed to investigate the effects of chronic hypoxia on the cellular response of the SHEP-2 and SH-SY5Y neuroblastoma cell lines, in terms of proliferation and drug resistance. Since the primary site of metastasis of neuroblastoma is the bone marrow, the research further investigates the role of HS-5 primary bone marrow cells on the neuroblastoma cell response in hypoxia. It was observed that proliferation of both SHEP-2 and SH-SY5Y cells was significantly increased in hypoxia, with a near 2-fold increase in proliferation. In co-culture with HS-5, the proliferation was significantly decreased in normoxia, while the proliferation was further increased in hypoxia, compared to the monoculture proliferation. The IC50 of vincristine, a chemotherapy drug commonly used in induction chemotherapy, in normoxia was found to be 0.031±0.008 μM and 0.0019±0.0004 μM for SH-SY5Y and SHEP-2 cells, respectively. In hypoxia the tolerance of the cells for vincristine was significantly increased by 3-fold for both cell lines. The co-culture with HS-5 bone marrow cells did not show a significant difference of the percentage viability compared to the monoculture. These results indicate that hypoxia significantly affects the proliferation of the SHEP-2 and SH-SY5Y neuroblastoma cell lines and the tolerance of both neuroblastoma cell lines to vincristine. Therefore, hypoxia is a microenvironment characteristic that should not be neglected in *in vitro* drug resistance and tumor behavior studies as it may strongly influence the results and translatability to the patient.

Content

Abbreviations

ADRN	Adrenergic
BM	Bone Marrow
BMM	Bone Marrow Microenvironment
CAR cell	CXCL12-Abundant Reticular cell
CBDCA	Carboplatin
CDDP	Cisplatin
CTX	Cyclophosphamide
CXCL12	CXC motif chemokine ligand 12
DMEM	Dulbecco's Modified Eagle Medium
EC	Endothelial Cell
FBS	Fetal Bovine Serum
HBSS	Hank's Balanced Salt Solution
HIF	Hypoxia Induced Factor
HSPC	Hematopoietic Stem and Progenitor Cells
MDR1	Multidrug Resistance Protein 1
MES	Mesenchymal
MRP1	Multidrug Resistance-associated Protein 1
MSC	Mesenchymal Stromal cell
NB	Neuroblastoma
PBS	Phosphate-Buffered Saline
PEMn	Pre-equilibrated Medium in normoxic condition
PEMh	Pre-equilibrated Medium in hypoxic condition
Pen/strep	Penicillin-Streptomycin
PGP	P-glycoprotein
ROS	Reactive Oxygen Species
VCR	Vincristine
VP-12	Etoposide

1. Introduction and Theoretical Background

In neuroblastoma pediatric cancer, one of the biggest clinical problems is that of relapse, resulting in low overall patient survival [1–3]. It is hypothesized that relapse is caused by a dormant and drug-resistant state of metastatic neuroblastoma tumor cells in the bone marrow that survive therapy and remain undetected due to the bi-directional communication with bone marrow resident cells in the hypoxic bone marrow microenvironment (~1-7% oxygen) [4–6]. However, many of the current co-culture studies are performed in normoxic conditions (standard oxygen concentration in the culture flask ~21% [7]), which does not reflect the biological microenvironment of the metastatic neuroblastoma cells. As hypoxia is known to strongly affect tumor cell characteristics [8–14] as well as to play a role in activating the bone marrow stromal cell behavior in mediating malignant behavior of tumor cells [15–17], this research project is aimed to elucidate the role of hypoxia in the malignant behavior of the SHEP-2 and SH-SY5Y neuroblastoma cells in monoculture and co-culture with HS-5 bone marrow cells in terms of proliferation and drug resistance.

1.1 High-risk neuroblastoma and the bone marrow microenvironment

Neuroblastoma (NB) is one of the most common extracranial solid childhood tumors, characterized by clinical heterogeneity ranging from spontaneous regression without medical intervention to therapy resistant tumors with metastasis [18–22]. Neuroblastoma tumors arise from sympathoadrenal cells of the neural crest, which differentiate to sympathetic ganglion cells and adrenal catecholamine-secreting chromaffin cells [18]. Primary neuroblastomas form along the sympathetic chain or in the adrenal gland [19]. Diagnosis and staging of neuroblastoma are achieved through a combination of histological, biochemical, and imaging approaches. A currently widely accepted risk classification system used for pretreatment risk stratification is the International Neuroblastoma Risk Group Staging System (INRGSS), which is based on a combination of prognostic factors, including clinical stage, patient age, histopathology, and genetic and molecular properties [23,24]. Patients are classified into low-, intermediate-, and high-risk groups, based on for example age, MYCN amplification, chromosome aberrations, and metastasis [3]. The most common metastatic site of neuroblastoma is the bone marrow (BM) [1,25]. More than 50% of patients present with metastasis to the bone marrow at the time of diagnosis and 90% of high-risk patients have BM metastasis [22]. Despite the aggressive multimodal therapies (including surgical resection, high-dose chemotherapy, radiation therapy and post-consolidation immunotherapy) for high-risk patients, the overall survival of children with metastatic neuroblastoma is poor (<40%) [1–3]. Over 50% of high-risk patients relapse [3], possibly due to a chemo-resistant, dormant-state of tumor cells in the BM, which survive therapy and remain undetected. As relapse or progression in the BM are major causes of death for neuroblastoma patients, it is of great importance to understand and study the complex interaction between BM-infiltrating neuroblastoma cells and the BM resident cells, as this might aid in identifying therapeutic strategies and improvement of the overall survival of patients with high-risk, metastatic NB.

Important to realize is the complexity of the bone marrow microenvironment (BMM). The BMM is not just one niche itself, but rather an assembly of multiple micro-niches composed of distinct cell populations and chemotactic gradients [12,13]. The micro-niches induce distinct hematopoietic stem and progenitor cell (HSPC) responses, including cell homing, quiescence, self-renewal, or lineage commitment. The two most referred to sub-niches in the human BM are the endosteal and the perivascular niche [26–29]. The perivascular niche, located in close proximity to the blood vessels, is comprised of endothelial cells (ECs) (constructing the BM sinusoids) accompanied by MSCs [30] and CXCL12-abundant reticular (CAR) cells [31]. The perivascular niche is associated with activated HSPCs [28]. The endosteal niche is situated at the interface tween trabecular bone and the BM, and is primarily comprised of osteoblasts (OBs), acting as an interface between calcified bone and the BM, CAR cells, stromal fibroblasts, and osteoclasts [27,30,31]. HSPCs isolated from the endosteal niche show higher hematopoietic potential [32,33], indicating there are separate, spatially distinct niches for quiescent and proliferating HSCs in BM [26,29,34]. Every cell type within the BM expresses receptors and ligands for communication with other cells via secreted soluble factors (e.g., growth factors, cytokines, and chemokines) or extracellular vesicles with various cargo (e.g., proteins, DNA fragments, metabolites, and RNA) [35,36]. The complex cross-talk between hematopoietic and non-hematopoietic cells is required for BM homeostasis. This physiological homeostasis may be altered

by the presence of a metastatic neuroblastoma tumor cell. The physiological functions of the bone marrow niches become commandeered by the tumor cells as such that the niches support tumor cell functions such as dormancy, relapse, and growth [10,37–39]. The metastatic niche of tumor cells in the bone marrow is believed to be composed of both the perivascular and endosteal niche [38]. Both the vascular and endosteal niche have shown to maintain cell dormancy, by release of stromal cell derived factor 1 (SDF-1), also known as CXC motif chemokine ligand 12 (CXCL12) that binds to CXCR4 on tumor cells [10,38]. For NB, the role of the different niches is not elaborately described.

Importantly, the entire BMM is regarded as hypoxic. Normoxia is generally approximated to be ~20-21% oxygen, with an oxygen tension (P_{O_2}) of 160 mmHg [7]. In the bone marrow, the P_{O_2} is much lower ($< 32\ mmHg$) [40]. However, local P_{O_2} in the BM is heterogeneous, resulting in an oxygen gradient (figure 1) [40–42]. The lowest P_{O_2} of $\sim 10\ mmHg$ is found deep in the BM center. The endosteal region is less hypoxic as these regions are perfused with small, nestin positive arterioles. In percentages, the oxygen concentration ranges from 1% to 7% [5,6,43]. Hypoxia is believed to be a necessity in maintaining SC quiescence [44,45]. For HSCs it is observed that hypoxia is associated with quiescence and retention in the BM, whereas high oxygen tension allows for HSC mobilization [46], also indicating the biological importance of the oxygen gradient in the BMM. In cancer cell biology, tumor cells alter signaling pathways to adapt to hypoxia, promoting malignant behavior such as proliferation, migration, epithelial-to-mesenchymal transition, and chemotherapy resistance [8,13,14,47,48]. The hypoxic microenvironment induces molecular changes to facilitate dormancy [37,38].

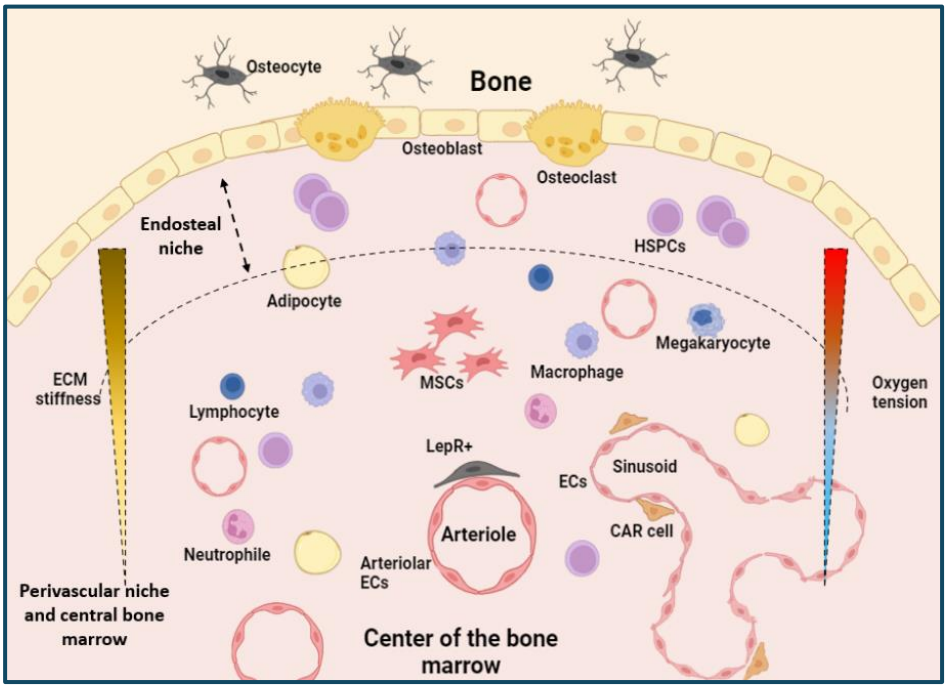

Figure 1: Simplified summary of the different cell types found in BMM of NB. Important cell types include the HSPCs and mature cells from the hematopoietic lineages, BMSCs, CAR cells, LepR⁺ cells, adipocytes, osteoblasts, osteoclasts, and ECs of the blood vessels. In addition, there is an indicated gradient in ECM stiffness (with higher stiffness in the endosteal niche) and oxygen tension (with higher oxygen tension in the endosteal niche). BMSC= bone marrow mesenchymal stromal cell, CAR= CXCL12 abundant reticular cell, LepR+= leptin receptor positive cells, EC= endothelial cell. Created with BioRender.com (05 Oktober 2023)

Hypoxia can be categorized in acute, intermittent, and chronic hypoxia [47]. Acute hypoxia is characterized by short term exposure to low oxygen (few minutes to a few hours) while chronic hypoxia is characterized by prolonged exposure to hypoxia. Intermittent hypoxia is the cyclic occurrence of high and low oxygen concentrations. In metastatic NB, the tumor cells reside in a naturally hypoxic environment. Therefore, in the case of high-risk neuroblastoma, metastatic neuroblastoma tumor cells are exposed to hypoxia for a longer period in the presence of BM resident cells, indicating chronic hypoxic conditions and co-culture of neuroblastoma cells with BM stromal cells is biologically most relevant to mimic high-risk neuroblastoma.

1.2 The SHEP-2 and SH-SY5Y neuroblastoma cell lines

Both the SHEP-2 and SH-SY5Y cell lines are derived from the SK-N-SH cell line, originally isolated from a bone marrow biopsy taken from a four-year-old female with neuroblastoma [49]. The SHEP-2 cell line is an S-phenotype subline [49]. They are epithelial-like, substrate adherent cells, which are flattened in shape without neuritic processes and no expression activity of the TH and DBH enzymes. The SH-SY5Y cell line is considered to be an N-phenotype subline [49–51], however, it is also suggested the SH-SY5Y cell line comprises both cell types [52,53]. These are neuroblast like cells, exhibiting a combination of adherent and suspension culture.

Based on master transcriptional regulators controlling gene expression of neuroblastoma, two distinct cell identities have been discriminated:

1. (nor)adrenergic (ADRN)-type cells, defined by a core regulatory circuitry (CRC) module including the PHOX2A/B, HAND1/2 and GATA2/3 transcription factors.
2. mesenchymal (MES)-type cells (close to human neural crest cells)

The ADRN and MES tumor cell types differ in phenotype, super-enhancers (SEs) and core regulatory circuitries (CRCs). SHEP-2 cells are MES-type cells, whereas SH-SY5Y cells are characterized as ADRN-type cells. Therefore, they form a frequently used isogenic cell line pair [50]. MES-type cells are considered to be more drug-resistant in comparison to ADRN-type cells [54]. Somewhat paradoxically, it has been reported that SHEP-2 cells are observed to be less aggressive, while the SH-SY5Y resemble a highly aggressive neuroblastic phenotype [55]. Both SHEP-2 and HS-SY5Y are MYCN non-amplified cell lines [53,55–57].

There is some discussion about the use of these cancer cell lines in regard to some inherent limitations. Namely, neuroblastoma cell lines, as well as other conventional cancer cell lines, do not properly recapitulate properties and phenotype of the original tumor properties [58]. They do not fully reflect the natural biology, complexity, and heterogeneity of the malignancy [59]. Therefore, they may not provide the ideal model for preclinical studies as the obtained results using these cell lines might not be translatable to patients. It is important to keep this in mind while drawing conclusions upon the results of this study and making recommendations for future research. Nonetheless, these cancer cell lines are very broadly implemented in fundamental biology studies due to their beneficial practical characteristics. Additional background readings for the different cell lines are included in Supplementary S1.

1.3 Neuroblastoma cellular response to hypoxia

Hypoxia can have a significant effect on the malignant behavior and cellular phenotype of cancer cells, including proliferation, dormancy, and chemotherapy resistance [60]. In order to determine the best course of action and most meaningful additions for filling current gaps of knowledge in research, it is important to assess what is already known about the specific response of neuroblastoma tumor cells in a hypoxic environment.

It is generally suggested that a hypoxic microenvironment increases drug resistance. This has also been observed for neuroblastoma tumor cells for several chemotherapeutics used in neuroblastoma treatment including etoposide and vincristine [11,61]. However, research upon drug resistance behavior for some chemotherapeutic agents is still limited the and the effects of hypoxia on chemotherapy resistance are yet to be examined and clarified. In NB, hypoxia is expected to evoke a more aggressive phenotype, showing more undifferentiated, stem-like cells correlated with poor prognosis and survival outcome. Hypoxia, for instance, can induce high levels of expression of drug resistance genes in cancer cells [62,63]. These include P-glycoprotein 1 (PGP) also known as multidrug resistance protein 1 (MDR1) and multidrug resistance-associated protein 1 (MRP1)[62].

In NB, Applebaum et al. [63] have combined several neuroblastoma tumor and cell line datasets to identify a hypoxia-upregulated signature correlated with poor patient outcome. This signature includes elevated expression of *LCO4A1, ENO1, HK2, PGK1, MTFP1, HILPDA, VKORC1, TPI1*, and *HIST1H1C*. When it comes to cell survival, upregulation of several survival and growth-related genes is observed in NB-derived cells under hypoxic conditions, including *VEGF, NEUROPILIN 1, ADRENOMEDULLIN* and *IGF2*. Hypoxia induced VEGF expression was found to cause apoptosis resistance in neuroblastoma cells by upregulation of B-cell leukemia 2 (Bcl-2) expression [64] as well

as extracellular-signal-regulated kinase (ERK1/2) phosphorylation [65]. It is hypothesized this apoptosis resistance is partially responsible for hypoxic-mediated chemoresistance.

In response to hypoxia, HIF-1α and HIF-2α stabilized is induced. HIF-1α and HIF-2α are expressed continuously, however, in an oxygen rich environment HIFs are degraded whereas low oxygen concentration allows for HIF stabilization. HIF-1α forms the initial response to acute hypoxia whereas HIF-2α is stabilized upon prolonged hypoxia exposure [66]. Hypoxia has been observed to provoke HIF-1α mediated resistance to chemotherapeutic agents [60,67,68]. It has been demonstrated that *HIF-1*α is preferentially expressed in MYCN-amplified neuroblastoma cells and primary tumors, compared to samples without MYCN amplification [69]. In addition, interplay between N-Myc and HIF-1α has a vital role in NB. For instance, high levels of N-Myc override HIF-1α cell cycle inhibition and allow for continued proliferation under hypoxia. Moreover, HIF-1α and N-Myc are vital for the Warburg effect, also known as aerobic glycolysis, commonly observed in tumor growth. Other studies report that MYCN-amplified neuroblastoma cells show increased apoptosis in hypoxia [70]. Moreover, HIF-1α has shown to protect neuroblastoma cells from apoptosis by promoting Survivin expression in SH-SY5Y cells [71].

HIF-2α also plays a significant role in neuroblastoma cell survival, by promoting hypoxic cell proliferation through the upregulation of c-Myc transcriptional activity [72]. Hypoxia is also known to trigger dedifferentiation of neuroblastoma cells towards a more immature SC phenotype and is associated with neuroblastoma metastasis [73]. HIF-2α leads to a neural crest-like neuroblastoma population with increased NOTCH1, HES-1, c-Kit, vimentin and dHAND expression [74]. HIF-2α additionally regulates OCT-4, affecting stem cell function and tumor growth [75]. Moreover, hypoxic neuroblastoma cells have shown to switch from primitive neuronal to chromaffin cell type with increased IGF2 and GAP-43 expression [76] and neuroblastoma cells under hypoxic culture conditions exhibit more stem cell like features with increased expression of proneuronal lineage specifying transcription factor inhibitors: ID2 and HES-1 [12,77]. High HIF-2α expression in neuroblastoma patients was correlated with a poor prognosis and more aggressive tumor phenotype [66].

As hypoxia induces a more aggressive cancer phenotype, this also includes an increase in proliferation [13]. However, limited data is available describing the relation between neuroblastoma tumor cell proliferation and hypoxia. A correlation between MYCN-amplification, HIF-1α, and proliferation has been suggested but the exact relation with hypoxic exposure has yet to be established [78]. It has also been suggested that hypoxia reduces the tumor cell proliferation, ultimately resulting in drug resistance, since anticancer drugs target rapidly dividing cells [79].

1.4 MSC specific response to hypoxia and BMSC in the tumor microenvironment

BM MSCs also respond to hypoxic cell culture. Increased expression of Oct4, C-Myc, Nanog, Nestin and HIF-1α have been observed in MSCs cultured under hypoxic conditions [15]. In addition, MSCs cultured under hypoxia conserve a higher level of MSC specific surface markers, as well as lower level of hematopoietic markers. Moreover, a significantly increased proliferation rate has been observed in MSCs cultured under hypoxic conditions, in combination with a higher percentage of cells in the S-phase of the cell cycle. Others, however, describe a reduction in proliferation and differentiation in response to hypoxia [4], indicating current literature is somewhat divided and additional research may elucidate the response of the HS-5 bone marrow cell line in hypoxia.

BMSCs are also known to mediate chemoresistance in tumor cells. In acute lymphoblastic leukemia (ALL), BMSCs have shown to mediate vincristine resistance through the CXCR4/CXCL12 axis [16]. In addition, extracellular vesicles containing specific micro-RNAs were excreted by hypoxic BMSCs, resulting in drug resistance in multiple myeloma [17]. BMSCs have in general been reported to be involved in increased tumor cell proliferation [80], tumor cell dormancy [81], stemness and chemoresistance [82–84].

1.5 Chemotherapy treatment regimens for neuroblastoma

In order to make a well substantiated decision on a chemotherapeutic agent for evaluating the drug-resistant behavior of neuroblastoma tumor cells in hypoxia, it is important to first gain insight in and understand the current treatment regimens of neuroblastoma patients. Treatment of neuroblastoma patients is based on the risk-classification. Patients with high-risk neuroblastoma constitute half of the total number of patients with newly diagnosed neuroblastoma. Multimodal therapy for high-risk patients starts with induction chemotherapy. The traditional most commonly implemented induction therapy, the current North American induction regimen, encompasses dose-intensive cycles of cisplatin and etoposide, alternating with vincristine, cyclophosphamide, and doxorubicin [85,86]. This regimen was elaborated with topotecan during the first two cycles of induction in the Children's Oncology Group (COG) trials [86,87]. The Society of Pediatric Oncology Europe Neuroblastoma Group (SIOPEN) have developed the rapid COJEC regimen. The rapid COJEC regimen encompasses eight cycles using combinations of cisplatin [C in the acronym, normally abbreviated P], vincristine [O], carboplatin [J], etoposide [E], and cyclophosphamide [C]. In comparison with the N5-MSKCC (Memorial Sloan Kettering Cancer Center) regimen, there is no difference in event free survival (EFS) or overall survival (OS), but COJEC showed lower frequency of toxicities [88–90]. In addition, the shorter time period of the rapid COJEC induction chemotherapy could in theory reduce the risk of drug resistance [91]. The standard rapid COJEC regimen [90,92,93] and N5-MSKCC [88–90] regimen have been depicted in figure 2, together with the COG regimen [94] and alternate OPEC/OJEC regimen [92,93].

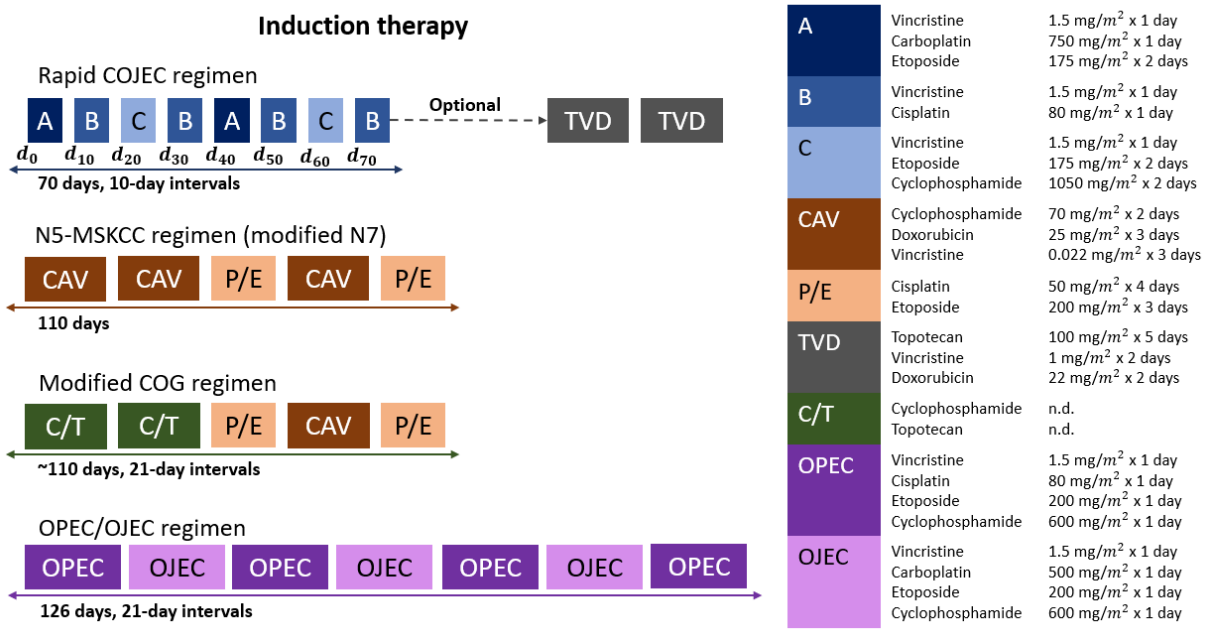

Figure 2: Induction chemotherapy regimens. SIOPEN recommend additional therapy with topotecan, vincristine, and doxorubicin (TVD) before consolidation transplantation if no adequate metastatic response to induction chemotherapy is shown in patients. Based on the works of [85–90,92–94].

SIOPEN recommend additional therapy with topotecan, vincristine, and doxorubicin (TVD) before consolidation transplantation if no adequate metastatic response to induction chemotherapy is shown in patients [90,94].

Induction therapy is followed by consolidation therapy and after consolidation therapy (or maintenance) [86]. The induction therapy phase does not only include chemotherapy, but also comprises stem cell collection and surgical resection of primary tumor. The consolidation phase encompasses high dose chemotherapy with autologous stem cell transplant (ASCT). The past consolidation phase or maintenance phase includes immunotherapy and retinoid therapy.

1.6 COJEC chemotherapeutic drugs mechanisms of action and (possible) mechanisms of drug resistance in normoxia and hypoxia

As previously described, the rapid COJEC regimen encompasses eight cycles of different combinations of five chemotherapeutics cisplatin (CDDP), vincristine (VCR), carboplatin (CBDCA), etoposide (VP-16), and cyclophosphamide (CTX). The chemical structures of the compounds are depicted in figure 3. The drugs have different mechanisms of action, and different underlying mechanisms of drug resistance. It is important to keep in mind that the cellular response to the chemotherapeutics is complex and depends on many factors including for instance the dose, schedule of administration, and exposure time [95].

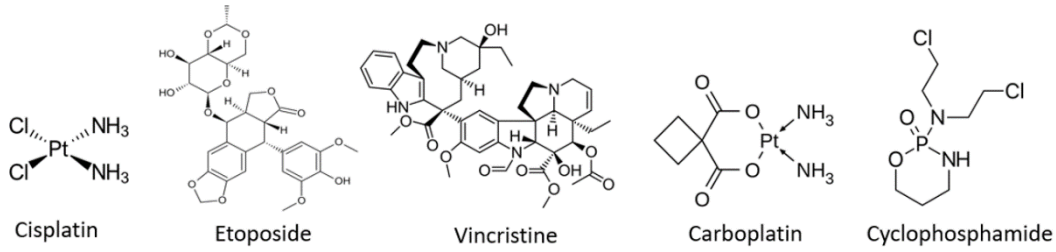

Figure 3: Overview of the chemical structures of the chemotherapeutics of the rapid COJEC regimen. Created 15-02-2024.

An overview of the characteristics of these chemotherapeutic drugs in pediatric cancer treatment have been included in table S2 (Supplementary S3). This includes the peak plasma concentration (Cmax), a standard measure in pharmacokinetics important to understand exposure-response effects [96]. Drug resistance is often measured using the IC50 value, i.e. the concentration of drugs that causes 50% growth inhibition [97,98]. For a further elaboration on the mechanism of action and possible mechanisms of drug resistance of cisplatin, carboplatin, etoposide, and cyclophosphamide, refer to Supplementary S3.

Vincristine

As described previously, VCR is included in each course of the rapid COJEC induction chemotherapy protocol, indicating its significance in neuroblastoma treatment. In addition, VCR is a bit less well-studied in comparison to for instance etoposide and cisplatin, and more unanswered questions remain. It has a clear mechanism of action and initial evidence was found to support the hypothesis that the response to VCR is influenced by hypoxia, also in neuroblastoma [11,99]. Therefore, based on the analysis of all drugs included in the rapid COJEC treatment, in this study, it was decided to investigate the effect of VCR on the SHEP-2 and SH-SY5Y neuroblastoma cell lines in normoxia and hypoxia.

Vincristine (VCR) is a vinca alkaloid, which can bind to the β-tubulin subunit of the tubulin dimers [100]. By formation of tubulin-drug complex, called paracystalline, the equilibrium between growth and shrinking of microtubules is pushed in favor of shrinking, by reducing the concentration of the tubulin dimers (figure 4). This inhibits the proper formation of mitotic spindles, causing cells to lose the ability to progress through the cell cycle, resulting in mitotic cell cycle arrest. Cells consequently undergo apoptosis. In the SH-SY5Y neuroblastoma cell line, VCR has shown to cause cell cycle arrest in the G2/M phase [99]. In addition to its effect on the mitotic process, VCR interferes with processes that require the microtubules, including molecular transport, secretion processes, and cellular structure [100].

There is limited literature on the mechanisms of drug resistance to VCR. One of the proposed causes of VCR drug resistance is P-glycoprotein-mediated multidrug resistance. In the breast cancer MCF7 cell line, VCR drug resistance is correlated with changes in microtubule proteins and drug metabolism pathways. In addition, drug resistance to VCR is related to changes in VEGFA and IL-1β expression [101]. Mutations in the tubulin protein or alternative tubulin expression leading to VCR drug resistance has been observed in leukemia [102,103].

In neuroblastoma cells, hypoxia promotes HIF1-α resistance to etoposide and VCR. In SH-EP1 and SH-SY5Y short hypoxic exposure (up to 16 hours) did not affect drug resistance. However, prolonged hypoxia between 1 and 7 days, results in reduced VCR- and etoposide-induced cell death. Short- and long-term hypoxic exposure did not induce cisplatin drug resistance. HIF1-α expression stabilized in 2 hours of hypoxia. After 48 hours of hypoxic exposure, the HIF1- α was not detectable. Downregulation of HIF1-α decreased the hypoxia-induced drug resistance [11].

In addition, VCR resistance in neuroblastoma cells was found to be related to upregulation of epidermal growth factor receptor (EGFR), dihydrofolate reductase (DHFR), microsomal epoxide hydrolase (EPHX1), MVP, cytochrome P450 3A4, and DNA topoisomerase II alpha and beta (TOP2A and TOP2B), that all have been linked to drug resistance mechanisms [104].

Chronic hypoxia has shown to induce HIF-1α dependent VCR and etoposide resistance in SH-EP1 and SH-SY5Y cells. In this study, short term exposure to hypoxia did not result in the drug-induced apoptosis, while prolonged exposure to hypoxic conditions did. Manually interfering with the HIF-1α expression showed the dependence of the increased drug-resistant on this HIF-1α function [11]. In addition, for SHEP-2 cells, VCR resistance was correlated with LIM-kinase 2 (LIMK2) expression. LIMK is a serine/threonine kinase, regulating actin dynamics [105].

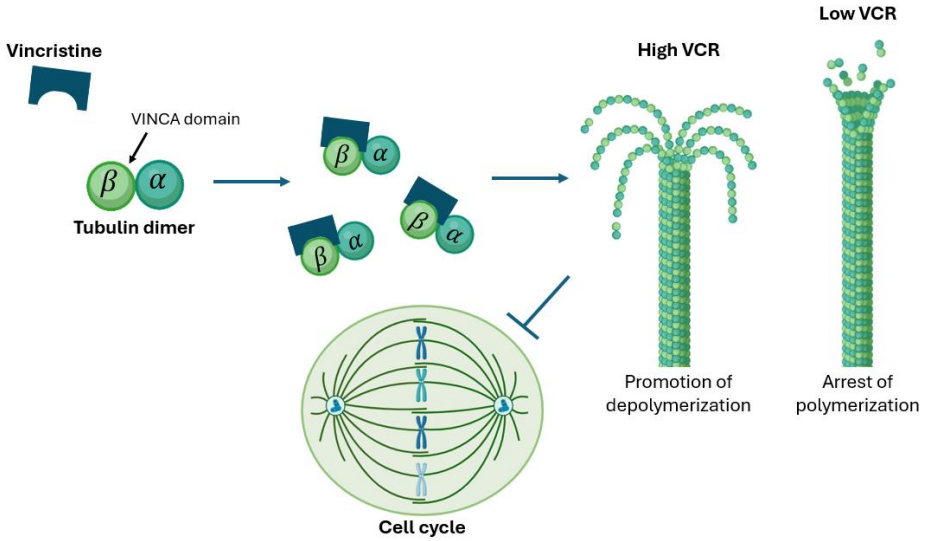

Figure 4: Mechanism of action VCR. Binding to β-tubulin, VCR interferes with the microtubule formation leading to cell cycle arrest and disruption of other microtubule involved processes. Created with BioRender.com (04 June 2024).

1.7 Drug resistance related membrane proteins in NB

Important in the chemotherapeutic drug resistance are a superfamily of membrane proteins linked to the ATP-regulated transport of many chemotherapeutic substrates across the membrane of tumor cells, known as the so-called ATP-binding cassette (ABC)-transports [106,107]. Examples of these ABC-transporters include MRP1, breast cancer resistance protein (BCRP), and PGP (also known as MDR1). MRP1 is considered to be the most important ABC transporter related to malignant and drug-resistant phenotype in neuroblastoma [108]. Etoposide and VCR are known substrates for the MRP1 transporter, as well as cisplatin [109]. MRP1 has been shown to contribute to tumor responsiveness to chemotherapy in MYCN amplified neuroblastoma primary tumors obtained from mice [110].

However, also PGP has been shown to be expressed in the SK-N-SH cell line (the parental cell line of SHEP-2 and SH-SY5Y). However, literature is limited [111]. PGP was associated with VCR resistance, as described above. In addition, PGP is correlated with etoposide resistance, but not with cisplatin resistance [109].

Finally, BCRP has been reported in neuroblastoma [112]. BCRP gene transcription was found to be influenced by hypoxia [113]. BCRP was associated with etoposide resistance, however, cisplatin and VCR were found not to be compatible substrates for BCRP [114].

2. Research aim and key objectives

Many of the current studies to evaluate the interaction between metastatic neuroblastoma cells and bone marrow resident cells are conducted under normoxic conditions. Little information is acquired on the neuroblastoma cell proliferation in hypoxia and also the drug-resistant behavior of neuroblastoma tumor cells in hypoxia is not fully understood. The interactions with bone marrow resident cells and its effect on proliferation and resistance in hypoxic conditions remains elusive. Although individual cell lines have been exposed to hypoxic culture conditions, current knowledge on the role of hypoxia in the tumor aggressive behavior and phenotype in neuroblastoma is limited.

We hypothesize, based on the presented literature, that exposure to hypoxia causes an increase in the proliferation of neuroblastoma cells as well as the drug resistance to VCR. In addition, we hypothesize that a co-culture with bone marrow cells increases the malignant behavior of neuroblastoma cells in the form of proliferation and drug resistance.

The aim of this thesis project is to investigate and understand the effect of hypoxia on the proliferation and VCR drug resistance of the neuroblastoma tumor cell lines SHEP-2 and SH-SY5Y as well as study how co-culture conditions with the HS-5 bone marrow cell line further affects these neuroblastoma cell behaviors. In order to achieve the aim, this research involves the following key objectives:

1. Determine the cellular proliferation of SHEP-2, SH-SY5Y and HS-5 cell lines in hypoxia compared to normoxia.

    a. Research question: What is the effect of exposure to chronic hypoxia (5% oxygen) in comparison to normoxia on the proliferation of the SH-SY5Y and SHEP-2 neuroblastoma cell lines and the HS-5 bone marrow cell line?
    b. Research question: What is the effect of bidirectional communication (co-culture) of SH-SY5Y or SHEP-2 with HS-5 on the proliferation rate? Is this altered in hypoxic conditions?

2. Determine the effect of hypoxia and co-culture with HS-5 bone marrow cells on the VCR drug resistance of the SHEP-2 and SH-SY5Y neuroblastoma cell lines.

    a. Research question: How is the IC50 for vincristine in the SHEP-2 and SH-SY5Y cell lines affected by hypoxia?
    b. Research question: Does communication with HS-5 affect the drug resistance for vincristine in the SHEP-2 and SH-SY5Y cell line in normoxia and/or hypoxia?

2.1 Approach

The research project can, roughly speaking, be divided in three main phases, each thoroughly optimized before continuation to the next phase of the project. In the initial phase, the cellular proliferation of the SHEP-2 and SH-SY5Y neuroblastoma cell lines are determined and protocols for using the hypoxic chamber and creating a hypoxic microenvironment are optimized. Subsequently, the drug resistance behavior of the neuroblastoma monocultures is determined using an IC50 determination experiment in normoxia and hypoxia. The mono-culture experiments provide the necessary basis for designing the co-culture experimental conditions, in terms of seeding densities, incubation durations, VCR concentrations, and handling of hypoxic medium pre-equilibration. The co-culture study and evaluation of the HS-5 bone marrow cell characteristics in hypoxia form the final phase of the project.

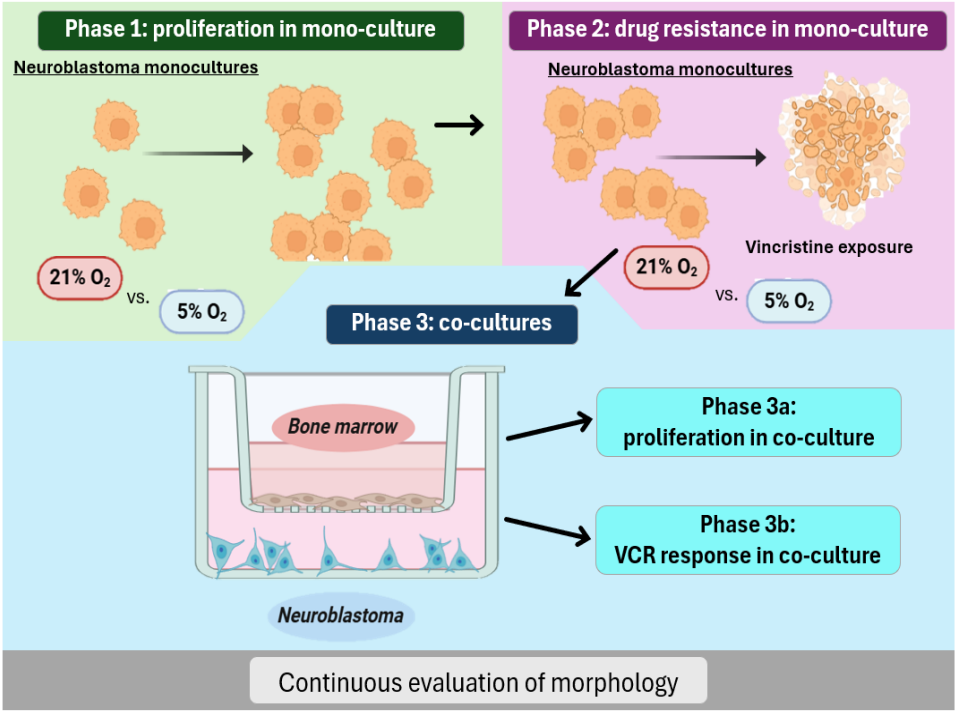

Figure 5: schematic representation of the study approach: 1) monoculture proliferative behavior is studied in hypoxia compared to normoxia; 2) monoculture drug response to vincristine is evaluated in hypoxia and normoxia; 3) all previous information on proliferation and drug resistance behavior is combined in the final phase of co-culture studies, evaluating the proliferation and drug response of neuroblastoma and bone marrow co-culture in hypoxia and normoxia.

3. Materials and methods

3.1 Cell culture

SH-SY5Y and SHEP-2 cells were cultured in DMEM High-glucose with L-glutamine (Capricorn, DMEM-HA) supplemented with 1% pen/strep (Capricorn, PS-B), 200 mM L-glutamine (Capricorn, GLN-B), 1% MEM non-essential amino acids (Gibco, 11140-050), 100 mM Sodium Pyruvate (Gibco, 11360070), and 10% Fetal Bovine Serum (FBS)(Sigma Aldrich, F7524).

For co-culture studies, HS-5 cells are used to resemble primary bone marrow mesenchymal stromal cells (BM-MSCs). Primary cells, isolated from donors, have a low proliferation rate, and lack homogeneity, which may result in experimental variation [115–117]. This mesenchymal stromal cell heterogeneity and associated variability in experimental results, may be reduced by using commercially available bone marrow-derived cell lines [115]. An example of an immortalized stromal cell line that can be used for in vitro models of the bone marrow microenvironment is HS-5. Twenty-seven immortalized clones, designated HS-1 to HS-27, were isolated from the stroma of a white, 30-year-old, male patient [118]. HS-5 is a fibroblast-like cell line demonstrating plastic adherence, cluster of surface differentiation marker (CD) expression, and fibroblastic morphology, resembling primary BM-MSCs [115–117]. HS-5 cells (ATCC, CRL-3611) were cultured in DMEM High-glucose with L-glutamine (Capricorn, DMEM-HA) supplemented with 1% pen/strep (Capricorn, PS-B), 100 mM Sodium Pyruvate (Gibco, 11360070), and 10% Fetal Bovine Serum (FBS)(Sigma Aldrich, F7524).

All experiments were performed using DMEM High-glucose with L-glutamine supplemented with 100 mM Sodium Pyruvate (Gibco, 11360070) and 10% Fetal Bovine Serum (FBS)(Sigma Aldrich, F7524) (referred to as Experiment DMEM).

3.1.1 Hypoxic cell culture

Prior to any exposure of cells to hypoxia or experimental conditions, cells were allowed to attach for a minimum of 24h in normoxic conditions. To establish hypoxic cell culture conditions, a modular incubator chamber (Billups-Rothenberg, MIC-101) was used. Cells in a well-plate or culture flask are placed on a tray in the hypoxic chamber containing a 100mm petri-dish with sterile milli-Q.

Subsequently, the chamber is tightly closed, using the O-ring clamp and the chamber is flushed with a gas mixture containing 5% O_2 and 5% CO_2 in nitrogen gas, for 4.5 minutes with a flow rate of 20 L/min using a single flow meter (Billups-Rothenberg, SFM-3001). The cylindrical shape of the chamber creates an even gas distribution. After flushing, the chamber is fully sealed using the in- and outlet tube-clamps, and the hypoxic chamber is placed in the standard incubator at 37°C.

3.1.2 Medium pre-equilibration

Culture medium in general contains oxygen. When placed in hypoxic conditions, it required a minimum of 24h for the medium to equilibrate to these hypoxic oxygen concentrations [119]. Therefore, if medium is used in hypoxic cell culture, the medium should be pre-equilibrated to hypoxic conditions, prior to the experiment. Medium pre-equilibration was performed by adding the required volumes of medium to the same well-format used for the subsequent experiment and placing these well plates in the hypoxic chamber 24h prior to the start of the experiment. After flushing the hypoxic chamber, it was placed either at 4°C in the fridge or at 37°C in the incubator, giving hypoxic pre-equilibrated medium (designated as PEMh). As a control, the same handling procedures were implemented but placing well-plates containing medium directly in the fridge or in the incubator (without use of the hypoxic chamber), at normoxic conditions, giving normoxic PEM (designated as PEMn). This control was included to account for any effects the pre-equilibration procedure might have on the quality of the medium.

3.2 Trypan blue cell counting assay to assess proliferation in monoculture

To assess the proliferation of the SH-SY5Y and SHEP-2 cells, cells were seeded in a 6-well plate at 10000 cells/cm^2 and 4200 cells/cm^2 for the SH-SY5Y and SHEP-2 cells, respectively. Cells were allowed to attach for 24h in normoxic conditions. Subsequently, cells were cultured for 48h in normoxic or hypoxic conditions with either standard pre-warmed Experiment DMEM or pre-equilibrated Experiment DMEM. After the culture period, cells were trypsinized and diluted in a 1:1 ratio with trypan blue (Gibco™ 15250061). Trypan blue is a cytotoxicity assay, used to determine the cell number and percentage of viable cells [120]. The assay is based on the principle that live cells present with an intact cell membrane and the trypan blue dye is impermeable, whereas for dead cells, the dye is permeable. Viable cells have a clear cytoplasm, while dead cells appear blue. After incubation, live cells were counted using the LUNA FL automated cell counter (Logos biosystems, L20001) using LUNA counting slides (Logos biosystems, L12001). To limit exposure of hypoxically cultured cells to high oxygen concentration, the cells are placed on ice after incubation with trypan blue until loading the samples in the counting slides, to reduce the metabolic activity of the cells in normoxic conditions. The analyzed imaged of the LUNA automated cell counter software are saved on an external hard drive and used to manually correct the total cell concentrations in case of miscounted cells. This manual correction was necessary due to the presence of small clusters of cells (especially for the SH-SY5Y cell line) that are not included in the automated counts, as well as errors in the number of dead cells due to wrongful cell counts as a result of some debris in the trypan blue solution. The experiment was performed in triplicates.

3.3 Trypan blue cell counting assay to assess proliferation in co-culture

To assess the proliferation of the SH-SY5Y and SHEP-2 cells in co-culture with HS-5 cells, neuroblastoma cells were seeded in the bottom well of a 12-well plate transwell system. The transwell system encompasses a standard tissue culture treated 12-well plate with in each well a movable, 12-mm diameter insert, containing a 10 μm thick polycarbonate membrane with 0.4 μm diameter pores (Corning, 3401). SHEP-2 cells were seeded at a density of 4200 cells/cm^2 and SH-SY5Y cells were seeded at a density of 11000 cells/cm^2. HS-5 cells were seeded in the transwell inserts at a density of 11000 cells/cm^2. As a control, to assess if the polycarbonate surface would affect the proliferative behavior of the HS-5 cells, a monoculture of HS-5 in the bottom well and HS-5 top transwell insert was established. To assess the proliferation of HS-5 in hypoxia compared to normoxia and compare the co-culture to neuroblastoma monoculture, HS-5 cells, SH-SY5Y cells, and SHEP-2 cells were seeded at 11000 cells/cm^2, 110000 cells/cm^2, and 4200 cells/cm^2 cells, respectively. Cells were allowed to attach for 24h at 37°C. Subsequently, medium for all conditions was changed, adding standard pre-warmed Experiment DMEM to the normoxic conditions and pre-equilibrated hypoxic Experiment DMEM to the hypoxic conditions. Hypoxic conditions were placed in the hypoxic chamber. The

chamber was flushed, and all cultures were incubated for 48h at 37℃. After the culture period, cells were trypsinized and diluted in a 1:1 ratio with trypan blue (Gibco™ 15250061). After incubation, live cells were counted using the LUNA-II automated cell counter (Logos biosystems, L40002) using LUNA counting slides (Logos biosystems, L12001), using the same method as previously described for the monocultures.

3.4 Morphology analysis

In addition to the proliferation analysis, cells were morphologically assessed for changes between normoxic and hypoxic culture conditions. After 48h culture, cells were fixated by incubating the cell culture with 4% paraformaldehyde (PFA) solution (prepared using PFA powder obtained from Sigma-Aldrich, 158127) for 15 minutes. Cells were subsequently washed two times with pre-warmed Hanks' Balanced Salt Solution (HBSS) (Gibco™ 14025092), after which the HBSS was replaced with fresh PBS before storage at 4℃. Cells were observed using a standard phase-contrast microscope.

3.5 Cell Titer Glo assay for IC50 determination in monoculture

To identify the IC50 value of vincristine for the neuroblastoma cell lines, cells were seeded in 96-well plates at 4200 cells/cm^2 and 9000 cells/cm^2 for SHEP-2 and SH-SY5Y, respectively and were allowed to adhere for 24h in normoxic conditions. For the treatment groups, cells were incubated for 24h with 100μL of 0.001, 0.01, 0.1, 1 or 10 μM vincristine (MedChemExpress, HY-N0488) in medium. As a control, cells were incubated with 100 μL of plain medium. After 48h exposure to the treatment or control condition, the plates are allowed to equilibrate to room temperature before addition of 100 μL of prepared CellTiter Glo Reagent (Promega, G7571). As a control for background luminescence, wells without cells containing solely medium and medium with the highest concentration vincristine are added (since the presence of a chemical compound may affect the background luminescence). The content is mixed for 2 minutes on an orbital shaker to induced lysis of the cells. Subsequently, the plate is incubated at room temperature for 10 minutes after which the contents of each well is translocated into a designated well of a white opaque 96-well plate and luminescence is recorded. The IC50 value is determined using sigmoidal curve fitting in the OriginLab software.

3.6 Assessment of the effect of co-culture condition on the IC50

To investigate the effect of the bi-directional communication of neuroblastoma cells and bone marrow cells in a co-culture setting on the drug resistance behavior of the neuroblastoma cells, the obtained results from the monoculture IC50 determination is used. For the co-culture, a 24-well plate transwell system (Corning, CLS3413) with a 10 μm thick polycarbonate membrane with 0.4 μm pores is used. In the bottom wells, SHEP-2 cells and SH-SY5Y cells were seeded at a density of 3000 cells/cm^2 and 9000 cells/cm^2, respectively. HS-5 cells were seeded in the transwell inserts at a density of 9000 cells/cm^2. For the monoculture controls, cells were seeded at the same densities in a standard 24-well plate. Cells are allowed to attach for 48h prior to adding any treatment. Subsequently, cells are incubated with 0 µM VCR or with the determined IC50 value of the monoculture study (distinct per cell type). Cells were incubated with the indicated treatments for 48h in normoxia and hypoxia. After incubation, the transwell inserts were translocated into a separate 24-well plate. A volume of Cell Titer Glo equal to the volume of culture medium is added to each well. The content is mixed for 2 minutes on an orbital shaker to induced lysis of the cells. Subsequently, the plate is incubated at room temperature for 10 minutes after which the contents of each well is translocated into a designated well of a white opaque 96-well plate and luminescence is recorded. For each condition incubated with VCR, the response in percentage viability is determined by normalizing the associated control condition (0 µM VCR) to 100 percent. This allows for a comparison of the monocultures and co-cultures and determine the effect of the co-culture on the percentage viability.

3.7 Statistical analysis

All experiments were repeated three times (biological replicates, n=3), with a minimum of three replicates for each experimental condition (technical replicates) per experiment, unless indicated differently. For data analysis, SPSS 13.0 software was used. To compare two groups, the t-test was applied. For the comparison between more groups, one-way ANOVA was used. All results are indicated at a means $\pm$ standard error. Differences were considered to be significant when $P<0.05$, and highly significant when $P<0.01$.

4. Results

4.1 Cellular morphology and distribution across cell culture surface differs per cell line

Cell morphology is evaluated based on the cellular shape and relative size, visually. Figure 6 shows morphological images of standard normoxic culture of SHEP-2, SH-SY5Y, and HS-5 cells. HS-5 cells have a fibroblast-like morphology (fig. 6A). They are very evenly distributed across the substrate surface (fig.6B). The SHEP-2 cells present as large, flattened cells that firmly attach to the culture substrate (fig. 6C). This is a characteristic of the MES-type or also called S-type neuroblastoma cell lines [121]. SHEP-2 cells present regions with lower and higher density of cells, with only mono-layer formation and relative spread over the surface (fig. 6D).

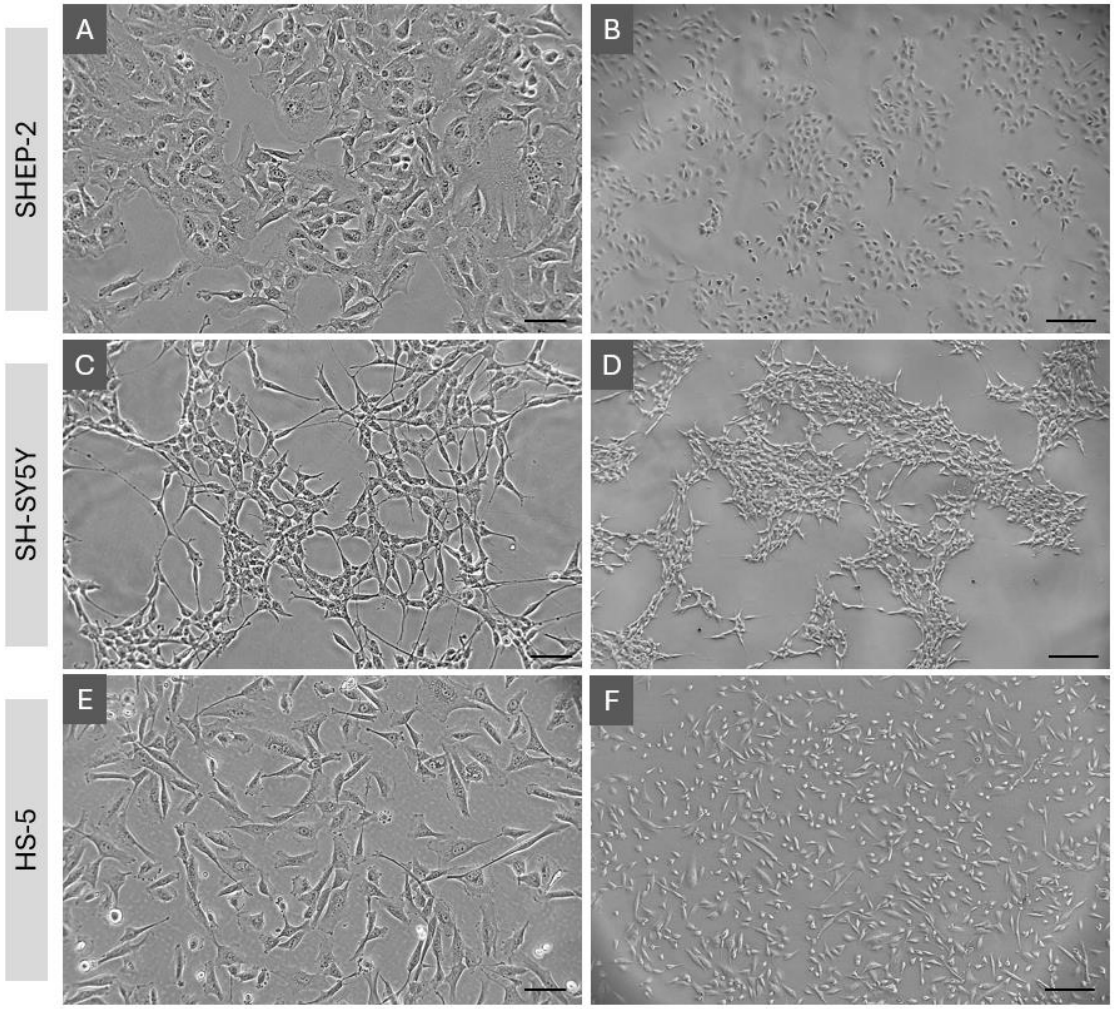

Figure 6: Cell distribution of HS-5, SHEP-2 and SH-SY5Y over the substrate of a standard T25 culture flask. (A, B) HS-5 (p+6, seeding density 8500 cells/cm2) show a uniform distribution across the surface. There is no cluster formation. (C,D) SHEP-2 (p24, seeding density 4200 cells/cm2) show a combination of a generally equal distribution and formation of cell cluster, always in the form of mono-layers. Since the SHEP-2 are more flattened and substrate adherent, they show with less contrast under the microscope in comparison to the other cell lines. (E, F) SH-SY5Y (p+20, seeding density 10000 cells/cm2) show specific cluster formation. In denser regions, cells start growing in multi-layers and clusters. At higher densities, SH-SY5Y cells start forming spheroids. Left column: 10x objective, scalebar = 25 µm; Right column: 4x objective, scalebar = 75 µm.

The SH-SY5Y cells present as more rounded, neuroblast-like cells (fig 6E). This is characteristic of the ADRN- or N-type cell lines [121,122]. The SH-SY5Y cells grow in focal aggregates (fig 6F). In the center of these clusters, cells tend to grow on top of each other, forming multilayers. As the cells attach more poorly to the substrate clumps of viable cells may detach and float in the culture medium. The SH-SY5Y cells show multiple fine and delicate processes, called tunnelling nanotubes (TNTs). These TNTs have been discovered to form connections between distant cells. They are thin (50 to 700 nm) and can

extent to a length from tens up to hundreds of microns (on average 20-100 um). TNTs allow for the intercellular transport of cellular components and molecules, such as organelles, pathogens, ions, proteins, DNA, mRNA, and micro-RNA [123]. In addition, they form a way of electrical coupling of cells [124].

4.2 The proliferation of SHEP-2 and SH-SY5Y cells is increased in chronic exposure to hypoxia

The proliferation of SHEP-2 and SH-SY5Y cells in hypoxia in comparison to normoxia was evaluated using a trypan blue cell counting assay. Cells were cultured for 48 hours in: 1) ambient conditions (normoxia) with standard Experiment DMEM; 2) normoxia with medium that was pre-equilibrated for 24h at ambient conditions in the incubator at 37℃; 3) hypoxia with standard Experiment DMEM; 4) and hypoxia with 24h medium equilibration at 37℃ and 5% O_2. For each cell line, the proliferation in the form of the total cell numbers per cm^2 was normalized to percentages, in which the control (normoxic cell culture with standard medium) was normalized to 100%. Experiments were repeated three times independently (n=3). According to the trypan blue assay and cell counting, proliferation (normalized to the control) for SH-SY5Y cells was $67.3 \pm 8.4\%$, $156.2 \pm 12.1\%$, and $143.9 \pm 14.8\%$, respectively (figure 7). For the SHEP-2 cells, the proliferation (normalized to the control) was $77.0 \pm 7.4\%$, $126.5 \pm 9.9\%$, and $95.0 \pm 8.6\%$, respectively. For both SH-SY5Y and SHEP-2, the hypoxic culture condition results in significantly higher (P=0.001) proliferation compared to the normoxic culture. However, use of the pre-equilibrated medium (prepared at ambient conditions for normoxic cell culture and prepared using the hypoxic chamber for hypoxic cell culture) results in a decrease of the overall proliferation for both cell lines in normoxia as well as hypoxia. This also complicates the assessment of the effect of hypoxia on the proliferation of the cells. Overall, the results indicate an increase in the proliferation rate of both SHEP-2 and SH-SY5Y cells in hypoxia and a negative influence of the pre-equilibration process.

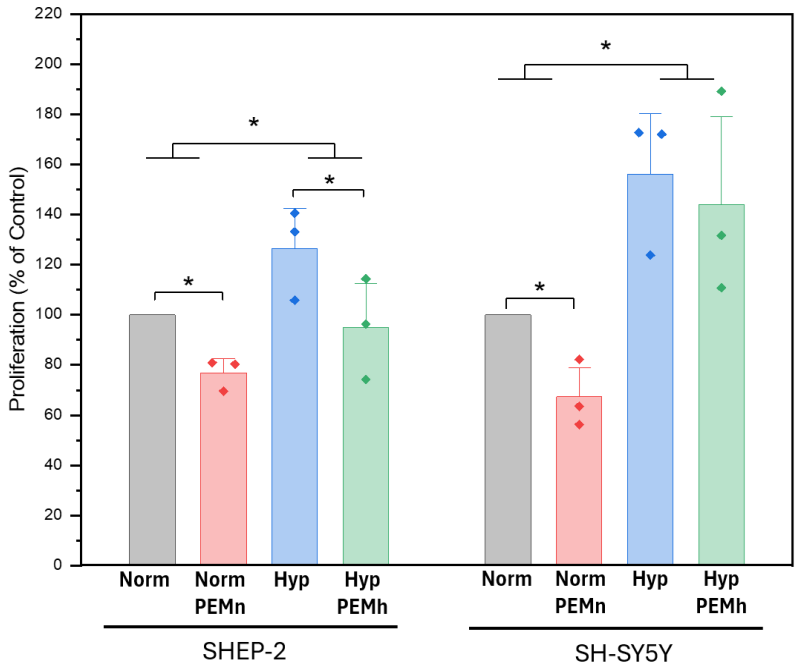

*Figure 7: Hypoxia influences the proliferation of SH-SY5Y and SHEP-2 cells. Cells are grown in normoxic (~21% O_2) and hypoxic (~5% O_2) conditions for 48 h with and without hypoxic or normoxic PEM (pre-equilibration at 37℃). The normoxic condition is normalized to 100%. Norm = Normoxia, Norm PEMn = Normoxia with normoxically pre-equilibrated medium, Hyp = Hypoxia, Hyp PEMh = hypoxia with hypoxically pre-equilibrated medium. Data represented as mean of independent experiments (individual marks), overall mean (bar) and SD (n=3). Statistical significance *P<0.05, **P<0.01, if nothing indicated, then it was found not significant.*

There is not yet sufficient data available when it comes to the effect of hypoxia on neuroblastoma tumor cell proliferation [13], however, these findings coincide with previous studies that have shown increased proliferation for SH-SY5Y in hypoxic conditions [125,126] as well as for SHEP-2 cells [127].

For SHEP-2 culture, a 1.4-fold increase in hypoxia was observed compared to normoxia when cells were exposed to 1% O_2 for 24 hours using a modular incubator chamber. It has also been shown that neuroblastoma tumor cells survive and proliferate in hypoxic conditions [9]. In a conflicting study however, hypoxic conditions have decreased the cellular proliferation in SH-SY5Y cells [128]. Nonetheless, when considering tumor cells in general, it is generally acknowledged that cancer cells increase proliferation in hypoxia [8,14,39].

On the other hand, the proliferation rate is influenced by the preparation of PEM (figure 7). Adding medium equilibrated for 24h at 37℃ at ambient oxygen conditions to cells cultured in normoxic atmosphere (PEMn), results in a significant decrease of the proliferation for both SHEP-2 (P=0.015) and SH-SY5Y (P=0.038). Adding hypoxically prepared pre-equilibrated medium (PEMh) to cells cultured in hypoxia, the same trend is observed, despite the lack of statistical significance. It was hypothesized that this decrease in proliferation was caused by the pre-equilibration process itself. It is described in literature that equilibration of medium at 37℃ can cause degradation of some components in the culture medium, including pyruvate and some amino acids, such as L-glutamine [119]. In addition, literature states that the degradation of L-glutamine can result in release of cytotoxic ammonia as a byproduct, which could result in decreased cell viability and proliferation [129]. This effect might be involved in the observed decrease in proliferation for the SHEP-2 and SH-SY5Y cells.

Therefore, it was decided to perform the pre-equilibration of the medium at 4℃ in subsequent experiments. Similar to previous experiments, as a control, medium was "pre-equilibrated" by placing medium at ambient conditions at 4℃ (PEMn) and medium was pre-equilibrated using the hypoxic chamber at 4 ℃ to prepare hypoxic medium (PEMh). Experiments were repeated three times independently (n=3). According to the trypan blue assay and cell counting, the proliferation (normalized to the control) for SH-SY5Y cells was $106.5 \pm 4.2\%$, $133.0 \pm 5.4\%$, $146.1 \pm 15.6\%$ and $186.1 \pm 18.8\%$ for, respectively the normoxic culture with PEMn, the normoxic culture with PEMh, the hypoxic culture, and the hypoxic culture with PEMh (figure 8). For the SHEP-2 cells, the proliferation (normalized to the control) was $104.0 \pm 6.9\%$, $120.1 \pm 9.7\%$, $148.0 \pm 7.0\%$ and $198.6 \pm 8.6\%$, respectively.

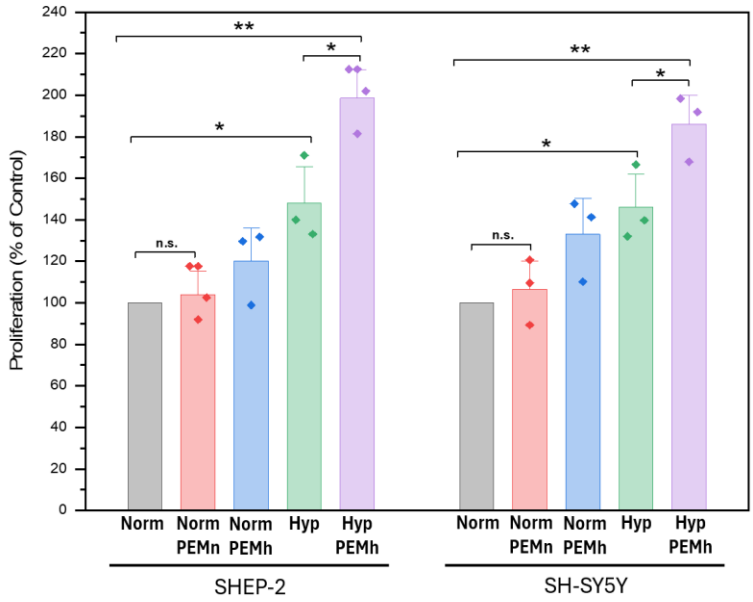

*Figure 8: Hypoxia influences the proliferation of SH-SY5Y and SHEP-2 cells. Cells are grown in normoxic (~20% O_2) and hypoxic (~5% O_2) conditions for 48 h with and without hypoxic or normoxic PEM (pre-equilibration at 4℃). The normoxic condition is normalized to 100%. Normoxic pre-equilibration of the medium at 4℃ does not lead to a decrease in proliferation. The hypoxic condition with hypoxic PEM is now much increased compared to the normoxic culture condition. Norm = Normoxia, Norm PEMn = Normoxia with normoxically pre-equilibrated medium, Norm PEMh = Normoxia with hypoxically pre-equilibrated medium. Hyp = Hypoxia, Hyp PEMh = Hypoxia with hypoxically pre-equilibrated medium. Data represented as mean of independent experiments (individual marks), overall mean (bar) and SD (n=3). Statistical significance *P<0.05, **P<0.01, n.s. not significant.*

When the medium is pre-equilibrated at 4℃, the difference in proliferation between the normoxic condition with standard pre-warmed Experiment DMEM and medium kept at ambient atmosphere and 4℃ in a 12-well plate before warming, is no longer significant (P=1 for SHEP-2, and P=1 for SH-SY5Y). In addition, the proliferation of SHEP-2 and SH-SY5Y cells in hypoxic conditions is further increased using pre-equilibrated medium hypoxically prepared at 4℃, in comparison to the use of non-equilibrated medium (P=0.023 for SHEP-2 and P=0.021 for SH-SY5Y).

Another culture medium characteristic that is influenced by temperature, is the oxygen solubility and the oxygen diffusion coefficient. The concentration of dissolved oxygen in medium is approximately doubled when medium is cooled from 37℃ to 5℃ [130]. In contrast, the oxygen diffusion is decreased at lower temperatures and the flux of oxygen is increased by ~15% when the temperature is increased from 25℃ to 37℃ [131,132]. This means that pre-equilibration of the medium at 4℃ may result in a higher concentration of remaining oxygen or the necessity of a longer pre-equilibration time. If the remaining oxygen concentration in the medium would be higher after pre-equilibration at 4℃, cells would be exposed to less hypoxic conditions, which in turn would result in a smaller difference in proliferation between normoxia and hypoxia. However, this is not observed. Looking at the results, we observe a slight but significant increase in proliferation when using hypoxic PEM on normoxically cultured cells. This indicates that the gradual change from a hypoxic state back to normoxia does not negatively affect cell proliferation. Cells appear to increase their proliferation for the duration of hypoxic exposure, to subsequently restore to normal proliferation when the oxygen concentration in the medium changes to normoxia.

For the HS-5 cells, there is no statistically significant difference in proliferation between normoxia and hypoxia on either a standard polystyrene culture surface of a standard well-plate or the polycarbonate transwell insert (figure 9). The proliferation of HS-5 cells was found to be $103.6 \pm 16.5(n = 3)\%$ in hypoxia compared to normoxia. The polycarbonate surface of the transwell insert does have a significant (P<0.05) effect on the proliferation. It shows a decrease to $64.9 \pm 0.02(n = 3)\%$ and $62.6 \pm 3.7(n = 3)\%$ in normoxia and hypoxia, respectively in comparison to standard normoxic culture.

It is suggested by the transwell insert manufacturer, that the cellular proliferation on the treated polycarbonate surface may differ from the proliferation in a standard tissue treated polystyrene well plate [133]. This should be kept in mind when deciding on seeding densities for co-culture experiments. Cells should be seeded at a higher density, to reach the same confluency over a set period of time.

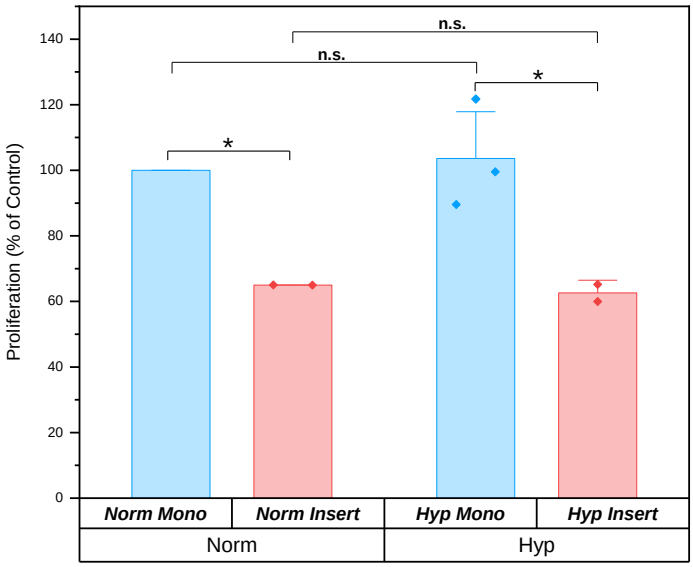

*Figure 9: The polycarbonate surface of the transwell insert affects the proliferation of HS-5 cells. Hypoxia does not affect the proliferation of HS-5 cell proliferation in either a standard polystyrene well plate or on the polycarbonate insert. Norm = Normoxia, Norm Mono = HS-5 proliferation in normoxia on standard polystyrene surface, Norm Insert = HS-5 proliferation in normoxia on polycarbonate transwell insert, Hyp = Hypoxia, Hyp Mono = HS-5 proliferation in hypoxia on standard polystyrene surface, Hyp Insert = HS-5 proliferation in hypoxia on polycarbonate transwell insert. Statistical significance *P<0.05, **P<0.01, n.s. not significant, n=3.*

The results combined showed that hypoxia influences the proliferation of SHEP-2 and SH-SY5Y neuroblastoma cells in monoculture. The proliferation is significantly (P=0.0005 for SH-SY5Y and P=0.0001 for SHEP-2) increased in hypoxia using pre-equilibrated medium in comparison to normoxia. The results also indicate the importance of using hypoxically pre-equilibrated medium (PEMh) for the hypoxic cultures and the necessity of performing the pre-equilibration at 4℃ to prevent possible

medium degradation. Finally, it was shown that the HS-5 proliferation is not affected by hypoxia (P=1), while the polycarbonate surface of the transwell insert causes a significant decrease (P=0.04 in normoxia and P=0.02 in hypoxia) of the proliferation.

4.3 The morphology of SHEP-2 and SH-SY5Y cells is not altered in hypoxia

The SHEP-2 cells present a healthy and ideal morphology in hypoxia and no clear differences between the various conditions (figure 10, left column). Hypoxia, thus, does not affect SHEP-2 morphology. For the SH-SY5Y cells, also, no clear differences in morphology are observed (figure 10, right column). SH-SY5Y cells demonstrate a healthy and ideal morphology in hypoxic conditions, indicating hypoxia does not affect the appearance of the neuroblastoma cell line. Based on these findings, both cell lines tolerate the hypoxic cell culture condition well. This supports the previous results of increased proliferation.

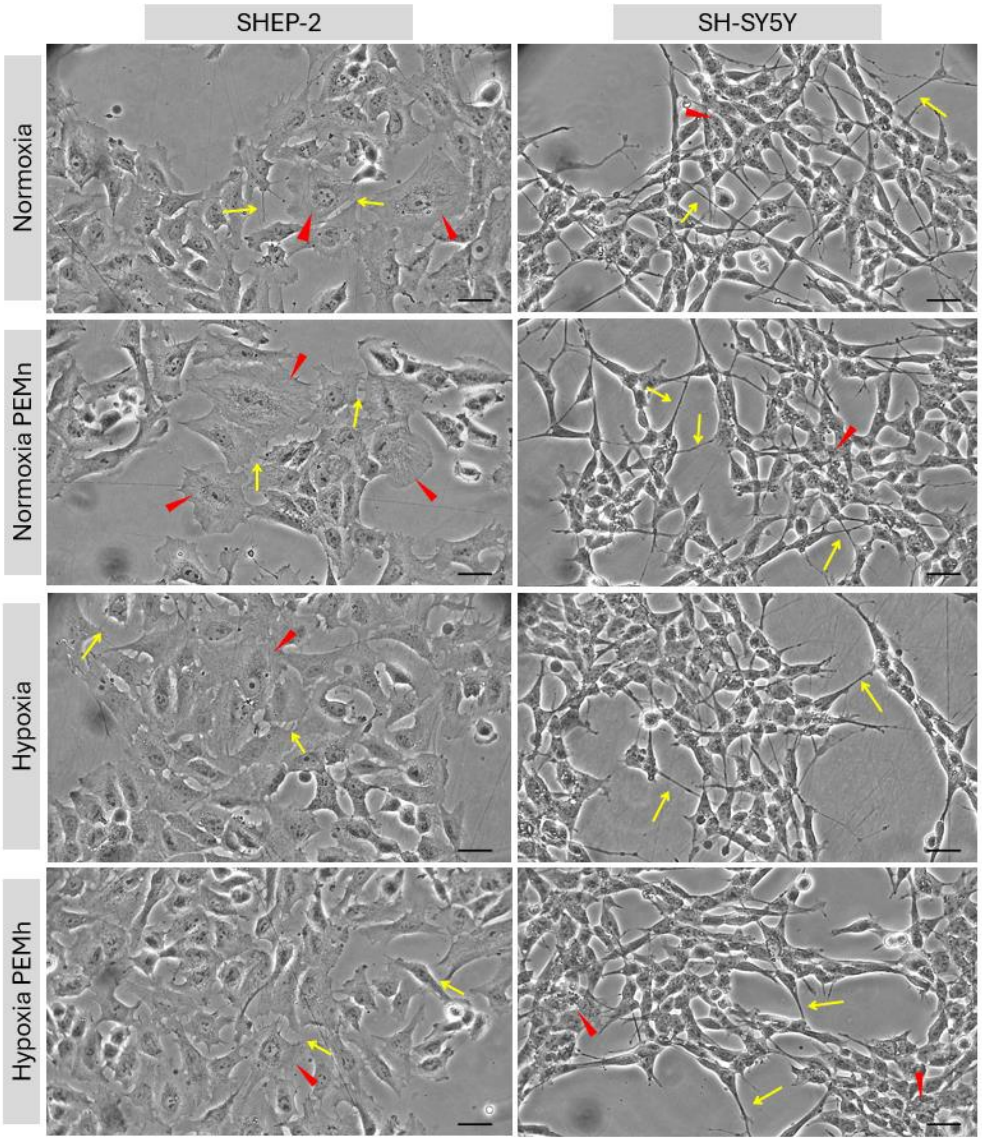

Figure 10: Left) Morphology images of SHEP-2 cells at passage p30 in normoxia in comparison to normoxia with pre-equilibrated medium and hypoxia in comparison to hypoxia with pre-equilibrated medium (top to bottom). Cells seeded at 4200 cells/cm² density cultured for 72h in total. Cells are properly attached to the culture substrate and multiple cells very vastly flatten over the surface (red pointed arrows). Cells form clear connections with adjacent cells through very fine protrusions (yellow arrows); Right) Morphology images of SH-SY5Y cells at passage p+21 in normoxia in comparison to normoxia with pre-equilibrated medium and hypoxia in comparison to hypoxia with pre-equilibrated medium (top to bottom). Cells seeded at 10000 cells/cm² density cultured for 72h in total. In denser regions of the clusters, cells appear to grow on top of each other (red pointed arrows). Cells form long, very fine TNTs (yellow arrows). Scalebar 10 µm.

In this study, an oxygen concentration of 5% is used to mimic the bone marrow microenvironment oxygen tension. As previously described, the oxygen concentration in the bone marrow presents a gradient from 2 – 7% [4,5,40], with a higher oxygen concentration in the endosteal niche and a lower oxygen concentration in the center of the bone marrow. However, it is yet unclear whether the neuroblastoma tumor cells reside in a specific niche, and it is suggested that both niches are involved in the malignant behavior of the cancer cells . 5% oxygen was suggested as more physiologically relevant [6,7,12,134]. In addition, the initial results show an effect of 5% oxygen on the proliferation of neuroblastoma cells, without affecting the morphology. Therefore, it was decided to use 5% oxygen in all subsequent experiments.

4.4 The tolerance to VCR is increased in hypoxia for both neuroblastoma cell lines

SHEP-2 and SH-SY5Y cells were allowed to attach in normoxia for 24h and subsequently treated with a range of VCR concentrations (0.001 – 100 uM) for 48h in either normoxia or hypoxia. A dose-dependent decrease of the relative cell viability was observed (figure 11). Experiments were repeated three times independently(n=3). According to the CellTiter Glo assay, the IC50 of VCR in SHEP-2 cells was found to be 0.031±0.008 µM for 48h incubation in normoxia and 0.096±0.02 µM for 48h incubation in hypoxia. The IC50 of VCR in SH-SY5Y cells was found to be 0.0019±0.0004 µM and 0.0058±0.001 µM for 48h incubation in normoxia and hypoxia, respectively. Both the SHEP-2 and SH-SY5Y cells, show a significant (P<0.05) 3-fold increase in the tolerance for VCR in hypoxia when compared to normoxia.

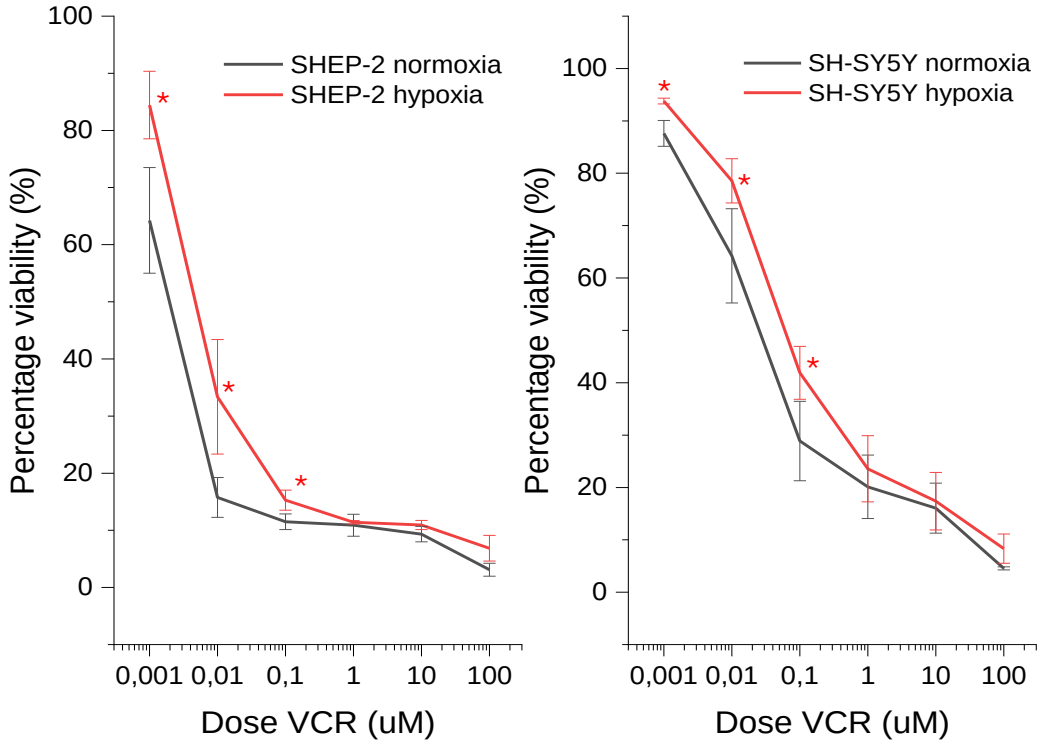

*Figure 11: SHEP-2 and SH-SY5Y neuroblastoma cells were treated with a range of VCR concentrations. The viability for both cell lines shows a dose-dependent reduction. Both cell lines show a shift of the dose-response curve to the right when exposed to hypoxia (red line) in comparison to normoxia (black line). Data represented as mean±SD, n=3. Statistical significance *P<0.05.*

These results indicate an influence of hypoxia on the drug resistance behavior in monoculture. For both neuroblastoma cell lines, an increase in the IC50 of VCR is observed when exposed to hypoxia. This designates the percentage cell viability at the same VCR concentration remains higher in hypoxia compared to normoxia, indicating a greater drug resistance. This coincides with the hypothesis that hypoxia increases the malignant behavior of tumor cells, including drug resistance [11,60,61].

4.5 Treatment with vincristine results in the disappearance of TNTs in the SH-SY5Y cell line

When incubated for 48h with different concentrations of VCR, the morphology clearly changes (figure 12). For the SH-SY5Y cells, the first morphological alteration is clearest visible at a 0.01 µM VCR concentration, showing a clear reduction of the length and number of TNTs. Additionally, the cellular bodies are slightly smaller. Furthermore, differences between normoxic and hypoxic culture can be observed. The cellular density is higher in hypoxia compared to normoxia, as expected from the previous experimental findings of an increase in proliferation. More importantly, at the 0.1 µM VCR concentration, the SH-SY5Y cells in hypoxia still show formation of TNTs, whereas these are no longer being formed in normoxia. This corresponds to the increase in the IC50 value and a greater tolerance for the VCR in hypoxia.

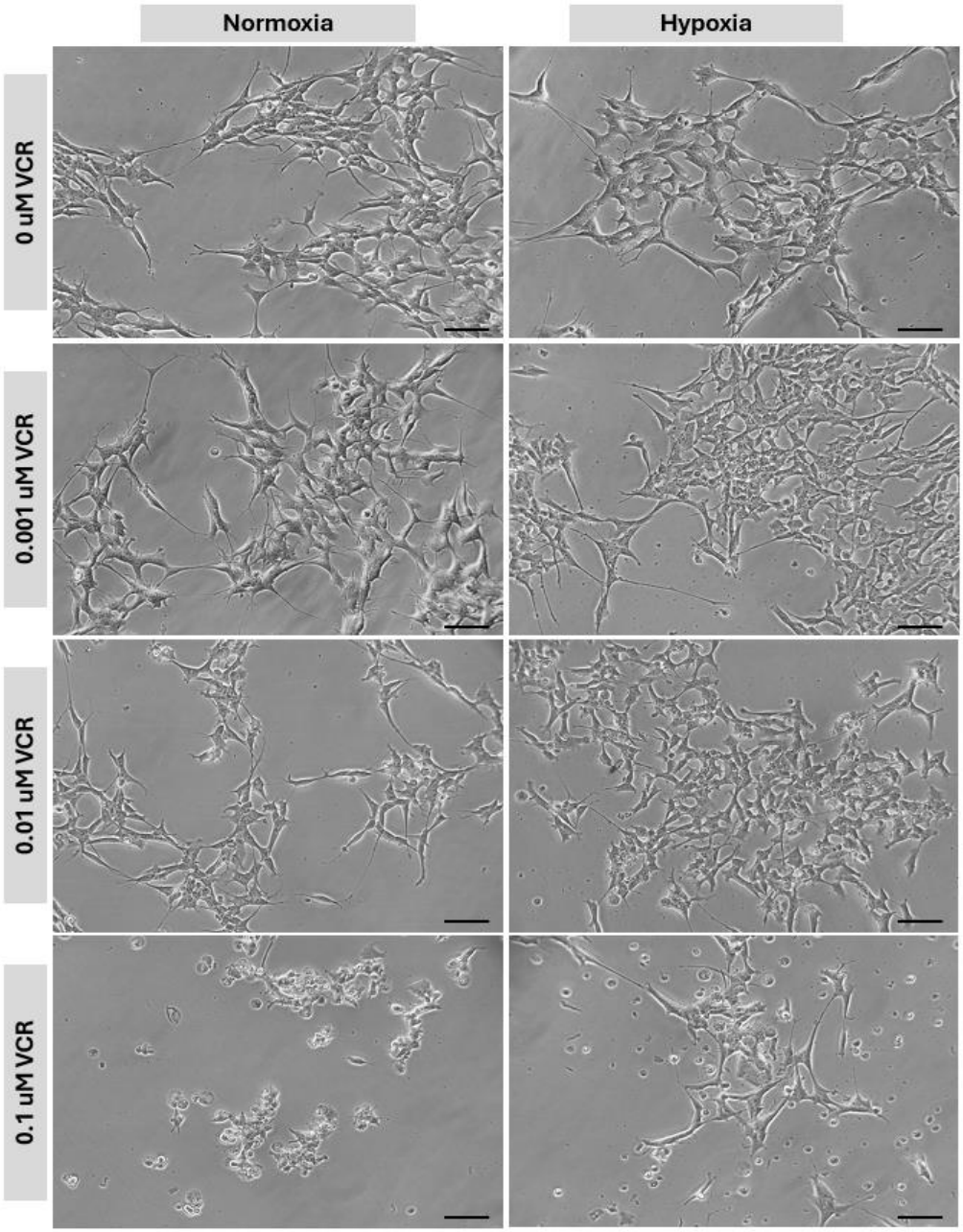

Figure 12: Representative images of SH-SY5Y cells (at passage 34, seeding density 11 000 cells/cm^2) allowed to attach for 24h and subsequently exposed for 48h to increasing VCR concentration (0 µM (control) – 0.1 uM). At a concentration of 0.001 µM VCR, the cellular morphology is relatively unchanged. At a concentration of 0.01 µM VCR the loss and decrease in length of the SH-SY5Y TNTs can be observed. At a concentration of 0.1 µM VCR the cell bodies have reduced in size and dead cells are visible in the clusters of cells that remain attached to the culture surface. Objective 10x, scalebar 25 µm.

The changes in morphology for the SHEP-2 (figure 13) cell line already appear at the lowest VCR concentration of 0.001 µM VCR. Cells are less stretched over the culture surface. Further morphological changes that are observed include detachment and dead cells (spherical and floating). At a 0.01 µM VCR concentration, the number of adherent cells with a normal morphology is drastically reduced. This corresponds with the results from the IC50 determination. However, still at high concentrations of VCR, some cells present a healthy morphology, being flattened, and attached to the culture surface. As such, the SHEP-2 cells differ from the SH-SY5Y cells. At the higher VCR concentration (≥0.1 µM VCR), SH-SY5Y remains a higher percentage viability, but all cells have changed in morphology with loss of TNTs and reduction if the size of the cell body. At the same VCR concentration, the number of SHEP-2 cells that appear viable is much lower compared to SH-SY5Y, however, most of the few SHEP-2 cells that remain, present a normal morphology.

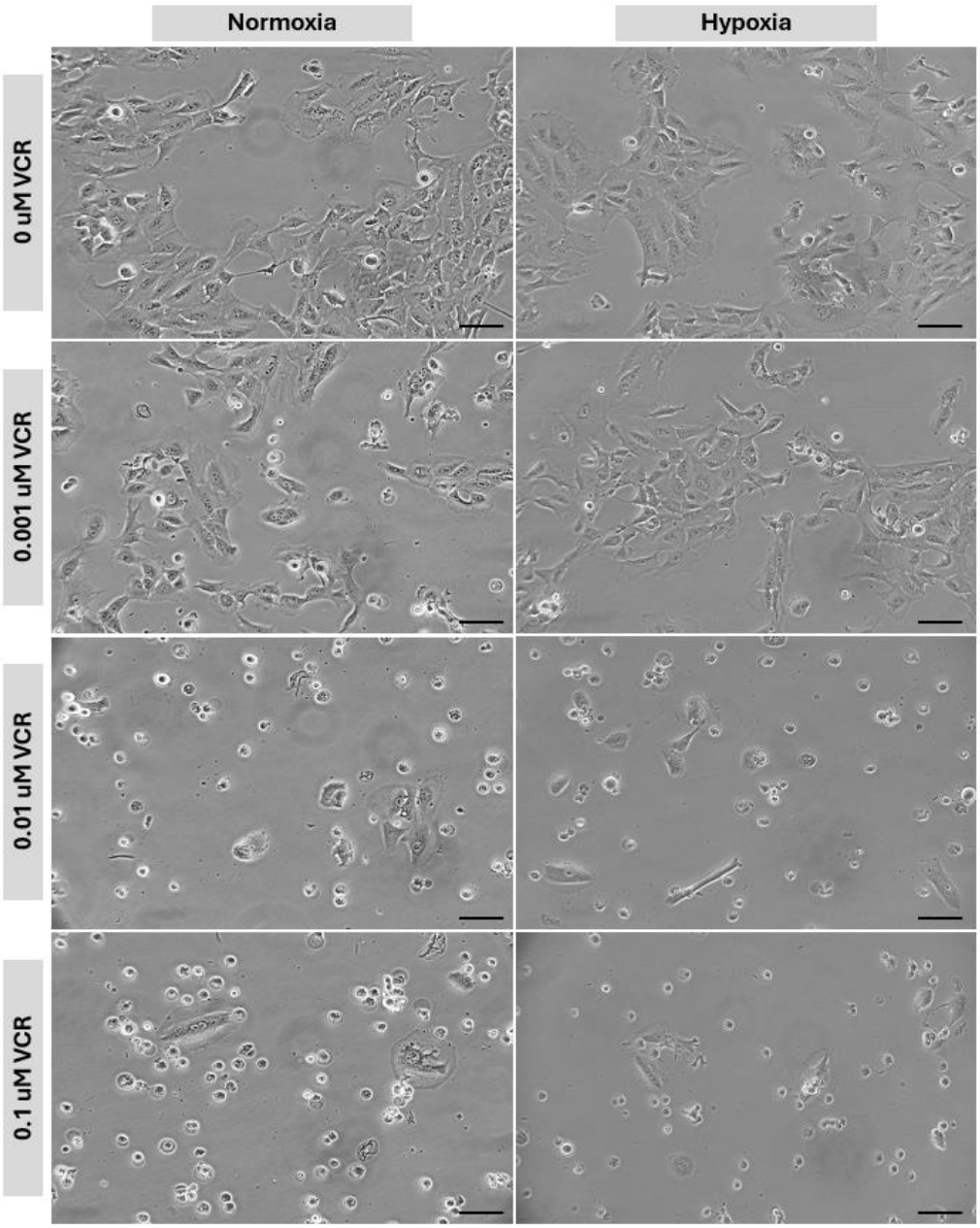

Figure 13: Representative images of SHEP-2 cells (at passage 44, seeding density 4200 cells/cm^2) allowed to attach for 24h and subsequently exposed for 48h to increasing VCR concentration (0 µM (control) – 0.1 uM). At a concentration of 0.001 µM VCR, cells have (partially) detached and dead cells are visible as floating, rounded cells. The majority of cells remain attached with a flattened morphology. At a 0.01 µM VCR concentration, the number of attached cells has drastically reduced and mostly round, dead cells are visible. At 0.1 µM concentration and higher (not shown in this figure panel) still few SHEP-2 cells remain viable with a normal, healthy morphology of flattened and attached cells. Objective 10x, scalebar 25 µm.

4.6 SHEP-2 and SH-SY5Y cells proliferate faster in co-culture with HS-5 cells in hypoxia

To assess the effect of the co-culture with HS-5 bone marrow cells on the proliferation of SHEP-2 and SH-SY5Y neuroblastoma cells, cells were incubated for 48h in monoculture and in a co-culture, using a transwell co-culture system. Cells were exposed to normoxia and hypoxia. Experiments were repeated three times independently (n=3).In normoxia, the proliferation was decreased in co-culture to $71.6 \pm 2.3\%$ and $74.2 \pm 1.8\%$ for SHEP-2 and SH-SY5Y cells, respectively (figure 14) in comparison with the mono-culture. In hypoxia, the proliferation of the monocultures is increased to $168.7 \pm 24.7\%$ and $151.7 \pm 9.8\%$ for SHEP-2 and SH-SY5Y, respectively, in comparison with the mono-culture in normoxia. This agrees with previous experimental results. The co-culture in hypoxia shows a further increase in proliferation to $212.9 \pm 8.2\%$ for SHEP-2 and $200.8 \pm 14.2\%$ for SH-SY5Y. The differences in proliferation between the monoculture and co-culture in both normoxia as well as hypoxia were found to be statistically significant.

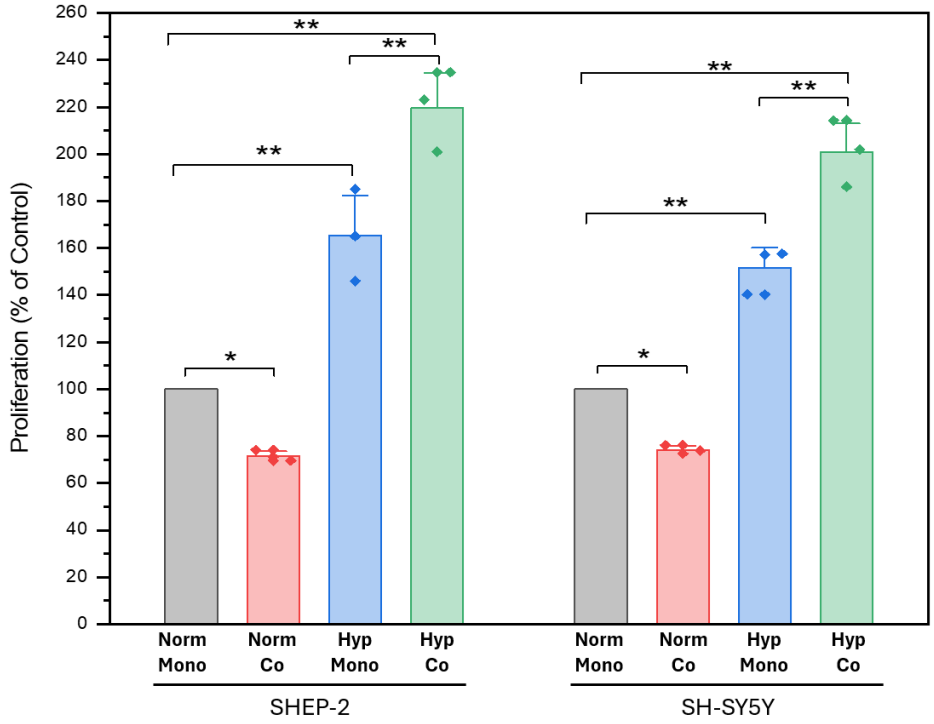

*Figure 14: Proliferation of SHEP-2 and SH-SY5Y in co-culture. The bi-directional communication with HS-5 cells affects SHEP-2 and SH-SY5Y proliferation in normoxia and in hypoxia. In normoxia, the proliferation is decreased, whereas in hypoxia the proliferation is increased in comparison to the monoculture conditions. Norm Mono= Normoxia Monoculture, Norm Co = Normoxia Co-culture, Hyp Mono = Hypoxia Monoculture, Hyp Co = Hypoxia Co-culture. Statistical significance *P<0.05, **P<0.01, n.s. not significant, n=3.*

These results show that the co-culture with HS-5 cells influences the proliferative behavior of both neuroblastoma cell lines, with a significant (P=0.01723 for SHEP-2 and P=0.03995 for SH-SY5Y) decrease in normoxia and a significant (P=0.0056 for SHEP-2 and P=0.0007 for SH-SY5Y) increase in hypoxia. It is generally suggested that co-culture with bone marrow cells contributes to tumor malignancy by an increase in proliferation [3,135]. However, this is not observed for the normoxic co-culture of HS-5 and neuroblastoma cells, which show a decrease in proliferation.

It is predicted that introducing the transwell insert in the bottom well, may cause for proteins in the medium to stick to the plastic of the transwell insert. It is hypothesized that this can result in a decrease of the concentration of medium components that is available for the cell culture in the well, which may negatively affect the proliferation of the cells. However, in a previous experiment, HS-5 cells were cultured in a standard 12-well plate as well as in the bottom well of a 12-well transwell system in a monoculture condition (just insertion of the transwell insert, only in presence of HS-5 cells). This experiment has shown that the proliferation in each set-up was equal and the insertion of the transwell insert did not reduce the proliferation (supplementary S4). Therefore, the observed reduction in proliferation for the co-culture condition is regarded as an effect of the bi-directional communication between the HS-5 and neuroblastoma cells.

A study by Chulpanova et al. (2020), has shown a small decrease in proliferation of SH-SY5Y neuroblastoma cells, PC3 cells and A549 cells when exposed to conditioned medium of adipose-tissue-derived-MSCs, in comparison to the use of fresh DMEM [136]. The study focused on the proliferation reduction in presence of MSCs with interleukin 2 overexpression. However, also a slight decrease in proliferation was observed for normal MSCs. To the best of my reckoning, no further studies were published on the proliferative behavior of neuroblastoma cells in co-culture with bone marrow cells. However, in for instance ovarian cancer, the opposite was observed in the form of increased proliferation in co-culture [80]. In contrast however, BMSC derived extracellular vesicles were observed to inhibit colorectal cancer progression [137]. In breast cancer, cell lines MDA-MB-232, MCF-7 and ZR-75-1 showed a 3-fold increase in proliferation in presence of adipose derived cells whereas the proliferation was not increased (and even slightly decreased) in presence of BMSCs [138]. Other studies again state the increase of breast cancer cell proliferation by exosome excretion from BMSCs [139]. Therefore, the existing literature is inconsistent and conflicting and does not provide a present reasoning for the observed findings.

On the other hand, in hypoxia an increase in proliferations is observed when SH-SY5Y and SHEP-2 cells are in co-culture with HS-5 cells. This is in line with the hypothesis. To the best of my knowledge, no literature is available on the proliferation behavior of neuroblastoma cells in co-culture with BMSCs in hypoxia. However, in lung cancer, EVs from hypoxically exposed BMSCs induced increased proliferation and EMT [140,141]. Similarly, in hepatocarcinoma cancer cells increased proliferation was observed as a result of hypoxic BMSC-derived exosomal micro-RNA [142]. The findings also follow the more generally accepted hypothesis that co-culture with bone marrow resident cells in hypoxia promotes the malignant behavior of cancer cells.

HS-5 proliferation is increased in hypoxia in co-culture with SHEP-2 as well as in co-culture with SH-SY5Y (supplementary S5), in comparison to the monoculture. Overall, these results indicate the co-culture of neuroblastoma cells and bone marrow cells results in changes in the proliferation of both cells, showing a decrease in proliferation of the neuroblastoma cells in co-culture with bone marrow cells in normoxia. In contrast, the proliferation of neuroblastoma cells is increased in co-culture in hypoxia, indicating the importance of the microenvironmental cue of oxygen tension.

4.7 Co-culture conditions in normoxia or hypoxia do not influence the cellular morphology of SHEP-2 and SH-SY5Y cells

When comparing the cellular morphology after 48h incubation in monoculture and co-culture, there are no clear differences for any of the cell lines (figure 15). SHEP-2 cells are properly attached to the culture surface, showing a large, flattened morphology. The SH-SY5Y cell line shows a stellate morphology with long and abundant TNTs in each culture condition. The HS-5 cells present a fibroblast like morphology of large, flat, and spindle-shaped cells with clear processes extending out of the cell body. Differences in density between mono- and co-culture conditions were somewhat, but not clearly visible. Based on the morphology, the co-culture condition was well-tolerated by each of the cell lines.

Importantly, this co-culture study uses the SH-SY5Y and SHEP-2 neuroblastoma cell lines, isolated from a bone marrow biopsy taken from a four-year-old female with neuroblastoma. In contrast, the HS-5 bone marrow cell line is isolated from the stroma of a white, 30-year-old, male patient. There is thus a difference in age and gender. Research has shown that infant BMSCs present a faster proliferation and increase in doubling times compared to adult BMSCs [143]. Infant BMSCs in addition exhibit a lower level of senescence, based on gene expression. Moreover, child BMSCs have a greater differentiation potential in chondrogenesis. Finally, gene expression has shown a higher expression of osteogenic, tenogenic, hepatogenic and adipogenic genes in differentiated infant BMSCs, but a decreased adipogenic differentiation potential. When comparing the adult and infant bone marrow mesenchymal niche, the infant BM niche was characterized by more primitive subsets of BMSCs with high expression of platelet-derived growth factor, Jagged-1 and CXCL-12 [144]. Interestingly, CXCL-12 has proven to be involved in neuroblastoma tumor cell dormancy [10,38]. Therefore, the co-culture response of the neuroblastoma cells might differ when making use of infant BMSCs.

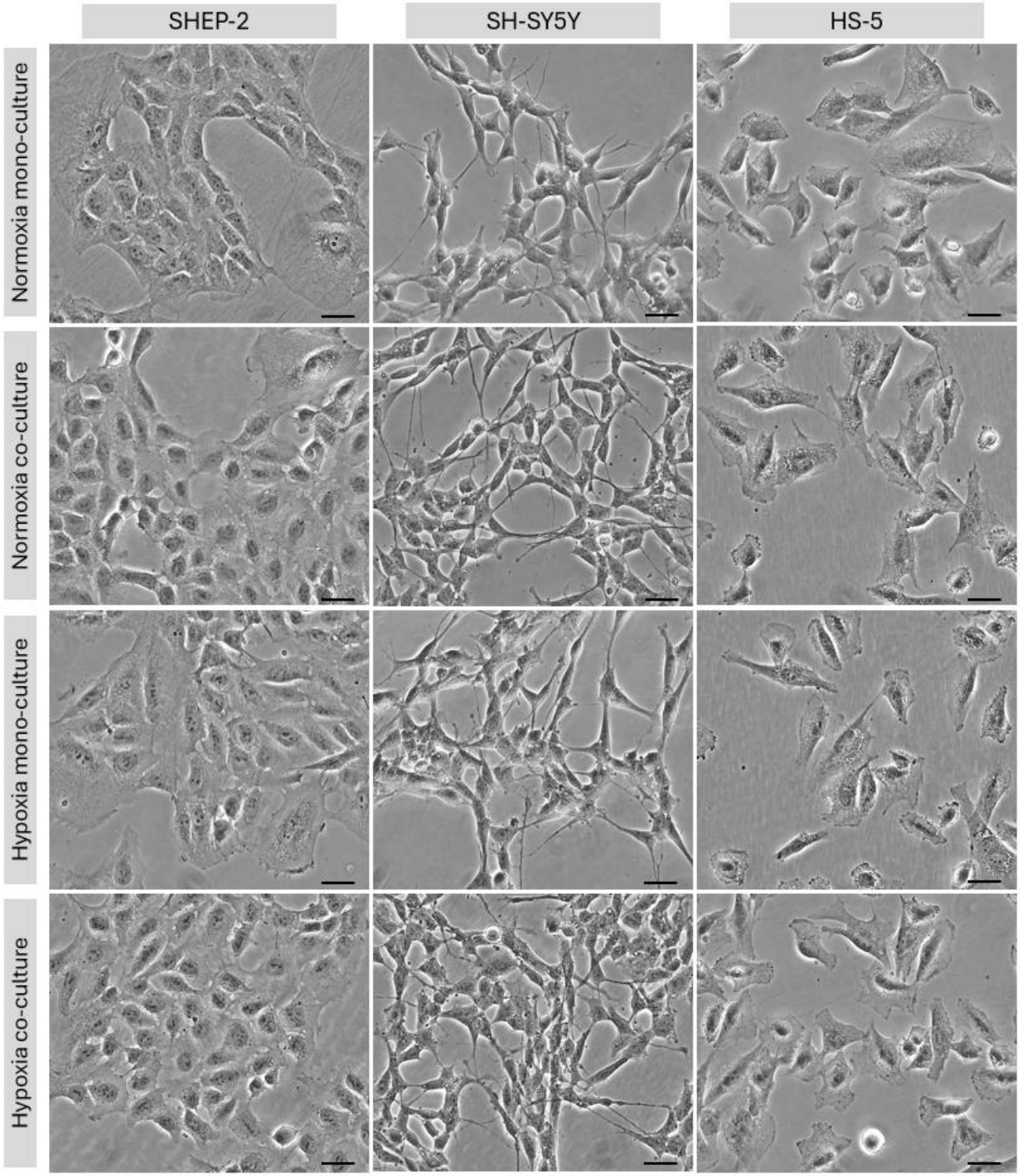

Figure 15: Representative images of the different culture conditions for SHEP-2 (p31, seeding density 4200 cells/cm^2), SH-SY5Y (p+10, seeding density 11 000 cells/cm^2) and HS-5 cells (p+21, seeding density 11 000 cells/cm^2), incubated for 72h in monoculture or co-culture, in hypoxia and normoxia. No clear differences in morphology were observed for the different cell culture conditions (normoxia, hypoxia, monoculture, and co-culture). Objective 20x, scalebar 10 μm.

4.8 The co-culture with HS-5 bone marrow cells does not significantly affect the drug resistance behavior of SHEP-2 or SH-SY5Y

To determine the effect of the co-culture with HS-5 cells on the VCR tolerance of the neuroblastoma cell lines, the results of the optimized monoculture IC50 determination experiments were used as a basis. Cells were seeded in mono- and co-culture and incubated in normoxia (37 ℃) for 48h. Subsequently, the medium was aspirated and either fresh Experiment DMEM (control) or Experiment DMEM with VCR was added. For SHEP-2 cells, a concentration of 0.0054 µM of VCR was added and for SH-SY5Y cells, a concentration of 0.09 µM of VCR was added. These concentrations correspond to the determined IC50 concentrations in hypoxia. Cells were incubated for 48h in absence or presence of VCR, after which the Cell Titer Glo assay was performed. The cells incubated without VCR were normalized to 100% for each condition (monoculture and co-culture in normoxia and hypoxia) and the cells incubated with VCR were normalized accordingly. The experiment was performed two times independently (n=2). The relative percentage viability of the SHEP-2 monoculture and co-culture in normoxia were found to be 34.7±0.6% and 37.0±1.4%, respectively. In hypoxia, the monoculture and co-culture percentage viability were 37.9±2.6% and 36.6±5.3%, respectively. The relative percentage viability of the SH-SY5Y monoculture and co-culture in normoxia were found to be 55.2±4.8% and 55.6±1.5%, respectively. In hypoxia, the monoculture and co-culture percentage viability were 44.9±0.8% and 54.1±3.5%, respectively.

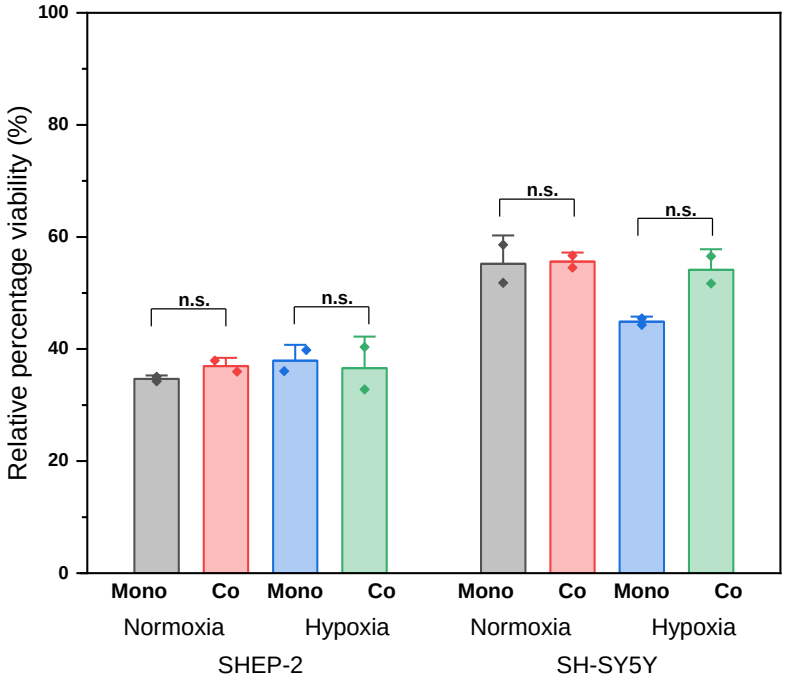

*Figure 16: The relative percentage viability of monocultures and co-cultures in normoxia and hypoxia exposed to VCR. Cells are allowed to attach and incubate for 48h in normoxia, after which the medium is replaced with to Experiment DMEM with VCR or without VCR as a control. For hypoxia, pre-equilibrated medium is used. SHEP-2 cells are incubated with 0.0054 µM of VCR. SH-SY5Y cells are incubated with 0.09 µM VCR. For each condition, the percentage viability of the cells incubated without VCR is normalized to 100% and the percentage viability of the treated conditions are normalized accordingly, resulting in the experimental results as represented. Statistical significance *P<0.05, **P<0.01, n.s. not significant, n=2.*

No statistically significant difference was identified between the response to VCR in co-cultured compared to the mono-culture for either SHEP-2 or SH-SY5Y in normoxia or hypoxia (figure 16). Despite the lack of statistical significance, for SH-SY5Y cells the percentage viability (as a measure of the tolerance to VCR) is higher in co-culture compared to the monoculture in hypoxia, possibly indicating the SH-SY5Y cells have a greater tolerance to VCR in co-culture with bone marrow cells. A possible explanation for not seeing any effect of the co-culture with HS-5 on the neuroblastoma drug resistance behavior could be the orientation of the co-culture system and used time of incubation. Cells on the top of the transwell insert directly excrete any soluble factors, proteins or EVs in the pores of the membrane. It is hypothesized that the apical-to-basolateral transport (top-to-bottom) is faster

compared to the basolateral-to-apical direction [145]. In contrast, molecules (or EVs) secreted by the cells in the bottom well are first diluted in the larger volume of the bottom well and subsequently have to make their way through the membrane. If some factor excreted from neuroblastoma cells is needed for the HS-5 cells to exhibit pro-tumor activity, the indicated time of incubation in the experiments may be too short. In addition, after 48h of attachment and incubation in normoxia, the medium is aspirated and Experiment DMEM is added (for each condition). This is a necessary handling procedure to add the pre-equilibrated medium for proper hypoxic cell culture. This procedure, however, also removes all excreted molecules or vesicles in the co-culture.

In addition, the transwell system only allows for analysis of the effects of long-distance cellular communication. Communication in the cancer microenvironment can entail direct communication, involving direct cell-cell contact in the form of gap junctions, ligand-receptor pairs and cell adhesion, or tunnel nanotubes, or indirect communication, involving signaling through extracellular vesicles, cytokines, chemokines, and/or growth factors [146]. When culturing HS-5 and SHEP-2 cells in direct co-culture, it can clearly be observed that cells form direct connections (supplementary S6). It could be hypothesized that changes in drug resistance behavior caused by bi-directional communication depends on direct cell-cell contact, causing it not to be observed in this long-distance communication study. Mechanisms involved may for instance be the presence of gap-junctions, ligand-receptor pairs and tunnel nanotubes [147–149]. However, literature suggest that changes in drug resistance behavior can also be induced by EV mediated cellular communication [150,151]. Therefore, further investigation is necessary.

The results of this experiment do form an internal control for the previous IC50 determination experiments of the neuroblastoma monocultures. In the monoculture experiments, the IC50 value was determined using sigmoidal curve fitting. It was observed that the percentage viability very rapidly decreases at low concentrations of VCR. These large leaps in the percentage viability may result in a less accurate IC50 value determination. It could therefore be valuable to include additional measurement points in the lower VCR concentration range (between 0.001 and 0.01 uM). However, addition of the determined IC50 concentrations from the monoculture study in this subsequent experiment to evaluate the effect of the co-culture, the percentage viability came close to 50%, indicating the determined IC50 values were accurate.

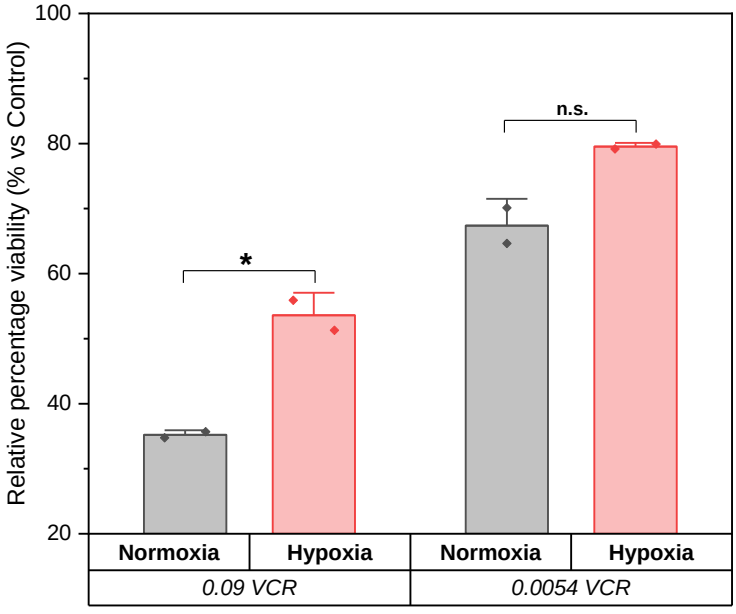

*Figure 17: The relative percentage viability of the HS-5 monoculture in normoxia and hypoxia exposed to 0.09 µM VCR or 0.0054 µM VCR. Cells are allowed to attach and incubate for 48h in normoxia, after which the medium is replaced with to Experiment DMEM with VCR or without VCR as a control. For hypoxia, pre-equilibrated medium is used. For each condition, the percentage viability of the cells incubated without VCR is normalized to 100% and the percentage viability of the treated conditions are normalized accordingly, resulting in the experimental results as represented. Statistical significance *P<0.05, **P<0.01, n.s. not significant, n=2.*

When looking at the HS-5 cells, the relative percentage viability was found to be 35.2±0.66(n=2)% when exposed to 0.09 µM VCR and 67.4±3.9(n=2)% when exposed to 0.0054 µM VCR in normoxia (figure 17). In hypoxia the relative percentage was found to be 53.6±3.3(n=2)% and 79.5±0.5(n=2)% when exposed to 0.09 µM VCR and 0.0054 µM VCR, respectively. Comparing normoxia and hypoxia, there is a significantly increased tolerance for VCR in hypoxia when incubated with 0.09 µM VCR (P=0.047). For 0.0054 µM VCR the same trend is observed, however, lacking the statistical

significance. Nonetheless, it is observed that HS-5 cells tolerate VCR better when incubated in hypoxia. The differences between the monoculture and co-culture conditions in normoxia were not found to be statistically significant for either SHEP-2 or SH-SY5Y (Supplementary S5). In general, the co-culture condition causes a minor decrease in the tolerance of the HS-5 cells for VCR (in hypoxia as well as normoxia), with a lack of statistical significance.

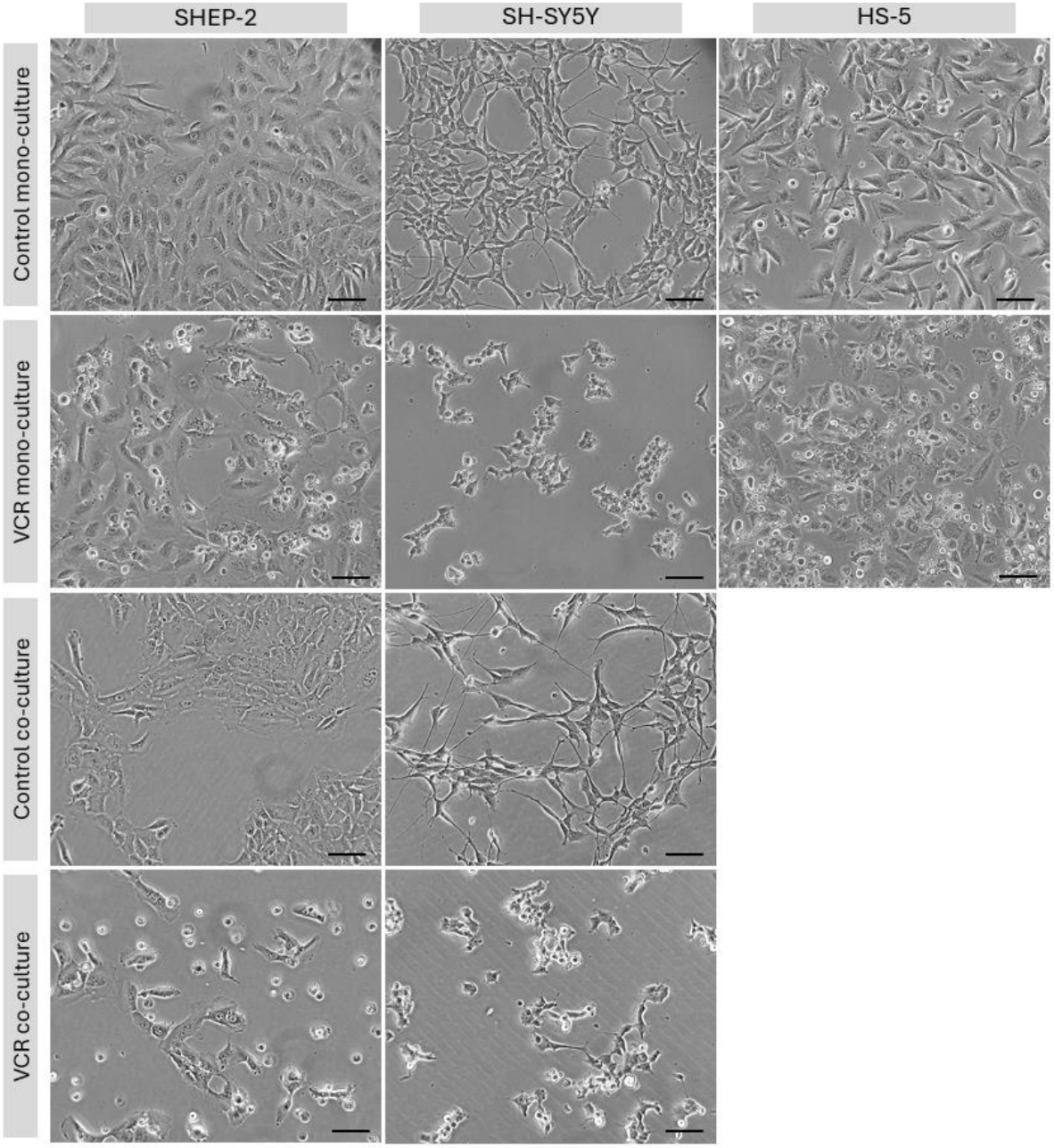

Figure 18: Morphology of cells treated with the IC50 concentration in monoculture and co-culture. Cells were seeded and allowed to grow in normoxia (in monoculture or co-culture) for 48h. Subsequently, Experiment DMEM without VCR (control) or with VCR was added (0.0054 µM for the cultures with SHEP-2 cells and 0.09 µM for cultures with SH-SY5Y) using pre-equilibrated medium for the hypoxic cultures. Finally, cells were incubated for 48h in normoxia or hypoxia. Left column: SHEP-2 cells (p20, seeding density 3000 cells/cm^2) show a lower confluence in co-culture. When treated with VCR, rounded, floating, dead cells appear, in both mono- and co-culture. In mono-culture, the remaining cells appear somewhat larger and more flattened. Middle column: for SH-SY5Y cells (p+16, seeding density 8500 cells/cm^2) the treatment with VCR results in the disappearance of the TNTs, in both mono- and co-culture. On top of the still attached cells, spherical, dead cells can be observed. Right column: when treated with 0.09 µM VCR, HS-5 culture (p+26, seeding density 9500 cells/cm^2) exhibits a chaos of cell debris and dead cells. Underneath, still viable and attached cells are visible. Objective 10x, scalebar 25 µm.

Looking at the morphology of the cells, there are no clear differences between the monoculture and co-culture conditions. Regarding the confluence of the cells, the co-culture condition showed a lower cell density in the center of the wells, underneath the transwell insert and a little higher cell density along the edges of the well.

In all IC50 determination experiments, cells were exposed to VCR for 48 hours. In this study, we are interested in chronic hypoxia. Therefore, the minimally desired period of exposure is 24 hours. This time-span of 24h exposure would be more relevant when looking at the administration and half-life of VCR in pediatric pharmacodynamics and pharmacokinetics. However, using a 24-hour incubation period with VCR resulted in a percentage viability only decrease to ~70%, and the luminescence remained high even in highest concentration of VCR. This readout did not support the observation of the morphology of the cells, that clearly showed similar results in comparison with the 48h exposure to VCR. Therefore, the incubation was increased to 48h. This resulted in proper dose-response curves with a sigmoidal curve to determine the IC50 values. It was decided to keep this incubation duration for the remainder of the experiments.

4.9 SHEP-2 cells are much less sensitive to VCR when exposed for a second time and show clear morphological changes

During the study, a new question arose: how do the neuroblastoma cells respond to a second treatment with VCR? Do the cells recover when the VCR is removed? And, if the cells are subsequently treated for a second time with VCR, will the percentage viability decrease in the same manner as observed in the first VCR exposure?

In order to investigate these questions, cells were seeded at a density of 3000 cells/cm^2 and 8500 cells/cm^2 for SHEP-2 and SH-SY5Y, respectively, and allowed to attach for 48h, followed by a 48h incubation with VCR (all in normoxia). Subsequently, the VCR containing medium was removed, cells were washed with pre-warmed PBS and fresh Experiment DMEM (without VCR) was added. Cells were allowed to recover for 72h. The morphology was imaged. Subsequently, cells were kept in fresh Experiment DMEM (as a control) or incubated for 48h with VCR (as a second VCR treatment). This means, after removal of the first VCR, cells were 1) allowed to recover in fresh medium for 5 days (120h) or 2) allowed to recover for 72h followed by second VCR incubation for 48h. Experiments were repeated two times independently (n=2).

When treated with VCR (0.0054 µM for SHEP-2 and 0.09 µM for SH-SY5Y), the percentage viability is reduced to 34.7±0.59% for SHEP-2 and 55.2±4.8% for SH-SY5Y (P=0.002 and P=0.01). When allowed to recover, the percentage viability of the SHEP-2 cells is restored to 103.6±10.6%, which is a significant (P=0.0017) increase compared to the treated cells. Interestingly, the relative percentage viability of the recovered cells does not significantly differ from the non-treated control (P=1). In contrast, the relative viability of the SH-SY5Y cells is not significantly (P=1) increased when allowed to recover. The cells incubated with VCR for 48h show a reduction of the viability to 55.2±4.8% and when allowed to recover, the percentage viability only goes increases a few percentages to 63.0±11.2%. Interestingly, when incubated with VCR for a second time, the relative percentage viability of the SHEP-2 cells is only reduced to 84.6±4.4%, which was not found to be statistically significant (P=0.181) compared to the recovered cells. This reduction is much less compared to the decrease in viability of the first incubation with VCR, indicating a greater tolerance to VCR. Conversely, the SH-SY5Y cell viability is further reduced to 30.1±7.8%, which is approximately half of the relative viability of the recovered cells, indicating the SH-SY5Y cells respond very similar to the consecutive VCR incubation in comparison to the first VCR exposure.

These results show that, upon a consecutive round of VCR exposure, SH-SY5Y cells exhibit the same tolerance (or sensitivity) to the VCR drug, while the SHEP-2 cells are much less sensitive to VCR in comparison to the first drug treatment. It is hypothesized there is sub-population of SHEP-2 cells that presents a mechanism of drug resistance, which survive the first exposure to VCR as a selection process. These surviving cells proliferate and grow, and upon the second round of VCR exposure, the more sensitive SHEP-2 cells that have remained in a first round of selection, cause the observed decrease in percentage viability, which as a result is smaller compared to the initial VCR treatment. The observations do support the proposition that MES-type neuroblastoma cells are more drug resistant as suggested in literature [54]. However, further investigation on the mechanisms behind the

observed increase in VCR tolerance is necessary. Nonetheless, these findings are interesting and relevant, as the situation in which cells are exposed to multiple consecutive rounds of drug treatment is very similar to the clinical scenario of induction chemotherapy treatment, in which patients receive multiple rounds of chemotherapy treatment.

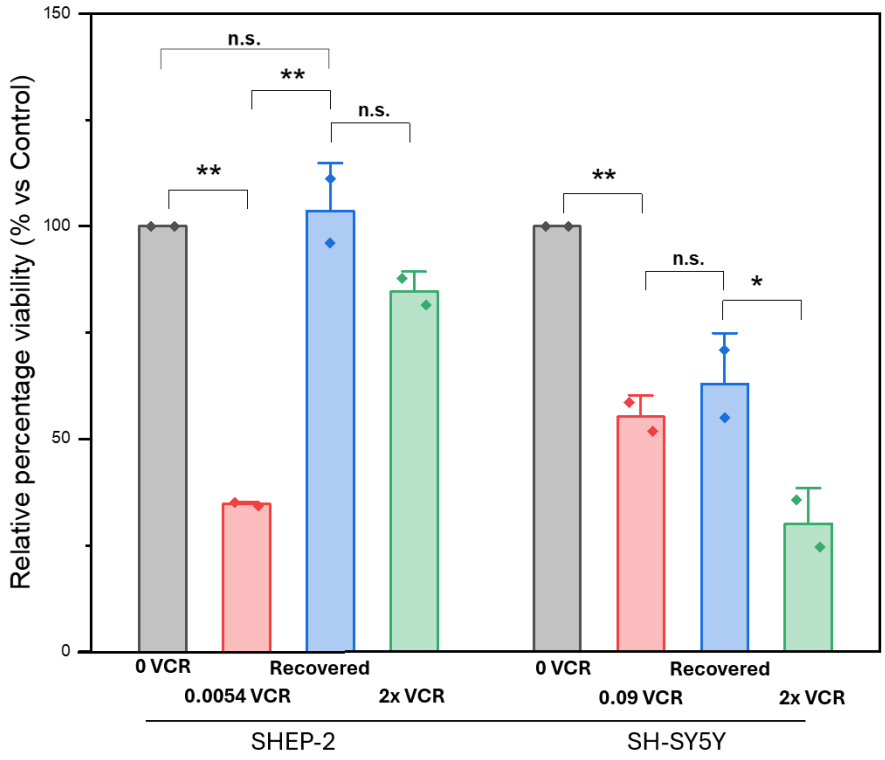

*Figure 19: The relative percentage viability of SHEP-2 and SH-SY5Y monocultures incubated with two consecutive rounds of VCR. These experiments are performed fully in normoxia. 0 VCR= control, cells cultured in normoxia for 96h without VCR; 0.0054 VCR= SHEP-2 cells allowed to attach for 48h and incubated with VCR for 48h; 0.09 VCR = SH-SY5Y cells allowed to attach for 48h and incubated with VCR for 48h; Recovered= 48h attachment, 48h incubation with VCR, and 120h recovery in fresh Experiment DMEM; 2x VCR= 48 attachment, 48h incubation with VCR, 72h recovery in medium without VCR, and 48h incubation with VCR (second treatment). For each condition, the percentage viability of the cells incubated without VCR is normalized to 100% and the percentage viability of the treated conditions are normalized accordingly. Statistical significance *P<0.05, **P<0.01, n.s. not significant, n=2.*

In addition to the change in the drug response, clear changes in morphology were observed for recovered and repeatedly exposed cells, especially in the SHEP-2 cell line. For SH-SY5Y it is observed that the long and fine TNTs are restored. Cells form very long processes to again connect to each other for communication. In addition, multiple dead cells are still visible as small clusters around the healthy cells. For the SHEP-2 cells, it was observed that the majority of the remaining, recovering cells, presented a very flattened, enlarged morphology (figure 20). Cells appear much larger compared to the normal morphology. In addition, there are some cells that form very long, thin processes, comparable to those observed for the SH-SY5Y cells. Multiple cells appear more stellate and elongated.

Studying the effects of multiple rounds of VCR treatment was only performed in normoxia, as it requires multiple handling steps and medium changes. This introduces one of the main limitations of this research. To create a hypoxic environment, a hypoxic chamber is used. The hypoxic chamber is flushed with a specific gas mixture, creating a stable oxygen tension inside the chamber. The moment the hypoxic chamber is opened (or the closing ring is compromised), oxygen is allowed to diffuse into the chamber, increasing the oxygen concentration and losing the hypoxic microenvironment. In cells, this rapid increase in oxygen can result in the generation of reactive oxygen species (ROS). ROS are free radicals, unstable molecules that contain oxygen and easily react with other cellular molecules. These ROS are considered cytotoxic [152–155]. A buildup of ROS can cause oxidative stress characterized by DNA damage, RNA damage and damage to proteins, resulting in cell death.

Radiotherapy is based on this principle to kill tumor cells [156]. In contrast, other studies suggest that intermitted hypoxia increases the malignant behavior of tumor cells in the form of increase proliferation, survival, and metastasis [157–159]. Anyhow, sudden reoxygenation can affect the experimental outcome. The bone marrow microenvironment has a constant hypoxic oxygen pressure, and therefore it is desired to minimize any effects of reoxygenation in these studies since it does not represent the physiological situation. When investigating proliferation and percentage viability, we are only interested in the effect of the hypoxia itself and want to minimize the effect of ROS. Therefore, it is important to limit the time cells are exposed to oxygen and it is not possible to manually manipulate the cells in between the start of the incubation and the final readout. Measuring multiple consecutive rounds of VCR exposure in hypoxia was therefore not possible with the given restrictions.

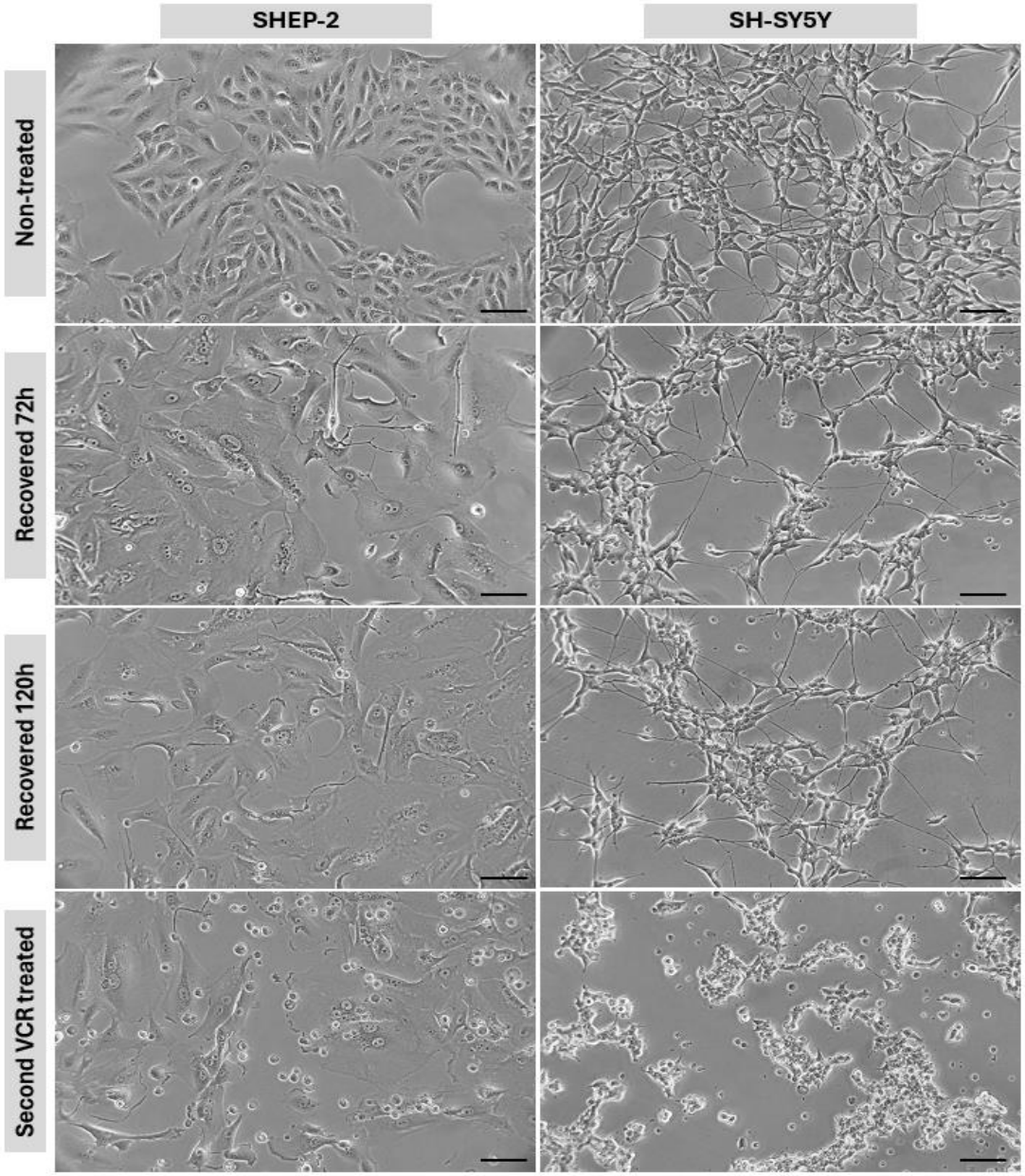

Figure 20: Morphology of cells treated with the IC50 concentration in monoculture and co-culture. SHEP-2 cells (p22) and SH-SY5Y (p+18) were seeded (3000 cells/cm^2 and 8500 cells/cm^2, respectively) and allowed to grow in normoxia for 48h. Subsequently, Experiment DMEM without VCR (control) or with VCR was added (0.0054 µM for the cultures with SHEP-2 cells and 0.09 µM for cultures with SH-SY5Y) and cells were incubated for 48h in normoxia or hypoxia. Cells were then allowed to recover in fresh medium for 72h. Finally, cells were kept in fresh medium or incubated with VCR for 48h. SHEP-2 cell morphology shows an increase in the cell size and a very flattened, stretched cytoplasm. In addition, several cells with a more stellate morphology and long, fine processes are observed. SH-SY5Y cells that are allowed to recover show a re-appearance of the long, fine TNTs, connecting the cells over relatively long distances.

Most often, an MTT assay is used for IC50 determination for different timepoints (generally 24h, 48h and 72h). However, this assay requires a 4h incubation of metabolically active cells. This would mean hypoxically cultured cells would be exposed to high (ambient) oxygen tension for 4 hours. This may allow for ROS to negatively affect viability and as such the measured percentage viability would not reflect the effect of the hypoxic environment alone but the combined effect of the ROS. The CellTiter Glo presented a suitable alternative assay, in which cells are lysed immediately after opening the hypoxic chamber and thus no exposure of cells to the high oxygen concentration. When performing proliferation assays, hypoxically cultured cells are kept on ice as much as possible after opening the hypoxic chamber to limit their metabolic activity. Nonetheless, use of the hypoxic chamber limits the choice of possible readouts. Not being able to open and close the hypoxic chamber during an experiment due to the negative effects of ROS also limits the options for analyzing different timepoints. The time-scale is determined by the moment of closing and flushing the chamber and opening it. The 48h exposure time presented with clear difference between normoxia and hypoxia and was therefore used in every experiment. 48h is in the range of chronic hypoxia and thus provided biologically relevant findings, as it resembles chronic hypoxia exposure of neuroblastoma cells in the hypoxic bone marrow. Finally, it is important to realize that use of the hypoxic chamber also provides a limitation in the medium equilibration process. When the medium is pre-equilibrated for 24h, the chamber has to be opened to take out the medium and, if necessary, further process the medium (for instance by adding the VCR). These handling steps require (some) time. Even though this time is limited as much as possible, and the medium is transferred to tubes of which the lids are kept closed as much as possible, there may be some exchange of oxygen with the medium and the medium will not be fully hypoxic. A set-up with a glovebox could provide means to circumvent these practical limitations by creating a fully hypoxic environment where all handling and incubation steps can be performed with a constant, fixed, and pre-set oxygen concentration. This would also allow for some diversification of the oxygen concentration.

5. Discussion and conclusions

Culturing SH-SY5Y and SHEP-2 neuroblastoma cells in hypoxia (5% O_2) significantly affected cellular proliferation. Using hypoxic pre-equilibrated medium, the proliferation was almost doubled for both cell lines after 48h incubation in hypoxia. Cell morphology was not affected by hypoxia for either SHEP-2 or SH-SY5Y. These results indicate that the hypoxic microenvironment is well tolerated by the neuroblastoma cell lines and increases the malignant behavior of the neuroblastoma cells. In co-culture with HS-5, the proliferation of both neuroblastoma cell lines is decreased in normoxia. In contrast, the presence of HS-5 cells in hypoxia results in an increase in proliferation of both neuroblastoma cell lines.

When introduced to hypoxia, the drug resistance is significantly increased as well as the proliferation of both the SHEP-2 and SH-SY5Y cell line. In the hypoxic microenvironment, the malignant behavior of the cells is thus increased. This corresponds to previously reported findings. The mechanism involved in hypoxia-mediated drug resistance in the neuroblastoma cells should be further investigated. It is possible that HIF-2α, one of the major players in response to chronic hypoxia, plays a role in this mechanism, as suggested by previously reported literature. It is also possible that, as suggested by Hussein at al. [11] that HIF-1α is involved in the drug resistance mechanism. Looking at the proliferation of the neuroblastoma cells in hypoxia, a possible proposed reason for the observed increase could be found in the membrane potential of the tumor cells. Hypoxia has been known to affect the resting membrane potential of cells [152,153]. In addition, a relation between the membrane potential and cellular proliferation has already been proposed in 1971 [154]. It is suggested that depolarized tumor cells have a higher proliferation rate compared to hyperpolarized cells that are observed to be more quiescent. However, to the best of our knowledge, there is no currently available data on the membrane potential of neuroblastoma tumor cells in hypoxia, indicating a valuable future research step. Bioelectrical signaling may also play a crucial role in hypoxia-mediated drug resistance in a co-culture setting [155].

An interesting observation is that the ADRN-type SH-SY5Y cells exhibited a greater tolerance to VCR in the first round of exposure to the chemotherapy drug, which did not follow the hypothesis based on the literature that indicated an expected higher drug resistance of MES-type neuroblastoma cells.

Interestingly, however, the MES-type SHEP-2 cells show some mechanism of drug resistance, allowing them to continue to proliferate and greatly increasing the percentage viability upon a second round of VCR exposure. This exact mechanism, however, is not yet fully understood. It can be hypothesized that a population of the SHEP-2 cell line contains a mechanism such as the presence of ABC-transporters to reduce the sensitivity to VCR. Alternatively, these cells may lack the membrane associated transporter to take up the VCR drug. Importantly, however, the cells that do remain after the initial VCR exposure present a very flattened and stretched morphology. As VCR affects the tubulin protein, a cytoskeletal component, this is an interesting observation. As possible mechanisms of resistance to microtubule affecting chemo-therapeutics, it is proposed in literature that cells [156]: 1) form tubulin mutations; 2) overexpress specific tubulin isotypes; 3) overexpress microtubule interacting proteins. It has been observed in children treated for ALL, that vincristine resistance was accompanied by increased levels of microtubule polymers [157]. As the microtubules are a cytoskeletal component of the cell, it is hypothesized, based on the change in morphology and cell size, that changes in the tubulin expression and microtubule polymer levels could be involved in the observed drug resistance increase. Nonetheless, further research is necessary to unravel this specific drug resistance behavior that is observed only in the MES-type SHEP-2 cells.

TNTs are described to be composed of primarily actin, but also tubulin has been described to be a possible minor component in TNTs [149,158–160]. The presence of tubulin in the TNTs would be a possible explanation for their disappearance in the SH-SY5Y cell line upon VCR exposure. Nonetheless it can be theorized that, since vincristine affects a cytoskeletal component, in general the disappearance of the small processes is a logical consequence. In the tumor microenvironment, the TNTs form communicative channels between tumor cells as well as between tumor cells, normal cells and immune cells. This facilitates the transport of organelles such as mitochondria, transport of proteins, transfer of calcium waves and transfer of lysosomes. This can contribute to the malignant behavior of tumor cells in the form of survival, metastasis, and chemoresistance [160]. It is hypothesized these TNTs play a crucial role in the malignant behavior of neuroblastoma cells, also in co-culture with BMSCs, since formation of these TNTs were observed in a direct co-culture (supplementary S6) for both cells (SHEP-2 and HS-5). When growing the SH-SY5Y cells, low seeding densities resulted in a very limited proliferation and growth of the cells. When proliferating, cells form these TNTs to form very distinct networks, as observed with microscopy. It can be speculated that with low seeding densities, the cells are too far apart to reach each other through the formation of the TNTs, resulting in poor proliferation, indicating their importance. Upon removal of the VCR drug, the first thing observed for the SH-SY5Y cells is the re-appearance of the TNTs, without an increase in proliferation. This may indicate the importance of the TNT communication network for the SH-SY5Y cell survival and proliferation. If indeed the VCR drug affects the formation of these TNT structures, this may indicate why the SH-SY5Y cells show an equally large sensitivity to VCR upon the second incubation with the drug. However, the functionality of TNTs has been observed to mainly be disrupted by drugs that target actin polymerization, rather than tubulin [159], meaning that further investigation of the TNT structure and dynamics upon VCR exposure is needed.

In the co-culture study, the effect of long-distance communication is studied. For both neuroblastoma cell lines, no statistically significant differences were observed between the monoculture and the co-culture when exposed to VCR. Importantly, however, it is observed that in hypoxia the HS-5 cells are significantly more tolerant to VCR (when exposed to 0.09 µM VCR). According to a previous study by Zhang et al. [17], BMSCs cells were activated in hypoxia to excrete extracellular vesicles containing specific micro-RNAs that cause drug resistance in multiple myeloma. BMSCs were also observed to mediate chemoresistance in tumor cells. In acute lymphoblastic leukemia (ALL), BMSCs have shown to mediate vincristine resistance through the CXCR4/CXCL12 axis [16]. In hypoxia, hypoxia-induced macrophage migration inhibitory factor (*MIF*) expression occurs in BMSCs that can function as a noncognate ligand for the CXCR4 receptor. Again, also HIF-1 and HIF-2α are involved in BMSCs response to hypoxia. Interestingly, bone marrow tolerance to VCR decreases when in co-culture with the neuroblastoma cells. It could be speculated that in hypoxia, the HS-5 cells are activated to increase their tolerance to VCR, with which they mediate the drug resistance behavior of the neuroblastoma tumor cells, leading to a reduction of their own drug resistance. However, no significant changes in the drug resistance of the neuroblastoma cells in co-culture were observed in this study and further research is necessary.

Overall, the experimental results highlight the importance of hypoxia and communication with HS-5 bone marrow cells in the tumor cell behavior of the SHEP-2 and SH-SY5Y neuroblastoma cell lines. These findings emphasize that these elements in the tumor microenvironment are highly relevant and should not be ignored when performing studies to evaluate drug resistance behavior and predict patient outcomes. The study contributes to currently available research by complementing on the knowledge on the proliferative behavior of neuroblastoma cells in chronic physiologically relevant hypoxia and showing the changes in tolerances to vincristine in hypoxia as well as the changes in the VCR sensitivity in consecutive rounds of exposure. In the contiguous weeks following my master thesis defense, I will study the PGP and MRP1 expression in the neuroblastoma cell lines in normoxia and hypoxia, and in mono- and in co-culture to see if there are correlations between the expression of these ABC-transporters and the culture condition. This follow-up experiment is aimed to investigate if the ABC-transporter expression is dependent on a hypoxic microenvironment and if the ABC-transport expression is influenced by or dependent on the presence of HS-5 bone marrow cells.

6. Future recommendations

The possible limitations of the use of the modular hypoxic chamber have been discussed above. For future research upon the role of hypoxia in the neuroblastoma development and malignant characteristics, it could be considered to use a glovebox. Having a constant, stable oxygen tension for every handling procedure of the cells, opens the doors for great elaboration of the work, including for example the addition of multiple timepoints, the evaluation of the drug resistance upon treatment in consecutive cycles of VCR in hypoxia, or a longer co-culture incubation timespan prior to the addition of VCR in hypoxia, without the need for removal of the medium. A second recommendation for a follow-up study would be to investigate if the co-culture orientation influences the experimental results of the co-culture studies. It could be valuable to check if culturing the neuroblastoma cells on the insert results in an observable difference in the drug-response. In addition, the current co-culture studies were performed in a static environment. The addition of flow, for instance by implementing a tilting plate, might improve the diffusion of excreted molecules and vesicles. Moreover, this may more accurately resemble human physiology of flow in the human body and tissue [161]. Thirdly, it was reported previously that MYCN amplification affects the malignant behavior of neuroblastoma tumor cells in terms of proliferation and drug resistance in the context of hypoxia [69,70]. The SHEP-2 and SH-SY5Y cell lines are MYCN non-amplified. As MYCN amplification is regarded as one of the biggest prognostic factors in high-risk neuroblastoma, it would be valuable to assess the response of MYCN amplified cell lines to these culture conditions. Finally, it could be attempted to develop a way to apply a direct co-culture to allow for direct cell-cell contact that still allows for the intended analysis. Alternatively, a co-culture on bottom and top of the transwell membrane could be studied to minimize the distance between cell types. Direct cell contact, for instance through TNTs or gap junctions [147–149], may influence the observed results, especially in the context of the drug resistance and proliferation. In addition, the approximate one-millimeter gap between the insert and the bottom well is too large for the TNTs to connect the two cell lines. It is expected that these connections are crucial for BMSC to mediate drug resistance behavior in hypoxia. These TNTs may provide means to relay electrical potentials, affecting tumor cell proliferation, as well as membrane proteins possibly aiding in drug resistance behavior. Finally, it would be impactful to study the microtubule polymer concentrations and tubulin protein expression levels in non-treated and VCR incubated cells to investigate if these responses are a possible mechanism of resistance to VCR in the SHEP-2 cells.

In my perspective, interesting remaining question beyond the scope of this study include: 1) what causes the increase in proliferation observed in hypoxia/co-culture? What signaling pathways may be involved? What could be the role of electrical cell-cell signaling and membrane potential in monoculture and co-culture in hypoxia? 2) How do extracellular vesicles come into play in the observed effects of co-culture? What changes in the EV composition are observed in hypoxia (HS-5 and neuroblastoma)? 3) Is there a role of an ADRN-to-MES switch that was previously reported in literature? Can it be observed in hypoxia? Could it be an explanation for the observed results, such as the increase in drug resistance? These questions, among others, and the above-described future recommendations and gaps in research may form a basis for compelling future research.

7. References

1. Brignole C, Pastorino F, Perri P, Amoroso L, Bensa V, Calarco E, et al. Bone Marrow Environment in Metastatic Neuroblastoma. Cancers (Basel). 2021 May 19;13(10):2467.
2. Shiozawa Y. The Roles of Bone Marrow-Resident Cells as a Microenvironment for Bone Metastasis. In: Birbrair A, editor. Tumor Microenvironments in Organs. Switzerland: Springer; 2020. p. 57–72.
3. Hochheuser C, Windt LJ, Kunze NY, de Vos DL, Tytgat GAM, Voermans C, et al. Mesenchymal Stromal Cells in Neuroblastoma: Exploring Crosstalk and Therapeutic Implications. Stem Cells Dev. 2021 Jan 15;30(2):59–78.
4. Holzwarth C, Vaegler M, Gieseke F, Pfister SM, Handgretinger R, Kerst G, et al. Low physiologic oxygen tensions reduce proliferation and differentiation of human multipotent mesenchymal stromal cells. BMC Cell Biol. 2010 Dec 28;11(1):11.
5. Chow DC, Wenning LA, Miller WM, Papoutsakis ET. Modeling pO2 Distributions in the Bone Marrow Hematopoietic Compartment. II. Modified Kroghian Models. Biophys J. 2001 Aug;81(2):685–96.
6. Muz B, de la Puente P, Azab F, Luderer M, Azab AK. The Role of Hypoxia and Exploitation of the Hypoxic Environment in Hematologic Malignancies. Molecular Cancer Research. 2014 Oct 1;12(10):1347–54.
7. McKeown SR. Defining normoxia, physoxia and hypoxia in tumours—implications for treatment response. Br J Radiol. 2014 Mar;87(1035):20130676.
8. Al Tameemi W, Dale TP, Al-Jumaily RMK, Forsyth NR. Hypoxia-Modified Cancer Cell Metabolism. Front Cell Dev Biol. 2019 Jan 29;7.
9. Påhlman S, Mohlin S. Hypoxia and hypoxia-inducible factors in neuroblastoma. Cell Tissue Res. 2018 May 14;372(2):269–75.
10. Ferrer A, Roser CT, El-Far MH, Savanur VH, Eljarrah A, Gergues M, et al. Hypoxia-mediated changes in bone marrow microenvironment in breast cancer dormancy. Cancer Lett. 2020 Sep;488:9–17.
11. Hussein D, Estlin EJ, Dive C, Makin GWJ. Chronic hypoxia promotes hypoxia-inducible factor-1α–dependent resistance to etoposide and vincristine in neuroblastoma cells. Mol Cancer Ther. 2006 Sep 1;5(9):2241–50.
12. Jögi A, Vallon-Christersson J, Holmquist L, Axelson H, Borg Å, Påhlman S. Human neuroblastoma cells exposed to hypoxia: induction of genes associated with growth, survival, and aggressive behavior. Exp Cell Res. 2004 May;295(2):469–87.
13. Huertas-Castaño C, Gómez-Muñoz MA, Pardal R, Vega FM. Hypoxia in the Initiation and Progression of Neuroblastoma Tumours. Int J Mol Sci. 2019 Dec 19;21(1):39.
14. Jing X, Yang F, Shao C, Wei K, Xie M, Shen H, et al. Role of hypoxia in cancer therapy by regulating the tumor microenvironment. Mol Cancer. 2019 Dec 11;18(1):157.
15. Kwon SY, Chun SY, Ha YS, Kim DH, Kim J, Song PH, et al. Hypoxia Enhances Cell Properties of Human Mesenchymal Stem Cells. Tissue Eng Regen Med. 2017 Oct 31;14(5):595–604.
16. Meyer LK, Hermiston ML. The bone marrow microenvironment as a mediator of chemoresistance in acute lymphoblastic leukemia. Cancer Drug Resistance. 2019;
17. Zhang H, Du Z, Tu C, Zhou X, Menu E, Wang J. Hypoxic Bone Marrow Stromal Cells Secrete miR-140–5p and miR-28–3p That Target SPRED1 to Confer Drug Resistance in Multiple Myeloma. Cancer Res. 2024 Jan 2;84(1):39–55.
18. Johnsen JI, Dyberg C, Wickström M. Neuroblastoma—A Neural Crest Derived Embryonal Malignancy. Front Mol Neurosci. 2019 Jan 29;12.
19. Qiu B, Matthay KK. Advancing therapy for neuroblastoma. Nat Rev Clin Oncol. 2022 Aug 25;19(8):515–33.
20. Louis CU, Shohet JM. Neuroblastoma: Molecular Pathogenesis and Therapy. Annu Rev Med. 2015 Jan 14;66(1):49–63.
21. Zeineldin M, Patel AG, Dyer MA. Neuroblastoma: When differentiation goes awry. Neuron. 2022 Sep;110(18):2916–28.
22. Shawraba F, Hammoud H, Mrad Y, Saker Z, Fares Y, Harati H, et al. Biomarkers in Neuroblastoma: An Insight into Their Potential Diagnostic and Prognostic Utilities. Curr Treat Options Oncol. 2021 Nov 27;22(11):102.
23. Monclair T, Brodeur GM, Ambros PF, Brisse HJ, Cecchetto G, Holmes K, et al. The International Neuroblastoma Risk Group (INRG) Staging System: An INRG Task Force Report. Journal of Clinical Oncology. 2009 Jan 10;27(2):298–303.
24. Shimada H, Ikegaki N. Genetic and Histopathological Heterogeneity of Neuroblastoma and Precision Therapeutic Approaches for Extremely Unfavorable Histology Subgroups. Biomolecules. 2022 Jan 5;12(1):79.
25. DuBois SG, Kalika Y, Lukens JN, Brodeur GM, Seeger RC, Atkinson JB, et al. Metastatic Sites in Stage IV and IVS Neuroblastoma Correlate With Age, Tumor Biology, and Survival. J Pediatr Hematol Oncol. 1999 May;21(3):181–9.
26. Galán-Díez M, Cuesta-Domínguez Á, Kousteni S. The Bone Marrow Microenvironment in Health and Myeloid Malignancy. Cold Spring Harb Perspect Med. 2018 Jul;8(7):a031328.
27. Braham MVJ, Li Yim ASP, Garcia Mateos J, Minnema MC, Dhert WJA, Öner FC, et al. A Human Hematopoietic Niche Model Supporting Hematopoietic Stem and Progenitor Cells In Vitro. Adv Healthc Mater. 2019 May 3;8(10).
28. Gattazzo F, Urciuolo A, Bonaldo P. Extracellular matrix: A dynamic microenvironment for stem cell niche. Biochimica et Biophysica Acta (BBA) - General Subjects. 2014 Aug;1840(8):2506–19.
29. Zhang P, Zhang C, Li J, Han J, Liu X, Yang H. The physical microenvironment of hematopoietic stem cells and its emerging roles in engineering applications. Stem Cell Res Ther. 2019 Dec 19;10(1):327.
30. Nelson MR, Ghoshal D, Mejías JC, Rubio DF, Keith E, Roy K. A multi-niche microvascularized human bone marrow (hBM) on-a-chip elucidates key roles of the endosteal niche in hBM physiology. Biomaterials. 2021 Mar;270:120683.

31. WILSON A, OSER GM, JAWORSKI M, BLANCO-BOSE WE, LAURENTI E, ADOLPHE C, et al. Dormant and Self-Renewing Hematopoietic Stem Cells and Their Niches. Ann N Y Acad Sci. 2007 Jun 16;1106(1):64–75.

32. Grassinger J, Haylock DN, Williams B, Olsen GH, Nilsson SK. Phenotypically identical hemopoietic stem cells isolated from different regions of bone marrow have different biologic potential. Blood. 2010 Oct 28;116(17):3185–96.

33. Haylock DN, Williams B, Johnston HM, Liu MCP, Rutherford KE, Whitty GA, et al. Hemopoietic Stem Cells with Higher Hemopoietic Potential Reside at the Bone Marrow Endosteum. Stem Cells. 2007 Apr 1;25(4):1062–9.

34. Kunisaki Y, Bruns I, Scheiermann C, Ahmed J, Pinho S, Zhang D, et al. Arteriolar niches maintain haematopoietic stem cell quiescence. Nature. 2013 Oct 31;502(7473):637–43.

35. Blavier L, Yang RM, DeClerck YA. The Tumor Microenvironment in Neuroblastoma: New Players, New Mechanisms of Interaction and New Perspectives. Cancers (Basel). 2020 Oct 10;12(10):2912.

36. Tirado HA, Balasundaram N, Laaouimir L, Erdem A, van Gastel N. Metabolic crosstalk between stromal and malignant cells in the bone marrow niche. Bone Rep. 2023 Jun;18:101669.

37. Butturini E, Carcereri de Prati A, Boriero D, Mariotto S. Tumor Dormancy and Interplay with Hypoxic Tumor Microenvironment. Int J Mol Sci. 2019 Sep 3;20(17):4305.

38. Haider MT, Smit DJ, Taipaleenmäki H. The Endosteal Niche in Breast Cancer Bone Metastasis. Front Oncol. 2020 Mar 13;10.

39. Chen Z, Han F, Du Y, Shi H, Zhou W. Hypoxic microenvironment in cancer: molecular mechanisms and therapeutic interventions. Signal Transduct Target Ther. 2023 Feb 17;8(1):70.

40. Spencer JA, Ferraro F, Roussakis E, Klein A, Wu J, Runnels JM, et al. Direct measurement of local oxygen concentration in the bone marrow of live animals. Nature. 2014 Apr 2;508(7495):269–73.

41. Xiao Y, McGuinness ChanelleAS, Doherty-Boyd WS, Salmeron-Sanchez M, Donnelly H, Dalby MJ. Current insights into the bone marrow niche: From biology in vivo to bioengineering ex vivo. Biomaterials. 2022 Jul;286:121568.

42. Congrains A, Bianco J, Rosa RG, Mancuso RI, Saad STO. 3D Scaffolds to Model the Hematopoietic Stem Cell Niche: Applications and Perspectives. Materials. 2021 Jan 26;14(3):569.

43. Holzwarth C, Vaegler M, Gieseke F, Pfister SM, Handgretinger R, Kerst G, et al. Low physiologic oxygen tensions reduce proliferation and differentiation of human multipotent mesenchymal stromal cells. BMC Cell Biol. 2010 Dec 28;11(1):11.

44. Suda T, Takubo K, Semenza GL. Metabolic Regulation of Hematopoietic Stem Cells in the Hypoxic Niche. Cell Stem Cell. 2011 Oct;9(4):298–310.

45. Mohyeldin A, Garzón-Muvdi T, Quiñones-Hinojosa A. Oxygen in Stem Cell Biology: A Critical Component of the Stem Cell Niche. Cell Stem Cell. 2010 Aug;7(2):150–61.

46. Zhang CC, Sadek HA. Hypoxia and Metabolic Properties of Hematopoietic Stem Cells. Antioxid Redox Signal. 2014 Apr 20;20(12):1891–901.

47. Liu Q, Palmgren VAC, Danen EH, Le Dévédec SE. Acute vs. chronic vs. intermittent hypoxia in breast Cancer: a review on its application in in vitro research. Mol Biol Rep. 2022 Nov 3;49(11):10961–73.

48. Emami Nejad A, Najafgholian S, Rostami A, Sistani A, Shojaeifar S, Esparvarinha M, et al. The role of hypoxia in the tumor microenvironment and development of cancer stem cell: a novel approach to developing treatment. Cancer Cell Int. 2021 Jan 20;21(1):62.

49. Gautier M, Thirant C, Delattre O, Janoueix-Lerosey I. Plasticity in Neuroblastoma Cell Identity Defines a Noradrenergic-to-Mesenchymal Transition (NMT). Cancers (Basel). 2021 Jun 10;13(12):2904.

50. van Groningen T, Koster J, Valentijn LJ, Zwijnenburg DA, Akogul N, Hasselt NE, et al. Neuroblastoma is composed of two super-enhancer-associated differentiation states. Nat Genet. 2017 Aug 26;49(8):1261–6.

51. Kovalevich J, Langford D. Considerations for the Use of SH-SY5Y Neuroblastoma Cells in Neurobiology. In 2013. p. 9–21.

52. Ferlemann FC, Menon V, Condurat AL, Rößler J, Pruszak J. Surface marker profiling of SH-SY5Y cells enables small molecule screens identifying BMP4 as a modulator of neuroblastoma differentiation. Sci Rep. 2017 Oct 19;7(1):13612.

53. Şahin M, Öncü G, Yılmaz MA, Özkan D, Saybaşılı H. Transformation of SH-SY5Y cell line into neuron-like cells: Investigation of electrophysiological and biomechanical changes. Neurosci Lett. 2021 Feb;745:135628.

54. Sengupta S, Das S, Crespo AC, Cornel AM, Patel AG, Mahadevan NR, et al. Mesenchymal and adrenergic cell lineage states in neuroblastoma possess distinct immunogenic phenotypes. Nat Cancer. 2022 Sep 22;3(10):1228–46.

55. Do JH, Kim IS, Lee JD, Choi DK. Comparison of genomic profiles in human neuroblastic SH-SY5Y and substrate-adherent SH-EP cells using array comparative genomic hybridization. Biochip J. 2011 Jun 20;5(2):165–74.

56. Peirce. High level MycN expression in non-MYCN amplified neuroblastoma is induced by the combination treatment nutlin-3 and doxorubicin and enhances chemosensitivity. Oncol Rep. 2009 Oct 14;22(06).

57. Smith DJ, Cossins LR, Hatzinisiriou I, Haber M, Nagley P. Lack of correlation between MYCN expression and the Warburg effect in neuroblastoma cell lines. BMC Cancer. 2008 Dec 14;8(1):259.

58. Krawczyk E, Kitlińska J. Preclinical Models of Neuroblastoma—Current Status and Perspectives. Cancers (Basel). 2023 Jun 23;15(13):3314.

59. Campos Cogo S, Gradowski Farias da Costa do Nascimento T, de Almeida Brehm Pinhatti F, de França Junior N, Santos Rodrigues B, Cavalli LR, et al. An overview of neuroblastoma cell lineage phenotypes and in vitro models. Exp Biol Med. 2020 Dec 12;245(18):1637–47.

60. Huertas-Castaño C, Gómez-Muñoz MA, Pardal R, Vega FM. Hypoxia in the Initiation and Progression of Neuroblastoma Tumours. Int J Mol Sci. 2019 Dec 19;21(1):39.

61. Wang D, Zhu Q, Zhang X, Zhang L, He Q, Yang B. Hypoxia promotes etoposide (VP-16) resistance in neuroblastoma CHP126 cells. Pharmazie. 2010;65:51–6.

62. Chen Z, Han F, Du Y, Shi H, Zhou W. Hypoxic microenvironment in cancer: molecular mechanisms and therapeutic interventions. Signal Transduct Target Ther. 2023 Feb 17;8(1):70.

63. Applebaum MA, Jha AR, Kao C, Hernandez KM, DeWane G, Salwen HR, et al. Integrative genomics reveals hypoxia inducible genes that are associated with a poor prognosis in neuroblastoma patients. Oncotarget. 2016 Nov 22;7(47):76816–26.

64. Wang D, Weng Q, Zhang L, He Q, Yang B. VEGF and Bcl-2 Interact Via MAPKs Signaling Pathway in the Response to Hypoxia in Neuroblastoma. Cell Mol Neurobiol. 2009 May 2;29(3):391–401.

65. Das B, Yeger H, Tsuchida R, Torkin R, Gee MFW, Thorner PS, et al. A Hypoxia-Driven Vascular Endothelial Growth Factor/Flt1 Autocrine Loop Interacts with Hypoxia-Inducible Factor-1α through Mitogen-Activated Protein Kinase/Extracellular Signal-Regulated Kinase 1/2 Pathway in Neuroblastoma. Cancer Res. 2005 Aug 15;65(16):7267–75.

66. Holmquist-Mengelbier L, Fredlund E, Löfstedt T, Noguera R, Navarro S, Nilsson H, et al. Recruitment of HIF-1α and HIF-2α to common target genes is differentially regulated in neuroblastoma: HIF-2α promotes an aggressive phenotype. Cancer Cell. 2006 Nov;10(5):413–23.

67. Hyun JY, Chun YS, Kim TY, Kim HL, Kim MS, Park JW. Hypoxia-Inducible Factor 1alpha- Mediated Resistance to Phenolic Anticancer. Chemotherapy. 2004;50(3):119–26.

68. Hussein D, Estlin EJ, Dive C, Makin GWJ. Chronic hypoxia promotes hypoxia-inducible factor-1α–dependent resistance to etoposide and vincristine in neuroblastoma cells. Mol Cancer Ther. 2006 Sep 1;5(9):2241–50.

69. Qing G, Skuli N, Mayes PA, Pawel B, Martinez D, Maris JM, et al. Combinatorial Regulation of Neuroblastoma Tumor Progression by N-Myc and Hypoxia Inducible Factor HIF-1α. Cancer Res. 2010 Dec 15;70(24):10351–61.

70. Rössler J, Schwab M, Havers W, Schweigerer L. Hypoxia Promotes Apoptosis of Human Neuroblastoma Cell Lines with Enhanced N-myc Expression. Biochem Biophys Res Commun. 2001 Feb;281(2):272–6.

71. Zhang B, Yin CP, Zhao Q, Yue SW. Upregulation of HIF-1α by Hypoxia Protect Neuroblastoma Cells from Apoptosis by Promoting Survivin Expression. Asian Pacific Journal of Cancer Prevention. 2014 Oct 23;15(19):8251–7.

72. Gordan JD, Bertout JA, Hu CJ, Diehl JA, Simon MC. HIF-2α Promotes Hypoxic Cell Proliferation by Enhancing c-Myc Transcriptional Activity. Cancer Cell. 2007 Apr;11(4):335–47.

73. Herrmann A, Rice M, Lévy R, Pizer BL, Losty PD, Moss D, et al. Cellular memory of hypoxia elicits neuroblastoma metastasis and enables invasion by non-aggressive neighbouring cells. Oncogenesis. 2015 Feb 9;4(2):e138–e138.

74. Pietras A, Gisselsson D, Øra I, Noguera R, Beckman S, Navarro S, et al. High levels of HIF-2α highlight an immature neural crest-like neuroblastoma cell cohort located in a perivascular niche. J Pathol. 2008 Mar 14;214(4):482–8.

75. Covello KL, Kehler J, Yu H, Gordan JD, Arsham AM, Hu CJ, et al. HIF-2α regulates Oct-4: effects of hypoxia on stem cell function, embryonic development, and tumor growth. Genes Dev. 2006 Mar 1;20(5):557–70.

76. Hedborg F, Ullerås E, Grimelius L, Wassberg E, Maxwell PH, Hero B, et al. Evidence for hypoxia-induced neuronal-to-chromaffin metaplasia in neuroblastoma. The FASEB Journal. 2003 Apr;17(6):598–609.

77. Jögi A, Øra I, Nilsson H, Lindeheim Åsa, Makino Y, Poellinger L, et al. Hypoxia alters gene expression in human neuroblastoma cells toward an immature and neural crest-like phenotype. Proceedings of the National Academy of Sciences. 2002 May 14;99(10):7021–6.

78. Zaatiti H, Abdallah J, Nasr Z, Khazen G, Sandler A, Abou-Antoun T. Tumorigenic proteins upregulated in the MYCN-amplified IMR-32 human neuroblastoma cells promote proliferation and migration. Int J Oncol. 2018 Jan 4;

79. Rohwer N, Cramer T. Hypoxia-mediated drug resistance: Novel insights on the functional interaction of HIFs and cell death pathways. Drug Resistance Updates. 2011 Jun;14(3):191–201.

80. Wang KH, Chang YH, Ding DC. Bone Marrow Mesenchymal Stem Cells Promote Ovarian Cancer Cell Proliferation via Cytokine Interactions. Int J Mol Sci. 2024 Jun 19;25(12):6746.

81. Zhao L, Zhang K, He H, Yang Y, Li W, Liu T, et al. The Relationship Between Mesenchymal Stem Cells and Tumor Dormancy. Front Cell Dev Biol. 2021 Oct 12;9.

82. Gao X, Zhou J, Wang J, Dong X, Chang Y, Jin Y. Mechanism of exosomal miR-155 derived from bone marrow mesenchymal stem cells on stemness maintenance and drug resistance in myeloma cells. J Orthop Surg Res. 2021 Dec 24;16(1):637.

83. Wang J, Hendrix A, Hernot S, Lemaire M, De Bruyne E, Van Valckenborgh E, et al. Bone marrow stromal cell–derived exosomes as communicators in drug resistance in multiple myeloma cells. Blood. 2014 Jul 24;124(4):555–66.

84. Matamala Montoya M, van Slobbe GJJ, Chang JC, Zaal EA, Berkers CR. Metabolic changes underlying drug resistance in the multiple myeloma tumor microenvironment. Front Oncol. 2023 Apr 6;13.

85. Kushner BH, LaQuaglia MP, Bonilla MA, Lindsley K, Rosenfield N, Yeh S, et al. Highly effective induction therapy for stage 4 neuroblastoma in children over 1 year of age. Journal of Clinical Oncology. 1994 Dec;12(12):2607–13.

86. Smith V, Foster J. High-Risk Neuroblastoma Treatment Review. Children. 2018 Aug 28;5(9):114.

87. Park JR, Scott JR, Stewart CF, London WB, Naranjo A, Santana VM, et al. Pilot Induction Regimen Incorporating Pharmacokinetically Guided Topotecan for Treatment of Newly Diagnosed High-Risk Neuroblastoma: A Children's Oncology Group Study. Journal of Clinical Oncology. 2011 Nov 20;29(33):4351–7.

88. Garaventa A, Poetschger U, Valteau-Couanet D, Castel V, Elliott M, Ash S, et al. The randomised induction for high-risk neuroblastoma comparing COJEC and N5-MSKCC regimens: Early results from the HR-NBL1.5/SIOPEN trial. Journal of Clinical Oncology. 2018 May 20;36(15_suppl):10507–10507.

89. Kushner BH, Kramer K, LaQuaglia MP, Modak S, Yataghene K, Cheung NK V. Reduction From Seven to Five Cycles of Intensive Induction Chemotherapy in Children With High-Risk Neuroblastoma. Journal of Clinical Oncology. 2004 Dec 15;22(24):4888–92.

90. Garaventa A, Poetschger U, Valteau-Couanet D, Luksch R, Castel V, Elliott M, et al. Randomized Trial of Two Induction Therapy Regimens for High-Risk Neuroblastoma: HR-NBL1.5 International Society of Pediatric Oncology European Neuroblastoma Group Study. Journal of Clinical Oncology. 2021 Aug 10;39(23):2552–63.

91. Peinemann F, van Dalen E, Berthold F. Rapid COJEC Induction Therapy for High-risk Neuroblastoma Patients – Cochrane Review. Klin Padiatr. 2016 Apr 4;228(03):130–4.

92. Pearson AD, Pinkerton CR, Lewis IJ, Imeson J, Ellershaw C, Machin D. High-dose rapid and standard induction chemotherapy for patients aged over 1 year with stage 4 neuroblastoma: a randomised trial. Lancet Oncol. 2008 Mar;9(3):247–56.

93. Peinemann F, van Dalen E, Berthold F. Rapid COJEC Induction Therapy for High-risk Neuroblastoma Patients – Cochrane Review. Klin Padiatr. 2016 Apr 4;228(03):130–4.

94. Qiu B, Matthay KK. Advancing therapy for neuroblastoma. Nat Rev Clin Oncol. 2022 Aug 25;19(8):515–33.

95. Meczes EL, Pearson ADJ, Austin CA, Tilby MJ. Schedule-dependent response of neuroblastoma cell lines to combinations of etoposide and cisplatin. Br J Cancer. 2002 Feb 11;86(3):485–9.

96. Rizk M, Zou L, Savic R, Dooley K. Importance of Drug Pharmacokinetics at the Site of Action. Clin Transl Sci. 2017 May 3;10(3):133–42.

97. Aykul S, Martinez-Hackert E. Determination of half-maximal inhibitory concentration using biosensor-based protein interaction analysis. Anal Biochem. 2016 Sep;508:97–103.

98. McDermott M, Eustace AJ, Busschots S, Breen L, Crown J, Clynes M, et al. In vitro Development of Chemotherapy and Targeted Therapy Drug-Resistant Cancer Cell Lines: A Practical Guide with Case Studies. Front Oncol. 2014 Mar 6;4.

99. TU Y, CHENG S, ZHANG S, SUN H, XU Z. Vincristine induces cell cycle arrest and apoptosis in SH-SY5Y human neuroblastoma cells. Int J Mol Med. 2013 Jan 30;31(1):113–9.

100. Triarico S, Romano A, Attinà G, Capozza MA, Maurizi P, Mastrangelo S, et al. Vincristine-Induced Peripheral Neuropathy (VIPN) in Pediatric Tumors: Mechanisms, Risk Factors, Strategies of Prevention and Treatment. Int J Mol Sci. 2021 Apr 16;22(8):4112.

101. Chen Y, Yang L, Wang C, Wang C. Exploring the mechanism of resistance to vincristine in breast cancer cells using transcriptome sequencing technology. Oncol Lett. 2023 Oct 5;26(6):502.

102. Kavallaris M, Tait AS, Walsh BJ, He L, Horwitz SB, Norris MD, et al. Multiple microtubule alterations are associated with Vinca alkaloid resistance in human leukemia cells. Cancer Res. 2001 Aug 1;61(15):5803–9.

103. Verrills NM, Walsh BJ, Cobon GS, Hains PG, Kavallaris M. Proteome Analysis of Vinca Alkaloid Response and Resistance in Acute Lymphoblastic Leukemia Reveals Novel Cytoskeletal Alterations. Journal of Biological Chemistry. 2003 Nov;278(46):45082–93.

104. Jemaà M, Sime W, Abassi Y, Lasorsa V, Bonne Køhler J, Michaelis M, et al. Gene Expression Signature of Acquired Chemoresistance in Neuroblastoma Cells. Int J Mol Sci. 2020 Sep 16;21(18):6811.

105. Gamell C, Schofield A V., Suryadinata R, Sarcevic B, Bernard O. LIMK2 Mediates Resistance to Chemotherapeutic Drugs in Neuroblastoma Cells through Regulation of Drug-Induced Cell Cycle Arrest. PLoS One. 2013 Aug 21;8(8):e72850.

106. Rees DC, Johnson E, Lewinson O. ABC transporters: the power to change. Nat Rev Mol Cell Biol. 2009 Mar;10(3):218–27.

107. Zhou X, Wang X, Li N, Guo Y, Yang X, Lei Y. Therapy resistance in neuroblastoma: Mechanisms and reversal strategies. Front Pharmacol. 2023 Feb 16;14.

108. Pajic M, Norris MD, Cohn SL, Haber M. The role of the multidrug resistance-associated protein 1 gene in neuroblastoma biology and clinical outcome. Cancer Lett. 2005 Oct;228(1–2):241–6.

109. Breier A, Gibalova L, Seres M, Barancik M, Sulova Z. New Insight into P-Glycoprotein as a Drug Target. Anticancer Agents Med Chem. 2012 Dec 1;13(1):159–70.

110. Burkhart CA, Watt F, Murray J, Pajic M, Prokvolit A, Xue C, et al. Small-Molecule Multidrug Resistance–Associated Protein 1 Inhibitor Reversan Increases the Therapeutic Index of Chemotherapy in Mouse Models of Neuroblastoma. Cancer Res. 2009 Aug 15;69(16):6573–80.

111. Kurowski Ch, Berthold F. Presence of classical multidrug resistance and P-glycoprotein expression in human neuroblastoma cells. Annals of Oncology. 1998 Sep;9(9):1009–14.

112. Natarajan K, Xie Y, Baer MR, Ross DD. Role of breast cancer resistance protein (BCRP/ABCG2) in cancer drug resistance. Biochem Pharmacol. 2012 Apr;83(8):1084–103.

113. Nakanishi T, Ross DD. Breast cancer resistance protein (BCRP/ABCG2): its role in multidrug resistance and regulation of its gene expression. Chin J Cancer. 2012 Feb 5;31(2):73–99.

114. Yuan J, Lv H, Peng B, Wang C, Yu Y, He Z. Role of BCRP as a biomarker for predicting resistance to 5-fluorouracil in breast cancer. Cancer Chemother Pharmacol. 2009 May 27;63(6):1103–10.

115. Adamo A, Delfino P, Gatti A, Bonato A, Takam Kamga P, Bazzoni R, et al. HS-5 and HS-27A Stromal Cell Lines to Study Bone Marrow Mesenchymal Stromal Cell-Mediated Support to Cancer Development. Front Cell Dev Biol. 2020 Nov 5;8.

116. Podszywalow-Bartnicka P, Kominek A, Wolczyk M, Kolba MD, Swatler J, Piwocka K. Characteristics of live parameters of the HS-5 human bone marrow stromal cell line cocultured with the leukemia cells in hypoxia, for the studies of leukemia–stroma cross-talk. Cytometry Part A. 2018 Sep 3;93(9):929–40.

117. Kabrah S, May JE, Donaldson C, Morse HR. Abstracts of the 38th Annual Meeting of the United Kingdom Environmental Mutagen Society, 12th - 15th July 2015 at Plymouth University, UK. Mutagenesis. 2015 Nov 1;30(6):851–80.

118. ATCC. HS-5 [Internet]. 2023 [cited 2024 Jan 12]. Available from: https://www.atcc.org/products/crl-3611#detailed-product-information

119. Bavister BD, Poole KA. Duration and temperature of culture medium equilibration affect frequency of blastocyst development. Reprod Biomed Online. 2005 Jan;10(1):124–9.

120. Strober W. Trypan Blue Exclusion Test of Cell Viability. Curr Protoc Immunol. 2015 Nov 2;111(1).

121. Gautier M, Thirant C, Delattre O, Janoueix-Lerosey I. Plasticity in Neuroblastoma Cell Identity Defines a Noradrenergic-to-Mesenchymal Transition (NMT). Cancers (Basel). 2021 Jun 10;13(12):2904.

122. Kovalevich J, Langford D. Considerations for the Use of SH-SY5Y Neuroblastoma Cells in Neurobiology. In 2013. p. 9–21.

123. Driscoll J, Gondaliya P, Patel T. Tunneling Nanotube-Mediated Communication: A Mechanism of Intercellular Nucleic Acid Transfer. Int J Mol Sci. 2022 May 14;23(10):5487.

124. Wang X, Veruki ML, Bukoreshtliev N V., Hartveit E, Gerdes HH. Animal cells connected by nanotubes can be electrically coupled through interposed gap-junction channels. Proceedings of the National Academy of Sciences. 2010 Oct 5;107(40):17194–9.

125. Yu T, Li L, Liu W, Ya B, Cheng H, Xin Q. Silencing of NADPH Oxidase 4 Attenuates Hypoxia Resistance in Neuroblastoma Cells SH-SY5Y by Inhibiting PI3K/Akt-Dependent Glycolysis. Oncology Research Featuring Preclinical and Clinical Cancer Therapeutics. 2019 May 7;27(5):525–32.

126. Chen S, Zhang M, Xing L, Wang Y, Xiao Y, Wu Y. HIF-1α Contributes to Proliferation and Invasiveness of Neuroblastoma Cells via SHH Signaling. PLoS One. 2015 Mar 26;10(3):e0121115.

127. Glass JJ, Phillips PA, Gunning PW, Stehn JR. Hypoxia alters the recruitment of tropomyosins into the actin stress fibres of neuroblastoma cells. BMC Cancer. 2015 Dec 16;15(1):712.

128. Currò M, Ferlazzo N, Giunta ML, Montalto AS, Russo T, Arena S, et al. Hypoxia-Dependent Expression of TG2 Isoforms in Neuroblastoma Cells as Consequence of Different MYCN Amplification Status. Int J Mol Sci. 2020 Feb 18;21(4):1364.

129. Jagušić M, Forčić D, Brgles M, Kutle L, Šantak M, Jergović M, et al. Stability of Minimum Essential Medium functionality despite l-glutamine decomposition. Cytotechnology. 2016 Aug 24;68(4):1171–83.

130. Place TL, Domann FE, Case AJ. Limitations of oxygen delivery to cells in culture: An underappreciated problem in basic and translational research. Free Radic Biol Med. 2017 Dec;113:311–22.

131. Al-Ani A, Toms D, Kondro D, Thundathil J, Yu Y, Ungrin M. Oxygenation in cell culture: Critical parameters for reproducibility are routinely not reported. PLoS One. 2018 Oct 16;13(10):e0204269.

132. Wenger R, Kurtcuoglu V, Scholz C, Marti H, Hoogewijs D. Frequently asked questions in hypoxia research. Hypoxia. 2015 Sep;35.

133. Corning. Guidelines for use: Transwell® Permeable Supports [Internet]. 2024 [cited 2024 Jun 8]. p. 1. Available from: https://www.corning.com/worldwide/en/products/life-sciences/products/permeable-supports/transwell-guidelines.html

134. Morrison SJ, Csete M, Groves AK, Melega W, Wold B, Anderson DJ. Culture in Reduced Levels of Oxygen Promotes Clonogenic Sympathoadrenal Differentiation by Isolated Neural Crest Stem Cells. The Journal of Neuroscience. 2000 Oct 1;20(19):7370–6.

135. Yu JL, Chan S, Fung MKL, Chan GCF. Mesenchymal stem cells accelerated growth and metastasis of neuroblastoma and preferentially homed towards both primary and metastatic loci in orthotopic neuroblastoma model. BMC Cancer. 2021 Dec 10;21(1):393.

136. Chulpanova DS, Solovyeva V V., James V, Arkhipova SS, Gomzikova MO, Garanina EE, et al. Human Mesenchymal Stem Cells Overexpressing Interleukin 2 Can Suppress Proliferation of Neuroblastoma Cells in Co-Culture and Activate Mononuclear Cells In Vitro. Bioengineering. 2020 Jun 17;7(2):59.

137. Ma T, Wang M, Wang S, Hu H, Zhang X, Wang H, et al. BMSC derived EVs inhibit colorectal Cancer progression by transporting MAGI2-AS3 or something similar. Cell Signal. 2024 Sep;121:111235.

138. Massa M, Gasparini S, Baldelli I, Scarabelli L, Santi P, Quarto R, et al. Interaction Between Breast Cancer Cells and Adipose Tissue Cells Derived from Fat Grafting. Aesthet Surg J. 2016 Mar;36(3):358–63.

139. Chen R, Liu X, Tan N. Bone Marrow Mesenchymal Stem Cell (BMSC)-Derived Exosomes Regulates Growth of Breast Cancer Cells Mediated by Hedgehog Signaling Pathway. J Biomater Tissue Eng. 2023 Jan 1;13(1):157–61.

140. Zhang X, Sai B, Wang F, Wang L, Wang Y, Zheng L, et al. Hypoxic BMSC-derived exosomal miRNAs promote metastasis of lung cancer cells via STAT3-induced EMT. Mol Cancer. 2019 Dec 13;18(1):40.

141. Liu X, Jiang F, Wang Z, Tang L, Zou B, Xu P, et al. Hypoxic bone marrow mesenchymal cell-extracellular vesicles containing miR-328-3p promote lung cancer progression via the NF2-mediated Hippo axis. J Cell Mol Med. 2021 Jan 21;25(1):96–109.

142. Li M, Zhai P, Mu X, Song J, Zhang H, Su J. Hypoxic BMSC-derived exosomal miR-652-3p promotes proliferation and metastasis of hepatocarcinoma cancer cells via targeting TNRC6A. Aging. 2023 Nov 30;15(22):12780–93.

143. Yeh S, Yu J, Chou P, Wu S, Liao Y, Huang Y, et al. Proliferation and Differentiation Potential of Bone Marrow–Derived Mesenchymal Stem Cells From Children With Polydactyly and Adults With Basal Joint Arthritis. CellTransplantation. 2024 Jan 2;33(1).

144. Lee GY, Jeong SY, Lee HR, Oh IH. Age-related differences in the bone marrow stem cell niche generate specialized microenvironments for the distinct regulation of normal hematopoietic and leukemia stem cells. Sci Rep. 2019 Jan 30;9(1):1007.

145. Ghaffarian R, Muro S. Models and Methods to Evaluate Transport of Drug Delivery Systems Across Cellular Barriers. Journal of Visualized Experiments. 2013 Oct 17;(80).

146. Dominiak A, Chełstowska B, Olejarz W, Nowicka G. Communication in the Cancer Microenvironment as a Target for Therapeutic Interventions. Cancers (Basel). 2020 May 14;12(5):1232.

147. Brücher BLDM, Jamall IS. Cell-Cell Communication in the Tumor Microenvironment, Carcinogenesis, and Anticancer Treatment. Cellular Physiology and Biochemistry. 2014;34(2):213–43.

148. Dominiak A, Chełstowska B, Olejarz W, Nowicka G. Communication in the Cancer Microenvironment as a Target for Therapeutic Interventions. Cancers (Basel). 2020 May 14;12(5):1232.

149. Eugenin E, Camporesi E, Peracchia C. Direct Cell-Cell Communication via Membrane Pores, Gap Junction Channels, and Tunneling Nanotubes: Medical Relevance of Mitochondrial Exchange. Int J Mol Sci. 2022 May 30;23(11):6133.

150. Dhamdhere MR, Spiegelman VS. Extracellular vesicles in neuroblastoma: role in progression, resistance to therapy and diagnostics. Front Immunol. 2024 Apr 9;15.

151. Marimpietri D, Airoldi I, Faini AC, Malavasi F, Morandi F. The Role of Extracellular Vesicles in the Progression of Human Neuroblastoma. Int J Mol Sci. 2021 Apr 12;22(8):3964.

152. Hyllienmark L, Brismar T. Effect of hypoxia on membrane potential and resting conductance in rat hippocampal neurons. Neuroscience. 1999 Jun;91(2):511–7.

153. Kravtsova V V., Fedorova AA, Tishkova M V., Livanova AA, Matytsin VO, Ganapolsky VP, et al. Short-Term Mild Hypoxia Modulates Na,K-ATPase to Maintain Membrane Electrogenesis in Rat Skeletal Muscle. Int J Mol Sci. 2022 Oct 6;23(19):11869.

154. Yang M, Brackenbury WJ. Membrane potential and cancer progression. Front Physiol. 2013;4.

155. McMillen P, Oudin MJ, Levin M, Payne SL. Beyond Neurons: Long Distance Communication in Development and Cancer. Front Cell Dev Biol. 2021 Sep 21;9.

156. Ganguly A, Cabral F. New insights into mechanisms of resistance to microtubule inhibitors. Biochimica et Biophysica Acta (BBA) - Reviews on Cancer. 2011 Dec;1816(2):164–71.

157. Ong V, Liem NLM, Schmid MA, Verrills NM, Papa RA, Marshall GM, et al. A Role for Altered Microtubule Polymer Levels in Vincristine Resistance of Childhood Acute Lymphoblastic Leukemia Xenografts. Journal of Pharmacology and Experimental Therapeutics. 2008 Feb;324(2):434–42.

158. Ottonelli I, Caraffi R, Tosi G, Vandelli MA, Duskey JT, Ruozi B. Tunneling Nanotubes: A New Target for Nanomedicine? Int J Mol Sci. 2022 Feb 17;23(4):2237.

159. Zurzolo C. Tunneling nanotubes: Reshaping connectivity. Curr Opin Cell Biol. 2021 Aug;71:139–47.

160. Melwani PK, Pandey BN. Tunneling nanotubes: The intercellular conduits contributing to cancer pathogenesis and its therapy. Biochimica et Biophysica Acta (BBA) - Reviews on Cancer. 2023 Nov;1878(6):189028.

161. Munson J, Shieh A. Interstitial fluid flow in cancer: implications for disease progression and treatment. Cancer Manag Res. 2014 Aug;317.

162. Thirant C, Peltier A, Durand S, Kramdi A, Louis-Brennetot C, Pierre-Eugène C, et al. Reversible transitions between noradrenergic and mesenchymal tumor identities define cell plasticity in neuroblastoma. Nat Commun. 2023 May 4;14(1):2575.

163. Piskareva O, Harvey H, Nolan J, Conlon R, Alcock L, Buckley P, et al. The development of cisplatin resistance in neuroblastoma is accompanied by epithelial to mesenchymal transition in vitro. Cancer Lett. 2015 Aug;364(2):142–55.

164. Siddik ZH. Cisplatin: mode of cytotoxic action and molecular basis of resistance. Oncogene. 2003 Oct 20;22(47):7265–79.

165. Galluzzi L, Senovilla L, Vitale I, Michels J, Martins I, Kepp O, et al. Molecular mechanisms of cisplatin resistance. Oncogene. 2012 Apr 12;31(15):1869–83.

166. Dilruba S, Kalayda G V. Platinum-based drugs: past, present and future. Cancer Chemother Pharmacol. 2016 Jun 17;77(6):1103–24.

167. Browning RJ, Reardon PJT, Parhizkar M, Pedley RB, Edirisinghe M, Knowles JC, et al. Drug Delivery Strategies for Platinum-Based Chemotherapy. ACS Nano. 2017 Sep 26;11(9):8560–78.

168. Dasari S, Bernard Tchounwou P. Cisplatin in cancer therapy: Molecular mechanisms of action. Eur J Pharmacol. 2014 Oct;740:364–78.

169. Dilruba S, Kalayda G V. Platinum-based drugs: past, present and future. Cancer Chemother Pharmacol. 2016 Jun 17;77(6):1103–24.

170. Galluzzi L, Senovilla L, Vitale I, Michels J, Martins I, Kepp O, et al. Molecular mechanisms of cisplatin resistance. Oncogene. 2012 Apr 12;31(15):1869–83.

171. Sun CY, Zhang QY, Zheng GJ, Feng B. Phytochemicals: Current strategy to sensitize cancer cells to cisplatin. Biomedicine & Pharmacotherapy. 2019 Feb;110:518–27.

172. Devarajan N, Manjunathan R, Ganesan SK. Tumor hypoxia: The major culprit behind cisplatin resistance in cancer patients. Crit Rev Oncol Hematol. 2021 Jun;162:103327.

173. Siddik ZH. Cisplatin: mode of cytotoxic action and molecular basis of resistance. Oncogene. 2003 Oct 20;22(47):7265–79.

174. Song X, Liu X, Chi W, Liu Y, Wei L, Wang X, et al. Hypoxia-induced resistance to cisplatin and doxorubicin in non-small cell lung cancer is inhibited by silencing of HIF-1α gene. Cancer Chemother Pharmacol. 2006 Dec 11;58(6):776–84.

175. Hao J, Song X, Song B, Liu Y, Wei L, Wang X, et al. Effects of lentivirus-mediated HIF-1α knockdown on hypoxia-related cisplatin resistance and their dependence on p53 status in fibrosarcoma cells. Cancer Gene Ther. 2008 Jul 18;15(7):449–55.

176. Zhang F, Duan S, Tsai Y, Keng PC, Chen Y, Lee SO, et al. Cisplatin treatment increases stemness through upregulation of hypoxia-inducible factors by interleukin-6 in non-small cell lung cancer. Cancer Sci. 2016 Jun 3;107(6):746–54.

177. Ahmed EM, Bandopadhyay G, Coyle B, Grabowska A. A HIF-independent, CD133-mediated mechanism of cisplatin resistance in glioblastoma cells. Cellular Oncology. 2018 Jun 28;41(3):319–28.

178. Chen X, Wang J, Fu Z, Zhu B, Wang J, Guan S, et al. Curcumin activates DNA repair pathway in bone marrow to improve carboplatin-induced myelosuppression. Sci Rep. 2017 Dec 18;7(1):17724.

179. Cheng Y ju, Wu R, Cheng M liang, Du J, Hu X wei, Yu L, et al. Carboplatin-induced hematotoxicity among patients with non-small cell lung cancer: Analysis on clinical adverse events and drug-gene interactions. Oncotarget. 2017 May 9;8(19):32228–36.

180. Sousa GF de, Wlodarczyk SR, Monteiro G. Carboplatin: molecular mechanisms of action associated with chemoresistance. Brazilian Journal of Pharmaceutical Sciences. 2014 Dec;50(4):693–701.

181. Fan J, Li H, Ruan Q, Zhu X, Jing P, Gu Z. The PRMT5 inhibitor C9 mitigates hypoxia-induced carboplatin resistance in lung cancer by inducing autophagy. Cell Biol Int. 2023 Oct 28;47(10):1702–15.

182. Gamal-Eldeen AM, Alrehaili AA, Alharthi A, Raafat BM. Perftoran® Inhibits Hypoxia-Associated Resistance in Lung Cancer Cells to Carboplatin. Front Pharmacol. 2022 Mar 24;13.

183. Zhang W, Gou P, Dupret JM, Chomienne C, Rodrigues-Lima F. Etoposide, an anticancer drug involved in therapy-related secondary leukemia: Enzymes at play. Transl Oncol. 2021 Oct;14(10):101169.

184. Hainsworth JD, Greco FA. Etoposide: Twenty years later. Annals of Oncology. 1995 Apr;6(4):325–39.

185. Sinkule JA. Etoposide: A Semisynthetic Epipodophyllotoxin Chemistry, Pharmacology, Pharmacokinetics, Adverse Effects and Use as an Antineoplastic Agent. Pharmacotherapy: The Journal of Human Pharmacology and Drug Therapy. 1984 Mar 4;4(2):61–71.

186. Jaffrezou JP, Chen G, Duran GE, Kuhl JS, Sikic BI. Mutation Rates and Mechanisms of Resistance to Etoposide Determined From Flucattion Analysis. JNCI Journal of the National Cancer Institute. 1994 Aug 3;86(15):1152–8.

187. Alpsoy A, Yasa S, Gündüz U. Etoposide resistance in MCF-7 breast cancer cell line is marked by multiple mechanisms. Biomedicine & Pharmacotherapy. 2014 Apr;68(3):351–5.

188. Cosse JP, Sermeus A, Vannuvel K, Ninane N, Raes M, Michiels C. Differential effects of hypoxia on etoposide-induced apoptosis according to the cancer cell lines. Mol Cancer. 2007 Dec 26;6(1):61.

189. Piret JP, Cosse JP, Ninane N, Raes M, Michiels C. Hypoxia protects HepG2 cells against etoposide-induced apoptosis VIA a HIF-1-independent pathway. Exp Cell Res. 2006 Sep;312(15):2908–20.

190. Sullivan R, Graham CH. Hypoxia prevents etoposide-induced DNA damage in cancer cells through a mechanism involving hypoxia-inducible factor 1. Mol Cancer Ther. 2009 Jun 1;8(6):1702–13.

191. Sermeus A, Cosse JP, Crespin M, Mainfroid V, de Longueville F, Ninane N, et al. Hypoxia induces protection against etoposide-induced apoptosis: molecular profiling of changes in gene expression and transcription factor activity. Mol Cancer. 2008 Dec 26;7(1):27.

192. Stork CM, Schreffler SM. Cyclophosphamide. In: Encyclopedia of Toxicology. Elsevier; 2014. p. 1111–3.

193. Gamcsik MP, Dolan ME, Andersson BS, Murray D. Mechanisms of resistance to the toxicity of cyclophosphamide. Curr Pharm Des. 1999 Aug;5(8):587–605.

194. Barnett S, Errington J, Sludden J, Jamieson D, Poinsignon V, Paci A, et al. Pharmacokinetics and Pharmacogenetics of Cyclophosphamide in a Neonate and Infant Childhood Cancer Patient Population. Pharmaceuticals. 2021 Mar 16;14(3):272.

195. Tasso MJ, Boddy A V., Price L, Wyllie RA, Pearson ADJ, Idle JR. Pharmacokinetics and metabolism of cyclophosphamide in paediatric patients. Cancer Chemother Pharmacol. 1992;30(3):207–11.

196. Veal GJ, Cole M, Errington J, Pearson ADJ, Gerrard M, Whyman G, et al. Pharmacokinetics of carboplatin and etoposide in infant neuroblastoma patients. Cancer Chemother Pharmacol. 2010 May 23;65(6):1057–66.

197. Riccardi R, Riccardi A, Lasorella A, Di Rocco C, Carelli G, Tornesello A, et al. Clinical pharmacokinetics of carboplatin in children. Cancer Chemother Pharmacol. 1994 Nov;33(6):477–83.

198. Newell DR, Siddik ZH, Gumbrell LA, Boxall FE, Gore ME, Smith IE, et al. Plasma free platinum pharmacokinetics in patients treated with high dose carboplatin. Eur J Cancer Clin Oncol. 1987 Sep;23(9):1399–405.

199. Peng B, English MW, Boddy AV, Price L, Wyllie R, Pearson ADJ, et al. Cisplatin pharmacokinetics in children with cancer. Eur J Cancer. 1997 Oct;33(11):1823–8.

200. Ivanov AI, Christodoulou J, Parkinson JA, Barnham KJ, Tucker A, Woodrow J, et al. Cisplatin Binding Sites on Human Albumin. Journal of Biological Chemistry. 1998 Jun;273(24):14721–30.

201. Liu B, Earl HM, Poole CJ, Dunn J, Kerr DJ. Etoposide protein binding in cancer patients. Cancer Chemother Pharmacol. 1995;36(6):506–12.

202. Bisogno G, Cowie F, Boddy A, Thomas H, Dick G, Pinkerton C. High-dose cyclosporin with etoposide - toxicity and pharmacokinetic interaction in children with solid tumours. Br J Cancer. 1998 Jun;77(12):2304–9.

203. van de Velde ME, Panetta JCarl, Wilhelm AJ, van den Berg MH, van der Sluis IM, van den Bos C, et al. Population Pharmacokinetics of Vincristine Related to Infusion Duration and Peripheral Neuropathy in Pediatric Oncology Patients. Cancers (Basel). 2020 Jul 4;12(7):1789.

204. Sethi VS, Kimball JimC. Pharmacokinetics of vincristine sulfate in children. Cancer Chemother Pharmacol. 1981 Oct;6(2).

205. Barnett S, Hellmann F, Parke E, Makin G, Tweddle DA, Osborne C, et al. Vincristine dosing, drug exposure and therapeutic drug monitoring in neonate and infant cancer patients. Eur J Cancer. 2022 Mar;164:127–36.

206. Wang L, Zhao X, Fu J, Xu W, Yuan J. The Role of Tumour Metabolism in Cisplatin Resistance. Front Mol Biosci. 2021 Jun 23;8.

207. Brock P, Rajput K, Edwards L, Meijer A, Simpkin P, Hoetink A, et al. Cisplatin Ototoxicity in Children. In: Hearing Loss - From Multidisciplinary Teamwork to Public Health. IntechOpen; 2021.

8. Supplementary S1: Additional background on the cell lines

HS-5 cell line has been previously implemented to study leukemia-stroma interaction in normoxic and hypoxic conditions [116]. Hypoxic culture conditions did not affect HS-5 cell viability, proliferation rate or cell cycle. Follow-up experiments have shown the stromal protection from chemo-induced cell death of leukemia cells, proving its relevance as an in vitro model to study stroma-tumor cell interaction.

Granulocyte colony-stimulating factor (G-CSF), granulocyte-macrophage-CSF (GM-CSF), macrophage-CSF (M-CSF), Kit-ligand (KL), macrophage-inhibitory protein-1 alpha, interleukin-6 (IL-6), IL-8, and IL-11 are significantly secreted by HS-5 cells [115]. Moreover, HS-5 cells support the proliferation of hematopoietic progenitor cells. Both primary BM-MSCs and HS-5 cell lines are positive for CD73, CD90, CD105, and HLA-ABC, while lacking expression of CD14, CD31, CD34, CD45, and HLA-DR surface molecules. However, for HS-5 statistically significant higher expression of CD73 and HLA-ABC was found, as well as lower expression of CD90 when compared to BM-MSCs. Nonetheless, HS-5 demonstrates a general expression pattern similar to primary BM-MSCs, in contrast to for instance the HS-27A cell line. Moreover, HS-5 cells have been suggested to be a suitable model to reproduce the typical MSC expression pattern responsible for pro-tumor cellular interactions and immunosuppressive activity. Primary MSCs and HS-5 cell line show high similarity in immunological activity. It has therefore been concluded that HS-5 stromal cell line can be used to reproduce the capacity of MSCs to influence tumor biology and to evaluate the molecular mechanisms that underly tumor immune escape.

A study by Thirant et al. (2023) [162] has shown *PHOX2B* and *CD44* as specific makers for the adrenergic and mesenchymal population, respectively. *CD44* expression at transcription level correlates with mesenchymal tumor cell identity. While CD44 is a cell surface marker, it can be used to sort the two populations, using FACS. $CD44^{neg}$ cells exhibit transcriptomic profiles close to the adrenergic SH-SY5Y cell line, while $CD44^{pos}$ sorted cells have profiles close to mesenchymal SHEP-2 cells. The mesenchymal/$CD44^{pos}$ cell population show higher chemotherapy resistance compared to the adrenergic/$CD44^{neg}$ cells. The CD44 surface marker is an alternative to the previously used CD133 cell surface protein used to discriminate between adrenergic and mesenchymal cells. The CD133 cell surface maker is found to be downregulated in response to *in vitro* culture with serum-containing medium.

Cells demonstrate an adrenergic to mesenchymal plasticity potential [121]. The spontaneous plasticity depends on epigenetic reprogramming. This reprogramming potential is maintained through multiple generations in the SK-N-SH cell line. The ADRN-to-MES switch has been associated with cisplatin and etoposide drug resistance [163]and has been correlated with hypoxia [39,48].

9. Supplementary S2: Detailed scheme of the rapid COJEC regimen for neuroblastoma treatment

The rapid COJEC regimen consists of three different courses (A, B and C) that are given to the patient in specific time intervals and orders. Table 1 indicates the different courses and the included chemotherapeutics as well as the administration protocol in pediatric cancer treatment. Course A (vincristine, carboplatin, etoposide) is given on day 0 and day 40. Course B (vincristine, cisplatin) starts on days 10, 30, 50 and 70. Course C (vincristine, etoposide, cyclophosphamide) is given on days 20 and 60.

Table S1: Detailed overview of the rapid COJEC induction chemotherapy treatment in pediatric treatment of neuroblastoma.

Course A (day 0 and day 40)

Drug	Time	Dose	Administration
Day 1			
Vincristine	H0	1.5 mg/m^2	Single IV bolus over 1 hour
Carboplatin	H1	750 mg/m^2	IV infused, 1 hour, in 5% dextrose
Etoposide	H2	175 mg/m^2	IV infused, 4 hours, 0.9% saline
Day 2			
Etoposide	H0	175 mg/m^2	IV infused, 4 hours, 0.9% saline

Course B (day 10, day 30, day 50, and day 70)

Drug	Time	Dose	Administration
Day 1			
Vincristine	H0	1.5 mg/m^2	Single IV bolus over 1 hour
Pre-hydration	H1	200 ml/m^2/h	Infused over 3 hours before cisplatin
Mannitol 20%	H1	40 ml/m^2	Short infusion IV
Mannitol 20%	H3.5	40 ml/m^2	Short infusion IV
Hydration during cisplatin	H4	125 ml/m^2/h	Infused over 24 hours in parallel with cisplatin
Cisplatin	H4	80 mg/m^2/24h	Over 24 hours in 0.9% sodium chloride alongside the hydration
Over day 2			
Post-hydration	H28-H52	125 ml/m^2/h	Same as hydration during cisplatin
Mannitol 20%	If needed	40 ml/m^2	If diuresis falls below 400 ml/m^2/6 hours, short infusion IV

Course C (day 20 and day 60)

Drug	Time	Dose	Administration
Day 1			
Vincristine	H0	1.5 mg/m^2	Single IV bolus over 1 hour
Etoposide	H1	175 mg/m^2	IV infused, 4 hours, in 5% dextrose
Mesna	H5	200 mg/m^2	Short infusion IV
Cyclophosphamide	H5	1050 mg/m^2	Over 1 hour
Hyperhydration + mesna	H5	125 ml/ m^2 h + 1.2 200 g/m^2/24h	Infused over 24 hours
Day 2			
Etoposide	H0	175 mg/m^2	IV infused, 4 hours, 0.9% saline
Cyclophosphamide	H4	1050 mg/m^2	Over 1 hour
Hyperhydration + mesna	H4	40 ml/m^2	Infused over 24 hours

In addition, G-CSF (5μg/kg/day subcutaneously) is administered 24-48 hours after the end of the chemotherapy and is ended 48 hours before the next chemotherapy. The minimum interval between the last G-CSF injection and the start of the next chemotherapy course is at least 24 hours. This means G-CSF is administered from day 3 to 8, day 12 to 18, day 23 to 28, day 32 to 38, day 43 to 48, day 52 to 58, day 63 to 68, and day 72 to 76.

Additional TVD cycles

If the rapid COJEC treatment protocol does not yield metastatic complete response (disappearance of all signs of metastatic cancer), the COJEC regimen is followed by two so-called TVD cycles, that include treatment with topotecan, vincristine and doxorubicin:

- Topotecan: IV administered in the morning, as a 30-minute infusion in saline 100 ml/m2 at dose of 1.5 mg/m2/day for 5 consecutive days (days 1 to 5).
- Vincristine: 48-hour continuous infusion administration at a dose of 1 mg/m2/day in 50 ml/m^2/day 0.9% saline (maximum dose 1mg/day), starting one hour after the final topotecan infusion (days 5 and 6).
- Doxorubicin: 48-hour continuous infusion administered simultaneously with vincristine at a dose of 22.5 mg/m2/day in 50 ml/m^2/day of 0.9% saline solution (days 5 and 6).

A second cycle is administered at the same dose 21-28 days from the start of the first cycle. In addition, the patient should be off G-CSF for at least 48 hours.

10. Supplementary S3: Detailed elaboration on the COJEC chemotherapeutics

Cisplatin

Originally in 1978 *cis*-diamminedichloroplatinum(II) (known as cisplatin, or CDDP), a platinum-based chemotherapeutic, was used to treat several malignancies including testicular, bladder, ovarian, colorectal, lung, and head and neck cancers [164–167]. It kills tumor cells by creating irreparable DNA lesions, causing cellular senescence, or activating apoptotic pathways [168]. Due to the relatively low concentration of chloride ions in the cell, the inert cisplatin is activated intracellularly by a series of aquation reactions, resulting in aquated cisplatin which is highly reactive [169,170]. This activated cisplatin can bind a variety of nucleophilic species, including cysteine and methionine residues on proteins and DNA bases. This leads to inter- and intra-strand adducts in the nucleus, that are recognized by DNA damage-sensing machinery. If the DNA damage is too extensive, DNA damage response (DDR) is activated, involving ATR kinase, CHEK1 and CHEK2, as well as the tumor suppressor protein p53. Activation of p53 results in transactivation of several pathways, facilitating mitochondrial outer membrane permeabilization, triggering intrinsic apoptosis. In addition, p53 activation results in transactivation of genes involved in extrinsic apoptotic pathway. The mitochondrial outer membrane permeabilization triggers the caspase cascade and several caspase-independent mechanisms. Multiple other signaling pathways are involved in cisplatin induced cell death following DNA damage. The interaction between cisplatin and GSH, metallothionein and/or mitochondrial proteins, elicits generation of reactive oxygen species (ROS). These can result in mitochondrial outer membrane permeabilization or cause an increase in cisplatin-induced DNA damage, leading to cytotoxicity.

However, little or no response in tumor cells is observed for many cancer patients, leading to therapy failure and cancer relapse [171]. Based on recent investigations this cisplatin resistance is assigned to the hypoxic microenvironment [172]. Many different mechanisms are believed to precede cisplatin resistance. These include decreased p53 expression, increased cancer stemness, regulation of non-coding RNAs, generation of reactive oxygen species, increased exosome secretion, loss of mismatch repair, cyclophilin overexpression, and surviving overexpression [169,173].

In hypoxic conditions, the cisplatin resistance is hypothesized to be related to the HIF-1α correlated response to hypoxia. Silencing of HIF-1α in hypoxic cells reverse cisplatin drug resistance in human non-small cell lung carcinoma cells [174]. p53 plays a significant role in this HIF-1 mediated cisplatin resistance [175]. Cisplatin kills tumor cells by upregulation of p53, which induces cell cycle arrest and triggers apoptosis in tumor cells. HIF-1 suppresses p53 expression in the hypoxic tumor microenvironment, thus creating a more cisplatin resistant cellular phenotype. In addition, IL-6 mediated HIF-1α synthesis promotes the stemness of cancer stem cells, inducing insensitivity to cisplatin therapy [176]. Moreover, the hypoxic microenvironment up-regulates the expression of stem cell marker CD133, which enhances their stem cell properties and increases cisplatin resistance, however knock-down of CD133 siRNA reduces cisplatin resistance via a HIF independent manner [177]. Interestingly, cisplatin resistance is accompanied by ADRN-to-MES-transition [163].

Carboplatin

To reduce the side effects of cisplatin, the less nephron- and neurotoxic carboplatin (*cis*-diamine(cyclobutene-1,1-dicarboxylate-O,O') platinum(II)) was developed as a second-generation platinum drug. The active form of carboplatin is the same as that of cisplatin. The mechanism of action of carboplatin is therefore similar to that of cisplatin. Carboplatin has prominent side effects concerning the bone marrow. The dose-limiting toxicity of carboplatin is myelosuppression. Carboplatin is known to inhibit bone marrow cell viability [178]. In comparison to cisplatin, carboplatin presents with a bigger risk of bone marrow suppression [179].

Intracellular mechanisms causing carboplatin drug resistance include [180]: increased drug detoxification by the thiol groups in metallothionein and glutathione, increased DNA repair, and improved tolerance to nuclear damage, resulting in reduced apoptosis and decreased accumulation of intracellular carboplatin. Comparable to cisplatin, metal transporters are involved in the mechanism of resistance to carboplatin, including copper transporters CTR1, ATP7A and ATP7B [180]. Under hypoxic conditions, hypoxia induced carboplatin resistance is mitigated by PRMT5 in lung cancer cells [181]. PRMT5 is an arginine methyltransferase, involved in regulation of gene expression, chromatin remodeling and signal transduction. It was observed that hypoxia resulted in PRMT5 upregulation and PRMT5 overexpression promoted carboplatin resistance. The underlying mechanism for PRMT5 mediated carboplatin resistance is correlated with ULK1 methylation. PRMT5 overexpression results in ULK1 hypermethylation, leading to upregulation of autophagy improving the survival of cancer cells in hypoxic conditions. In addition, several other hypoxia-linked pathways are involved in platinum resistance. These include [182]:

1. hypoxia induced apoptosis suppression: for instance, hypoxia inhibits sirtuin 1 (SIRT1), leading to low 5' adenosine monophosphate (AMP)-activated protein kinase and inhibiting apoptosis;
2. hypoxia induced increase in mediators of the survival signaling pathway such as nucleotide excision repair pathways and nuclear factor κB (NF-κB);
3. hypoxia induced adaptation through two key proteins, hypoxia-inducible factor-1 (HIF-1) and HIF-2, where HIF controls tumor growth, cell metabolism, differentiation, and angiogenesis and HIF potentiating the development and progress of cancer.

Etoposide

Etoposide is a topoisomerase type II (TOP2) inhibitor [183]. TOP2 plays a crucial role in DNA replication and regulates under- and over-winding of DNA by creating double stranded breaks and resealing the double stranded DNA. Etoposide inhibits TOP2 by stabilization of the transient TOP2-DNA cleaved complex. Without repair of this complex, nuclease, or tyrosyl-DNA-phosphodiesterase-2 (TDP2) will remove TOP2 from the complex, resulting in irreversible double-strand DNA breaks.

Etoposide is relatively well-tolerated. Most common toxic side effects of etoposide include alopecia and gastrointestinal toxicity. This includes nausea, vomiting, and stomatitis. However, in comparison to other chemotherapeutic medication, the gastrointestinal toxicity is relatively mild. Myelosuppression is the dose-limiting side effect of etoposide [184,185]

Mechanisms of resistance to etoposide may include altered TOP2 expression, DNA damage response proteins, and multidrug resistance by MDR1 and MRP [186,187]. The literature on hypoxia-induced drug resistance to etoposide is somewhat contradictory. It is suggested that etoposide-induced DNA damage is not influenced by hypoxia [188]. However, in many studies, hypoxia is observed to cause etoposide resistance [61,189–191]. This effect is also observed in neuroblastoma CHP126 cells [61].

Cyclophosphamide

Cyclophosphamide is a nitrogen mustard drug, affecting cells through alkylation of DNA [192]. Cyclophosphamide has to be metabolically processed by enzymes in the liver to form its active metabolites. First hydroxy-cyclophosphamide is formed, followed by aldo-phosphamide and finally the active agent phosphoramide mustard and acrolein. Phosphoramide mustard causes cross-linkage between DNA strands, leading to apoptosis.

Cyclophosphamide drug resistance is hypothesized to be caused by glutathione detoxification, repair of the DNA lesions trough nucleotide excision repair, and the repair enzyme O6-alkylguanine-DNA-alkyltransferase [193].

Table S2: Overview of rapid COJEC chemotherapeutics in pediatric cancer treatment

	Vincristine	Etoposide	Cisplatin	Carboplatin	Cyclophosphamide
Molecular weight	824.92	588.56	301.1	371.25	261.086
Common abbreviation	VCR or VNCR	VP-16 or EPEG	CDDP	CBDCA	CTX
Plasma protein binding	75%	94 – 97%	65 – 98%	29% for carboplatin, 85 – 90% for platinum	12 – 14%
Cmax total (μM)	0.104 (for 1.5 mg/m^2)	56.07 (for 150 mg/m^2 1h infusion)	19.9 (for 100 mg/m^2 as 24h infusion)	-	-
Cmax free (μM)	-	42.3 (for 100 mg/m^2 infusion for 2h)	1.03 (for 100 mg/m^2 as 24h infusion)	155.2 (for 600 mg/m^2 1h infusion)	Phosphoramide mustard: 90.5 (for 1500 mg/m^2/day)
Time to Cmax	At the end of infusion	1 – 1.5h	At the end of infusion	~ 2 – 4h	~ 1 – 2h
Terminal half-life	2.5h	3 – 12h	30 min for free drug	~ 2 – 5h	~ 2.5 – 6.5h
Time to 5% Cmax	~ 6 – 10h	~ 20 – 46h	2 – 3h (after end of infusion) 26 – 27h including infusion time	~7 – 9h	Phosphoramide mustard: ~ 5 – 7h Cyclophosphamide : ~17h
Mechanism of action in short	Interference with microtubule formation	Interference with Topoisomerase-II result in irreversible double-strand DNA breaks	Formation of DNA adducts (damage) and mitochondrial DNA damage	Formation of DNA adducts (damage) and mitochondrial DNA damage	DNA alkylation and not cell-cycle phase-specific protein synthesis inhibition
Literature	[203–205]	[184,185,196,201,202]	[168,199,200]	[196–198]	[194,195]

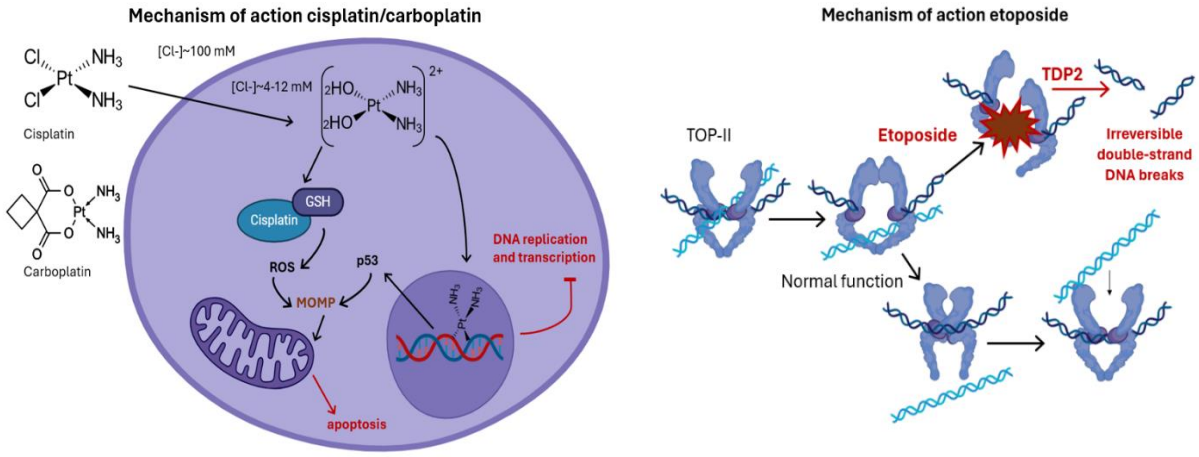

Fgure S1: Simple overview of the mechanism of action of cisplatin and carboplatin (left) and etoposide (right). Cisplatin and carboplatin perform cytotoxic effects by forming DNA adducts that suppresses DNA replication and transcription. Subsequent p53 activation results in transactivation of several pathways, facilitating mitochondrial outer membrane permeabilization (MOMP). Also, the interaction between cisplatin and GSH cause generation of ROS resulting in MOMP. Altogether, apoptosis is induced. Etoposide functions by impairing topoisomerase-II function, resulting in double stranded DNA breaks. Created with biorender (13-06-24), based on [183,206,207].

11. Supplementary S4: HS-5 proliferation in monoculture with and without presence of a transwell insert

To assess if introducing the transwell insert affects the proliferation in a monoculture situation, HS-5 cells were cultured in an empty, standard 12-well plate and in a 12-well plate with the insertion of a transwell insert. Proliferation was normalized to the standard monoculture in normoxia.

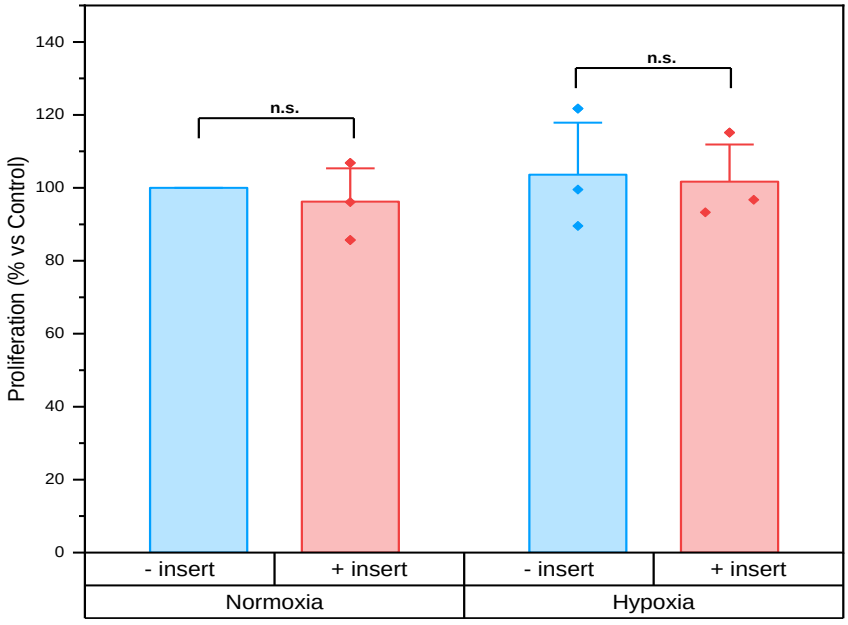

*Figure S2: The addition of a transwell insert into the culture plate does not affect the proliferation of HS-5 cells. Hypoxia does not affect the proliferation of HS-5 cell proliferation. Normoxia, - insert = Normoxia without a transwell insert; Normoxia, + insert = Normoxia with a transwell insert; Hypoxia, - insert = Hypoxia without a transwell insert; Hypoxia, + insert = Hypoxia with a transwell insert. Statistical significance *P<0.05, **P<0.01, n.s. not significant, n=3.*

No significant difference in proliferation was found in presence of the transwell insert compared to the absence of transwell insert. This indicates that, despite culture medium proteins and components may adhere to the plastic of the transwell insert, this does not further affect the proliferation of the cells.

12. Supplementary S5: HS-5 proliferation and response to chemotherapy in monoculture and in co-culture with the neuroblastoma cell lines

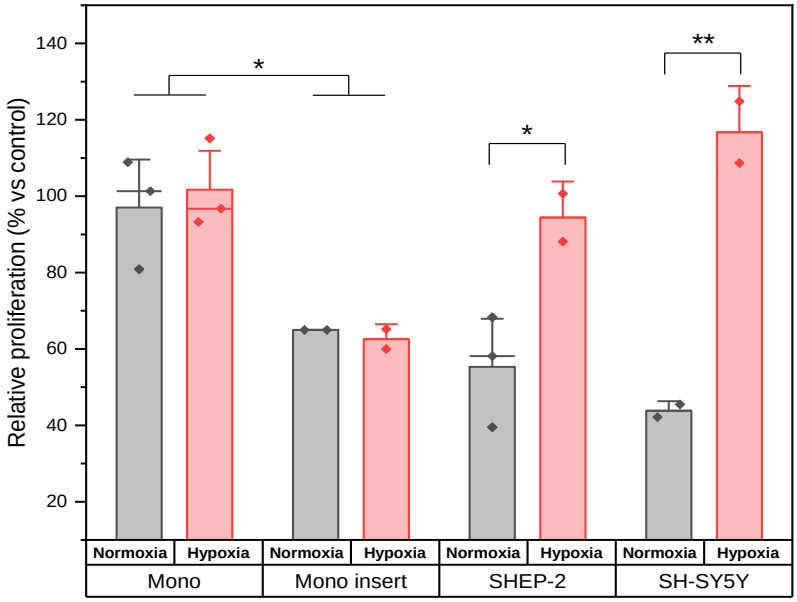

*Figure S3: HS-5 proliferation in mono-culture and co-culture. 1) Mono: the culture of HS-5 in a standard 12-well plate (VWR, 734-2324) in comparison to the culture in a standard 12-well plate by Corning (3513) showing the manufacturer of the 12-well plate does not affect the proliferation. 2) Mono insert: the proliferation of HS-5 cells is significantly (P= 0.04572) reduced when cultured on the polycarbonate transwell insert. 3) SHEP and SH-SY5Y indicate the co-culture conditions. In co-culture with SH-SY5Y, the proliferation of the HS-5 is significantly increased in hypoxia in comparison to normoxia (P=0.0011). The same is observed for the co-culture of HS-5 and SHEP-2 cells (P=0.0227). Statistical significance *P<0.05, **P<0.01, n.s. not significant, n=3.*

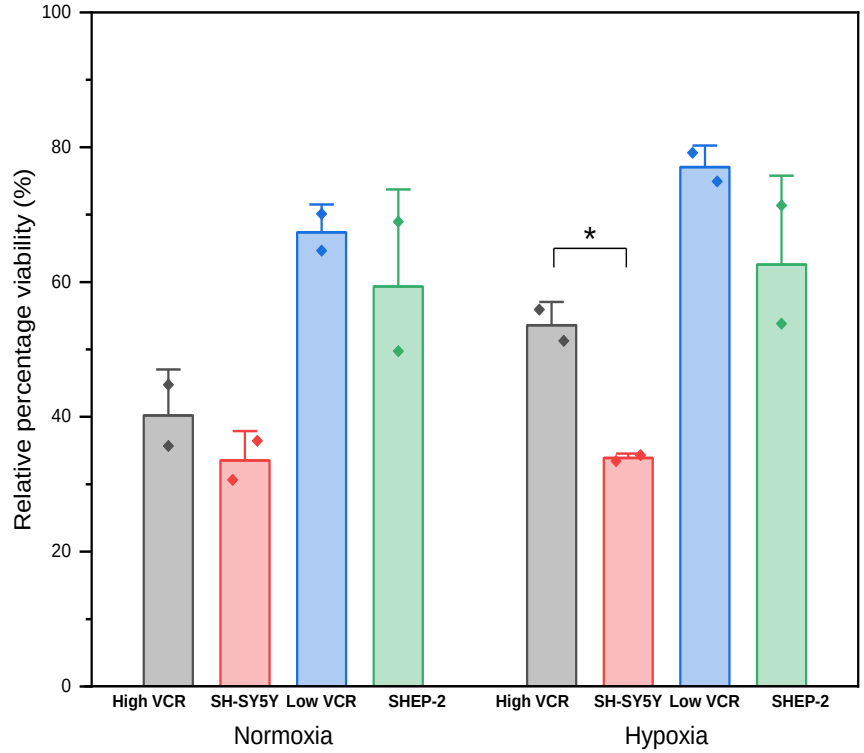

*Figure S4: Relative percentage viability of HS-5 in monoculture and co-culture in normoxia (left) and hypoxia (right). High VCR = 0.09 µM in monoculture, Low VCR = 0.0054 µM in monoculture, SH-SY5Y= co-culture with SH-SY5Y and 0.09 µM VCR, SHEP-2= co-culture with SHEP-2 and 0.0054 µM VCR. The differences between the monoculture and co-culture conditions in normoxia were not found to be statistically significant for either SHEP-2 or SH-SY5Y. In hypoxia, there was a statistically significant difference between the monoculture and co-culture with SH-SY5Y cells (P=0.0169). In general, the co-culture condition appears to cause a decrease in the tolerance of the HS-5 cells for VCR, despite the lack of statistical significance. Statistical significance *P<0.05, **P<0.01, n.s. not significant, n=3.*

13. Supplementary S6: Direct co-culture of HS-5 and SHEP-2 show direct cellular connections

When SHEP-2 and HS-5 cells are in direct co-culture, HS-5 cells form direct connections with SHEP-2 cells through long, fine processes (figure S4). In addition, the cells appear to connect to each other through larger parts of the cell membrane or thicker, short processes (figure S5).

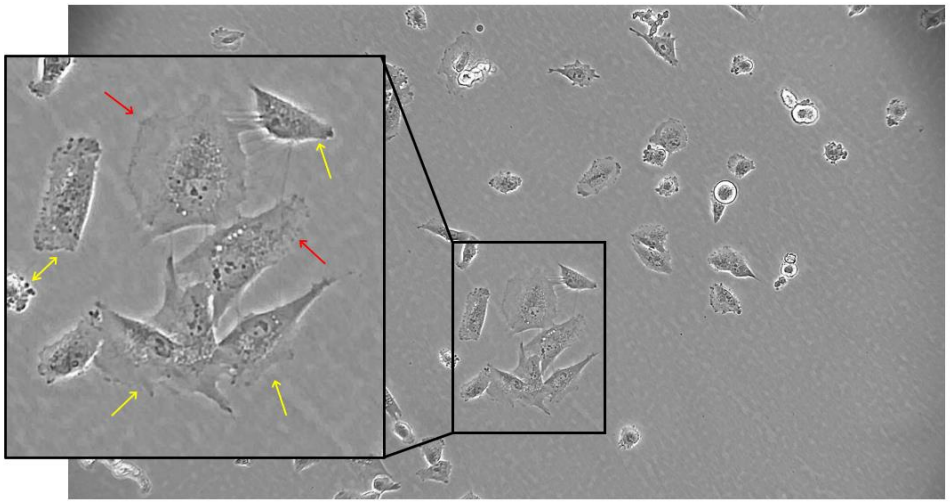

Figure S4: Co-culture of SHEP-2 (p46) and HS-5 (p+9) cells in T25 culture flask. HS-5 cells (indicated with yellow arrows) form long, fine processes to connect with SHEP-2 cells (red arrows).

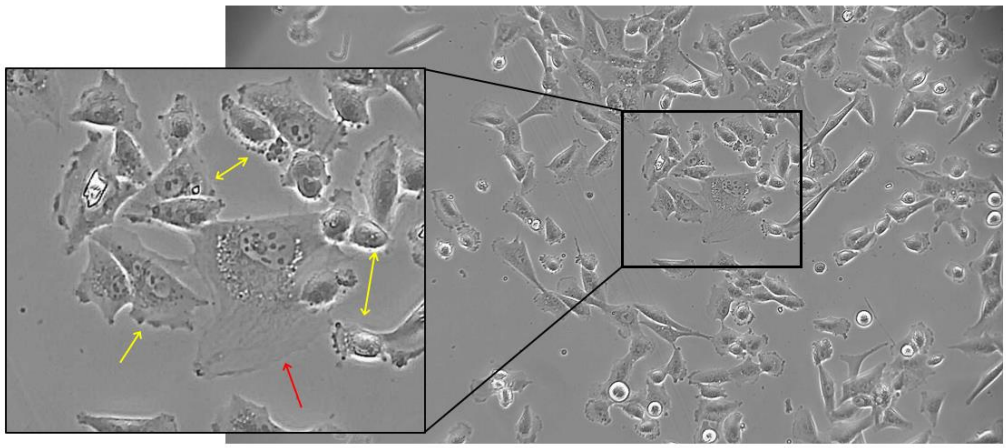

Figure S5: Co culture of SHEP-2 (p46) and HS-5 (p+9) cells on a 24-well coverslip. HS-5 cells (indicated with yellow arrows) appear to connect with SHEP-2 cells (red arrows) through larger parts of the cell membrane and with thicker, short processes.